Chem Soc Rev

Hexaazatriphenylene (HAT) derivatives. From synthesis to molecular design, self-organization and device applications

Journal:	*Chemical Society Reviews*
Manuscript ID:	CS-SYN-02-2015-000181.R2
Article Type:	Review Article
Date Submitted by the Author:	25-Jun-2015
Complete List of Authors:	Segura, Jose; Universidad Complutense, Quimica Organica I Juárez, Rafael; Universidad Rey Juan Carlos, Department of Environmental and Technological Chemistry Ramos, María del Mar; Universidad Rey Juan Carlos, Department of Environmental and Technological Chemistry Seoane, Carlos; Universidad Complutense, Quimica Organica I

Cite this: DOI: 10.1039/c0xx00000x

www.rsc.org/xxxxxx

ARTICLE TYPE

Hexaazatriphenylene (HAT) derivatives. From synthesis to molecular design, self-organization and device applications

Jose Luis Segura,[a*] Rafael Juarez,[a,b] Mar Ramos[b] and Carlos Seoane[a]

Received (in XXX, XXX) Xth XXXXXXXXX 20XX, Accepted Xth XXXXXXXXX 20XX
DOI: 10.1039/b000000x

Dipyrazino[2,3-f:2',3'-h]quinoxaline also known as 1,4,5,8,9,12-hexaazatriphenylene (**HAT**) is an electron deficient, rigid, planar, aromatic discotic system with an excellent π-π stacking ability. Because it is one of the smallest two-dimensional *N*-containing polyheterocyclic aromatic systems, it has been used as the basic scaffold for larger 2D *N*-substituted polyheterocyclic aromatics. Furthermore, it is the building block of choice in a plethora of molecular, macromolecular and supramolecular systems for a variety of applications. This review is aimed to critically review the research performed during the almost three decades of research based on **HAT** from the synthetic, theoretical and applications point of view. The design principles and synthetic strategies towards **HAT** derivatives will be established and its use in n-type semiconductors, sensors, nonlinear optical chromophores, liquid crystals, microporous polymers for energy storage and nano and microstructures will reveal the relevance of **HAT** as a basic scaffold in the areas of organic materials and nanoscience.

1 Introduction

Polycyclic aromatic hydrocarbons (PAHs) have been attracting a great deal of interest in materials science and nanoscience due to their tailorability and the appealing features of their electronic structure.[1] Those composed of laterally fused benzene rings, the so called linear PAHs (Figure 1), have received particular attention[2,3] because of their highly desirable electronic properties, including remarkable charge-carrier mobilities.[4,5,6] It has been found that increased conjugation length enhances electronic coupling and reduces reorganization energies in the solid state thus leading to several linear acenes with high charge-carrier mobilities.[3,7] Nevertheless, it has been also observed that linear acenes longer than five rings are not stable due to their low ionization potentials (IPs) and narrow band gaps.[8]

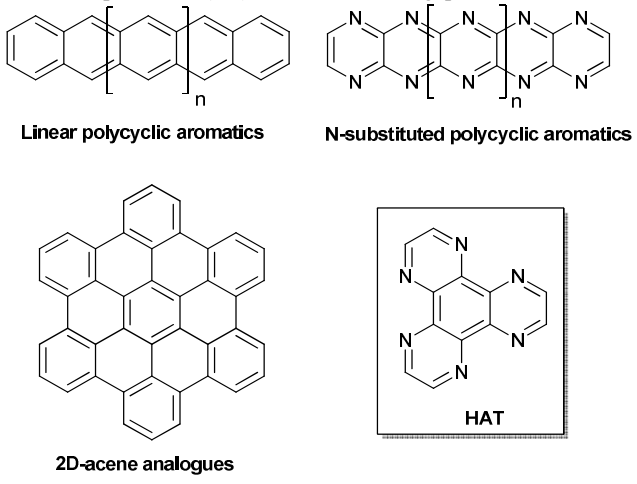

Fig. 1 Selected examples of linear polycyclic aromatics, N-substituted polycylic aromatics, 2D-acene analogues and structure of 1,4,5,8,9,12-hexaazatriphenylene (**HAT**)

Among the different approaches used for the stabilization of higher linear PAHs,[9] it has been found that (i) replacing CH atoms by heteroatoms such as nitrogen and (ii) annellating aromatic rings onto two neighboring rings, thus creating two-dimensional (2D) acene analogues[10] (Figure 1), are efficient routes to more stable compounds. Thus, *N*-substituted polycyclic aromatic analogues of PAHs (Figure 1) are less susceptible to degradation through oxidation or dimerization than their non-*N*-containing equivalents.[11] In contrast, 2D compounds that represent various fragments of graphene have large, planar π surfaces that can provide increased intermolecular surface overlap and effectively increase electron delocalization.[12]

In the frame of this research field, one of the smallest 2D *N*-containing polyheterocyclic aromatic systems is the dipyrazino[2,3-f:2',3'-h]quinoxaline or 1,4,5,8,9,12-hexaazatriphenylene (**HAT**, Figure 1). **HAT** is an electron deficient, rigid, planar, aromatic discotic system with an excellent π-π stacking ability which has been used not only as the basic scaffold for larger 2D *N*-substituted polycyclic aromatics but also as a building block in a plethora of molecular, macromolecular and supramolecular systems for a variety of applications.

This review summarizes the design principles and synthetic strategies for **HAT** derivatives and its use as a basic scaffold in n-type semiconductors, magnetic materials, sensors, nonlinear optical chromophores, liquid crystal, nano and microstructures and microporous polymers for energy storage.

Besides the above important applications of **HAT** derivatives as organic materials, for many years the main application of **HAT** was its use as ligand with three chelating sites. In this respect, the extensive literature related with metal complexes of HAT and its derivatives were already reviewed by Kitagawa and Masaoka[13] and therefore, in order to avoid duplication of these aspects, the readers interested in this particular use of **HAT** derivatives are referred to this comprehensive review.

In the present review (i) we will start with a description of the main characteristics of the hexaazatriphenylene moiety including its electron deficient character, D_{3h} symmetry, planarity and tendency for π-stacking. (ii) We will continue with a section dedicated to the synthesis of **HAT** derivatives including those with trigonal D_{3h} symmetry as well as those with non-trigonal symmetry (no D_{3h} symmetry). We will also describe methods for the synthesis of 2D-**HAT** derivatives with extended π-conjugation and for the post-synthesis functionalization of **HAT** derivatives. (iii) The next section will cover aspects related with the self-assembly of **HAT** derivatives. This section starts with the study of the supramolecular aggregation properties of **HAT** derivatives in solution. It will continue with the self-assembly in the bulk including many examples of their liquid crystal behavior and the relationship with the charge transport properties. We will also review selected examples of self-assembly of **HAT** derivatives on solid surfaces and finally the building of nano and microstructures by self-assembly. (iv) Different applications found for **HAT** derivatives will be also reviewed, including their use for the investigation of energy transfer processes, their nonlinear optical properties and their use as multiphoton-absorbing materials, their use for molecular recognition and sensors, their role as photoinitiators for polymerization reactions and their incorporation as scaffolds for microporous frameworks. (v) Hexaazatriphenylene hexacarbonitile (**HAT-CN**) will be treated as a special case of study and one section will be dedicated to this particular **HAT** derivative with a strong electron-defficient discotic character and a deep-lying LUMO level which has proved to be an interesting molecular material. (vi) In the last section, the main conclusions will be discussed, stressing the fact that the **HAT** moiety is a widely tunable and highly stable platform for developing materials in a broad spectrum of applications. We will critically comment the strengths and weaknesses for the use of **HAT** derivatives in the different areas outlined in the review, finishing with the current challenges in the field.

2 Structural and electronic characteristics of HAT

HAT is a symmetric molecule that belongs to the symmetry point group D_{3h} and is constituted by three fused pyrazine rings. The molecule contains six nitrogen atoms with sp^2 hybridization giving to the molecule an electron deficient character in agreement with the computational study performed for several hexaazatriphenylene derivatives.[14] The structure of naked **HAT** has been investigated by using a B3LYP functional and a 6-31G** level of theory (Figure 2) showing that the HOMO in **HAT** is doubly degenerate with E' [E'']' symmetry, separated by 0.16 [0.19] eV from the A_1' [A_1'']' HOMO-1 orbital. In contrast, the LUMO in **HAT** is a non-degenerate orbital with A_2'' symmetry, very close in energy (0.02 eV) to the E'' degenerate LUMO+1 orbitals. Thus, the HOMO-LUMO gap calculated for HAT is of 4.73 eV.[15]

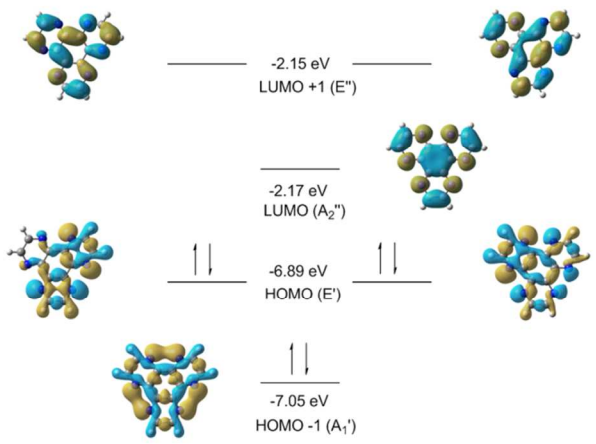

Fig. 2 Theoretical electronic structure of **HAT** frontier orbitals. B3LYP/6-31G**.

From the structural point of view, while theoretical calculations predict that **HAT** is completely flat in the gas phase, the resolved crystal structure of **HAT** shows that the molecule deviates, if only slightly, from planarity.[16] Thus, a maximum atomic deviation of only 0.07 Å is observed in the needle-like formed light beige crystals prepared from recrystallization of **HAT** in a mixture of chloroform/acetonitrile (4:1) at 5 ˚C. **HAT** crystallizes in the orthorhombic system, space group $Pca2_1$ with a = 18.187 Å, b = 9.2576 Å and c = 6.9672 Å parameters (figure 3). The HAT molecules pack in columns with an average interplanar distance of 3.29 Å that is shorter than the expected van der Waals distance (3.54 Å)[17] and comparable to the separation quoted for aromatic π-donor/acceptor molecules.[18] This short distance is indicative of an effective π-stacking of the **HAT** molecules. Additionally, water molecules in the crystal provide links between the columns of stacked molecules through hydrogen bonds.

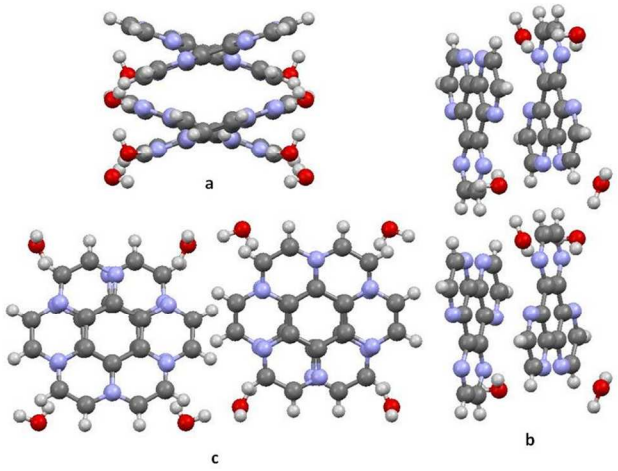

Fig. 3 HAT·$2H_2O$ packing viewed from a: *a* axis, b: *b* axis and c: *c* axis.

Comparison between experimental[16] and theoretical data[14] shows a good agreement in bond lengths (figure 4) and bond angles for which discrepancies between predicted and experimental data are less than 2°. These slight differences could be due to the fact that the theoretical calculations performed do not take into account

intermolecular interactions.

On the other hand, the molecular aggregation of **HAT** has been also theoretically explored by QM/MM calculations on a dimer model, thus showing that an antiparallel π-stacking interaction is the most stable conformation of **HAT**. Electrostatic interactions are responsible for the stabilization of the antiparallel cofatial arrangement with respect to the parallel one.[15]

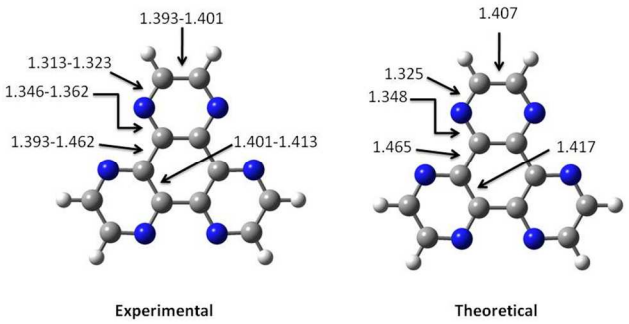

Fig. 4 Experimental[16] and theoretical[14] bond distances (all values in Å) determined for **HAT**.

Owing to its D_{3h} symmetry, **HAT** gives very simple NMR spectra. For example, in the ^{13}C-NMR spectrum there is one signal at 147.0 ppm for the six hydrogen-bearing carbons and one signal at 142.3 ppm for the six quaternary carbons.[19] The absorption spectra of **HAT** has a main peak at 4.77 eV (260 nm) with a broad unresolved band around 4.13 eV (300 nm). This is in good agreement with excited-state TD-DFT/B3LYP/6-31G** calculations, which predict the greatest oscillator strength for HAT at 4.86 eV (f = 1.14). On the other hand, **HAT** presents a very low fluorescence quantum yield which can be related to: 1) the fact that the $S_0 \rightarrow S_1$ transition has a forbidden character; and 2) the significant contribution of n-π* character in these excitations imparted by the lone electron pairs of the nitrogen atoms, which is known to quench the fluorescence emission.[15]

The electrochemical behavior of **HAT** has been investigated by using cyclic voltammetry measurements. They show several reduction processes of the **HAT** core (E^1_{RED}= -1.44 V, E^2_{RED}= -1.64 V and E^3_{RED}= -2.10 V) which are attributed to the consecutive reduction of the three pyrazine rings.[20] This good electron acceptor ability of **HAT** is in agreement with the ionization energy (IE) and electron affinity (EA) values deduced from the UPS/IPES spectra of **HAT** deposited on gold substrate by vaccum evaporation. Thus, EA value of -2.12 eV and IE value of 7.23 eV were obtained by means of this experimental methods and are in good agreement with the values obtained from gas phase DFT calculations.[15]

The electron deficient, rigid, highly symmetric, planar character of HAT together with its excellent π-π stacking ability make it a basic building block for the synthesis of a variety of organic materials. In the next section we will summarize the main synthetic strategies toward different types of **HAT** derivatives.

2 Synthesis of HAT derivatives.

2.1 A historical approach

The first synthesis of 1,4,5,8,9,12-hexaazatriphenylene (**HAT**) was not reported until 1981 by Nasielski-Hinkens *et al*. by using a three step reaction sequence (scheme 1) in the search of new metal ligands for low valent transition metals. The synthetic route starts with the amination of nitroderivative **1** to yield intermediate **2**, which was subsequently reduced with hydrazine to afford diamine **3**. This was finally reacted with glyoxal to afford the target **HAT** with an overall yield of 34 % based on nitroderivative **1**.[21]

Despite this late synthesis of basic **HAT**, research on π-deficient polycyclic aromatic compounds containing the **HAT** moiety started as early as 1888 when Nietzki and Schmidt reported the reaction between the sodium salt of the rhodizonic acid (**4**) and *o*-phenylenediamine from which they isolated what they called benzenetriphenazine.[22] In 1962 Eistert *et al*. reinvestigated this reaction between rhodizonic acid (**4**) with *o*-phenylendiamine and isolated the same compound to which they assigned the structure of 5, 6, 11, 12, 17, 18-hexaazatrinaphthyl-ene (**HATNA**) (Scheme 1).[23] The structure of this condensation product was postulated almost entirely on the basis of analytical data. It was not until 1969 that the first spectroscopic and structural evidences for the structure of **HATNA** were reported.[24,25]

The first systematic synthesis of functionalized **HAT** derivatives was reported in 1985[26] and consisted in the condensation between different α–diketones (**5**a-i) and hexaaminobenzene (**6**) (Scheme 2). This efficient synthesis provided a general protocol for the synthesis of functionalized **HAT** derivatives. At that time, the synthesis of hexaaminobenzene involved the reduction of explosive aromatic nitrocompounds with different hidrazynes which prevented the production of **6** in large scale. This problem was resolved by Rogers who reported the synthesis of hexaaminobenzene (**6**) in large amounts and high yields using sodium in liquid ammonia to reduce 1,3,5-triamino-2,4,6-trinitrobenzene (TATB, **8**, Scheme 2).[27]

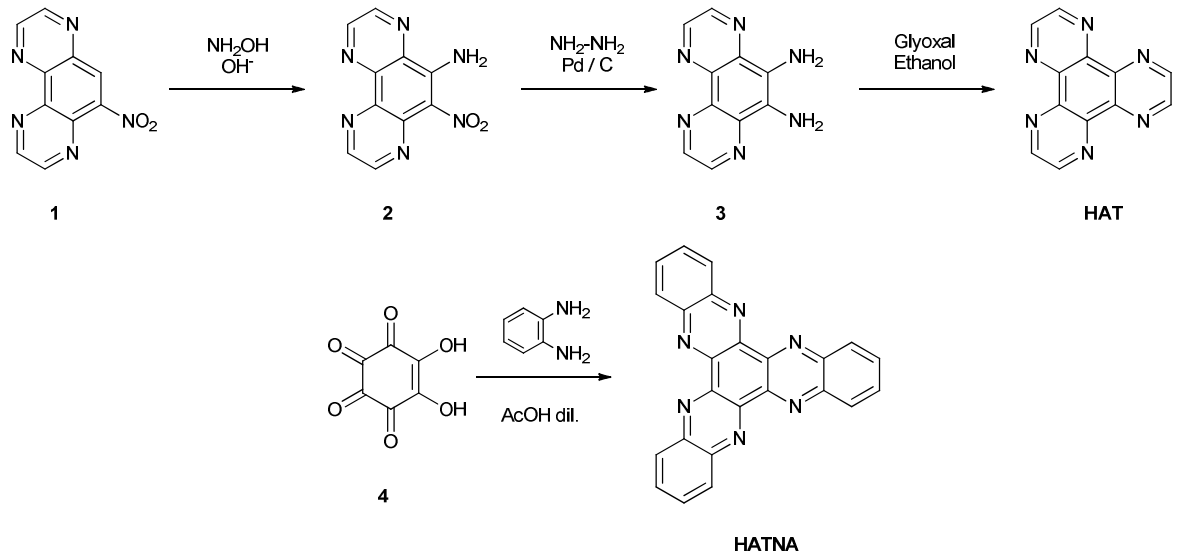

Scheme 1 *Top:* The first synthesis of **HAT**; Bottom: The first synthesis of a **HAT** derivative, **HATNA**.

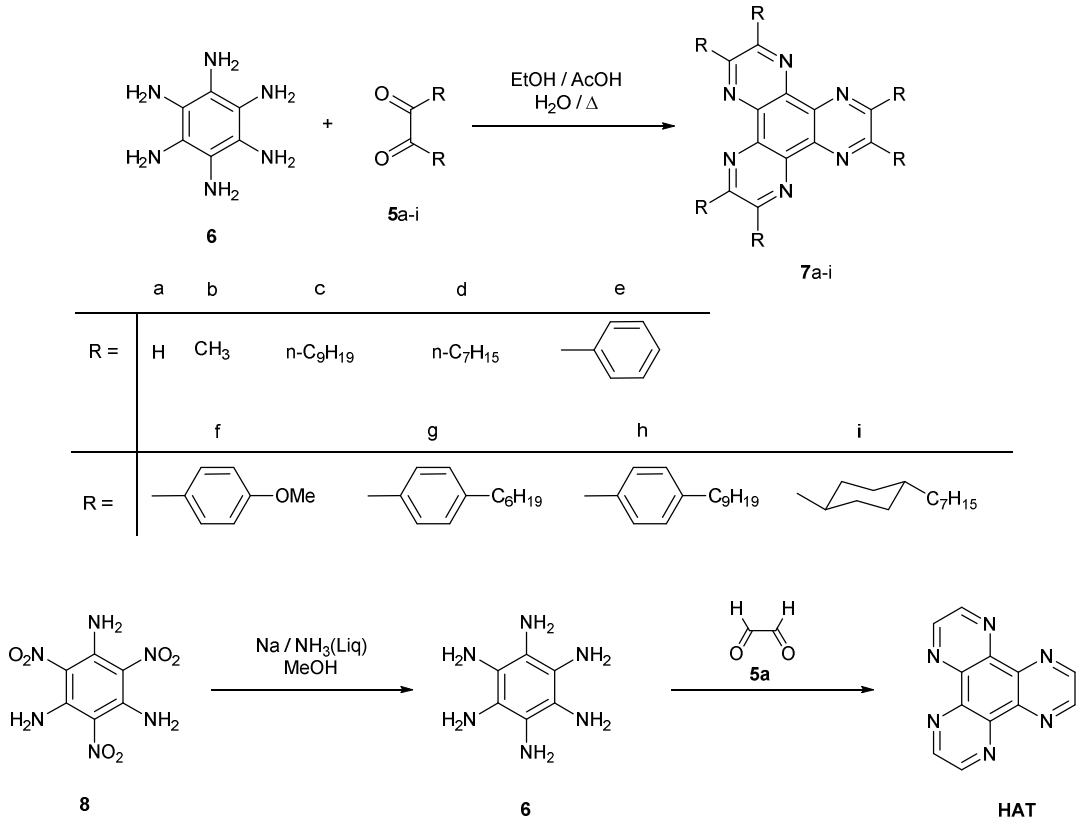

Scheme 2 *Top:* First systematic synthesis of a series of **HAT** derivatives. *Bottom:* Rogers' synthesis of **HAT**.

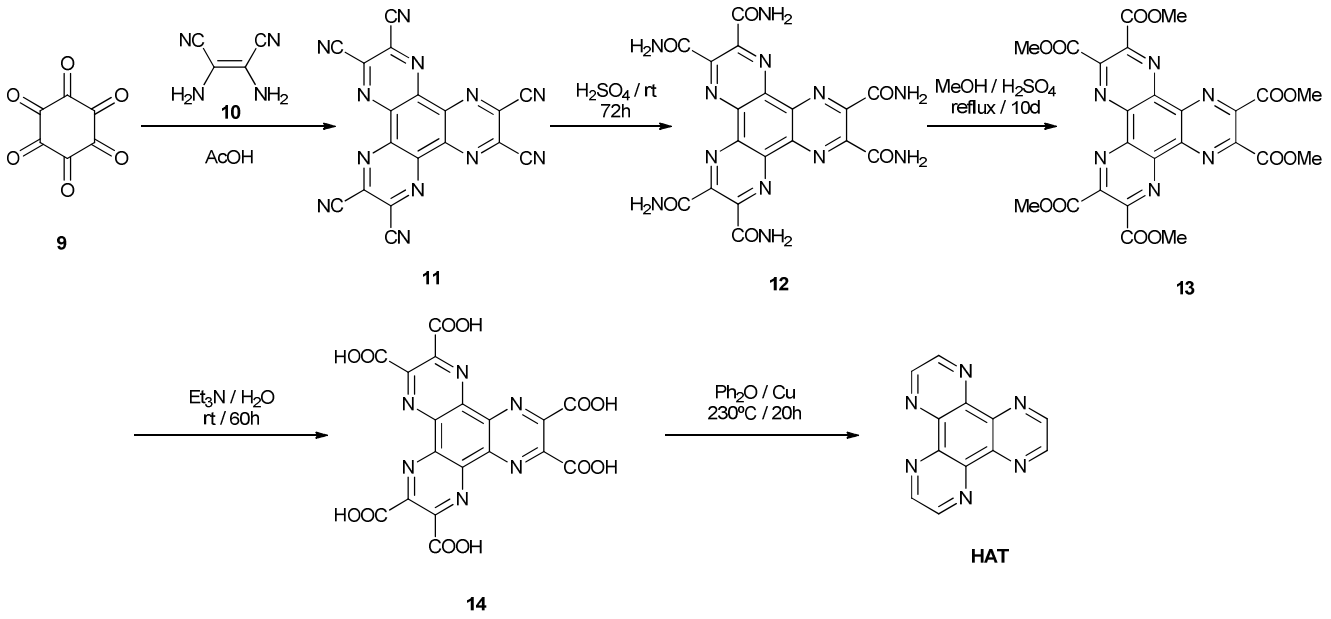

Scheme 3 Multistep synthetic route for the production of **HAT** from hexaketocarbonyle (**9**)

Although TATB (**8**) is used as an explosive, it is perhaps the most thermostable and insensitive explosive known because of its low sensibility to shock that makes it stable enough for laboratory handling and can be produced and stored in multigram scale.[28] In order to avoid the use of **8**, a multistep synthetic route towards unsubstituted **HAT** was also developed. This synthetic procedure starts with the reaction of hexaketocyclohexane (**9**) with 2,3-diaminomaleonitrile (**10**) to yield 2,3,6,7,10,11-hexacyanoHAT (**HAT-CN**, **11**), which can be subsequently used to obtain hexaazatriphenylene-2,3,6,7,10,11-hexacarboxylic acid (**14**). This can be finally decarboxylated to afford pristine **HAT** (Scheme 3).[29, 30] However, in order to obtain this basic **HAT**, the synthetic route depicted in Scheme 3 requires 15 days of work in contrast with Rogers´ method (Scheme 2)[27] with which **HAT** or other **HAT** derivatives can be obtained in multigram scale in less than a week.

In 1969 it was already shown that the use of hexaketocyclohexane (**9**) as starting material for the synthesis of **HAT** derivatives is effective not only for the condensation with diaminomaleonitrile, as shown in scheme 3, but also with a variety of *o*-phenylenediamine derivatives.[24] Thus, the condensation of hexaketocyclohexane (**9**) with unsaturated 1,2-diamines has become a good alternative for the general synthesis of differently functionalized **HAT** derivatives as is depicted in scheme 4 for a family of **HATNA** derivatives (**16a-h**) with a variety of substituents.[31,32] Introduction of rigid acetylenes with bulky silyl substituents in positions that force the aromatic core to deviate from planarity, leads to twisted-**HATNA** derivatives **16f-h** (Scheme 4). [32] Interestingly, it has been observed that modifying the size of twist angles in **HATNA** derivatives allows tuning their emission characteristics and electrochemical potentials.

By using hexaketocyclohexane (**9**) as starting material, Hsu and coworkers have synthesized a series of **HATNA** derivatives **17a-d** (Figure 5) as electron deficient liquid crystal materials,[33] and Marder and coworkers have synthesized unsubstituted **HATNA** and **HATNA** derivatives **18a-c** (Figure 5) in which the solid state ionization potentials and electron affinity can be tuned by means of the different substitution pattern.[34] Wang and coworkers also started from hexaketocyclohexane to synthesize a series of film-forming low-bandgap chromophores with a **HATNA** skeleton and multiple electron-donating groups at the appropriate positions of the acceptor core (**19a,b**, Figure 7).[35] Piglosiewicz et al. reported in 2005 a new synthetic procedure for the synthesis of **HATNA** which consists on the dehydroaromatization reaction of quinoxaline (**20**) using a Ti complex for the activation of the C-H bonds followed by a reaction with iodine to afford the pristine **HATNA** (scheme 5).[36] Nevertheless, this last approach has not been widely studied or used as a common synthetic way to **HATs**.

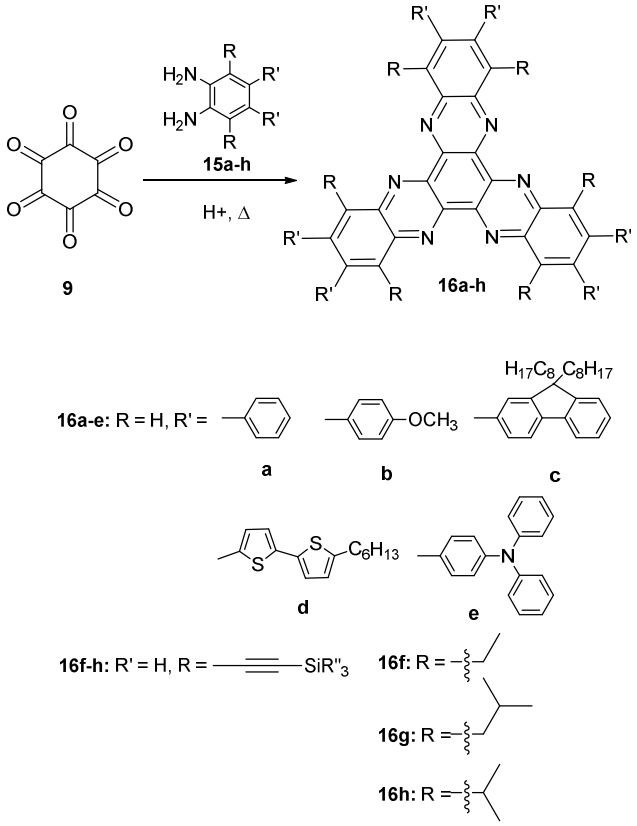

Scheme 4 Synthesis of a family of **HATNA** derivatives using hexaketocyclohexane (**9**) as starting material.

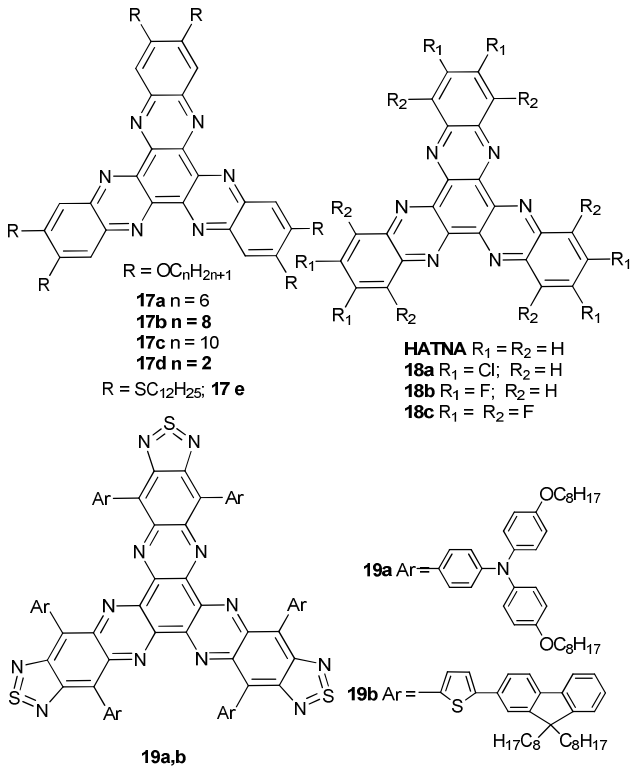

Figure 5 Selected examples of **HATNA** derivatives synthesized using hexaketocyclohexane (**9**) as starting material.

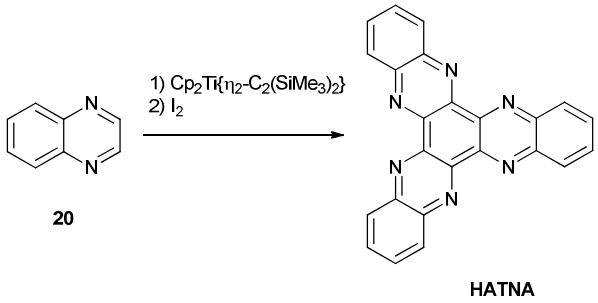

Scheme 5 Metal mediated synthesis of **HATNA**.

Thus, the synthetic strategies for the production of the **HAT** skeleton used to date are summarized in Scheme 6. The most extensively used strategies involve i) the condensation of hexaketocyclohexane (**9**) with unsaturated 1, 2-diamines and ii) the condensation of hexaaminobenzene (**6**) with α-diketones. The other, less general, route which has been used for the synthesis of **HATNA** is based on the cyclodehydrogenation of quinoxaline (**20**) mediated by titanium complexes.

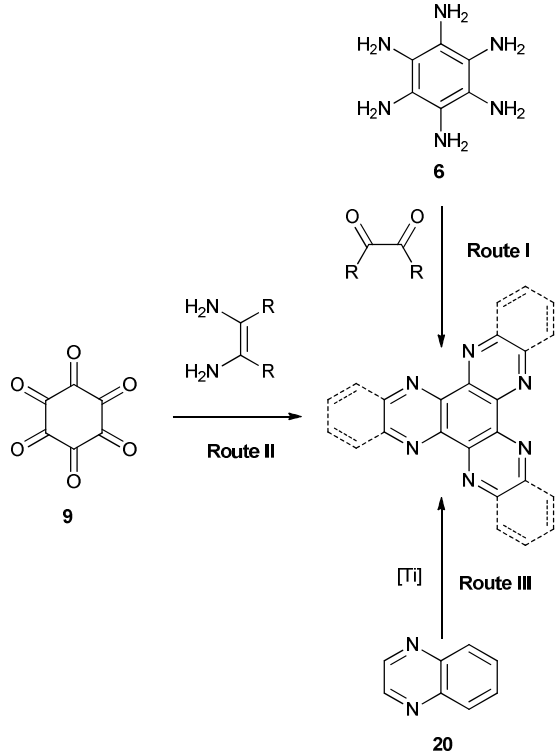

Scheme 6 Synthetic approaches to trigonal **HAT** derivatives.

It is worth mentioning that these approaches lead to the synthesis of trigonal **HAT** derivatives with D_3h symmetry containing a C_3 symmetry axis perpendicular to the **HAT** plane (Figure 6).

In the meantime, the need of synthesizing other non-trigonal **HAT** derivatives for specific applications was brought into play. It has been necessary to develop other synthetic strategies in order to obtain this kind of non-trigonal derivatives. Thus, **HAT** derivatives that present a C_2 (usually in the same plane of the **HAT** ring) or lower symmetry axis (Figure 6) have been synthesized and the synthetic procedures used for their synthesis will be summarized in the following section.

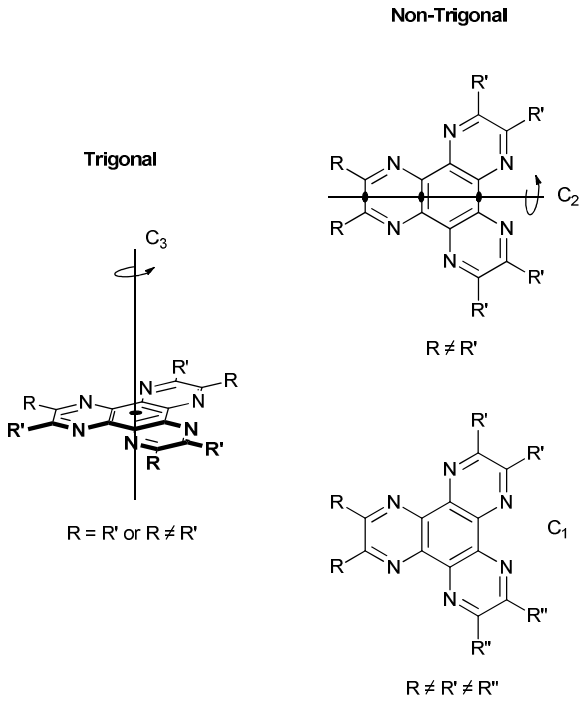

Fig. 6 Some samples of trigonal and non-trigonal symmetries of **HATs**.

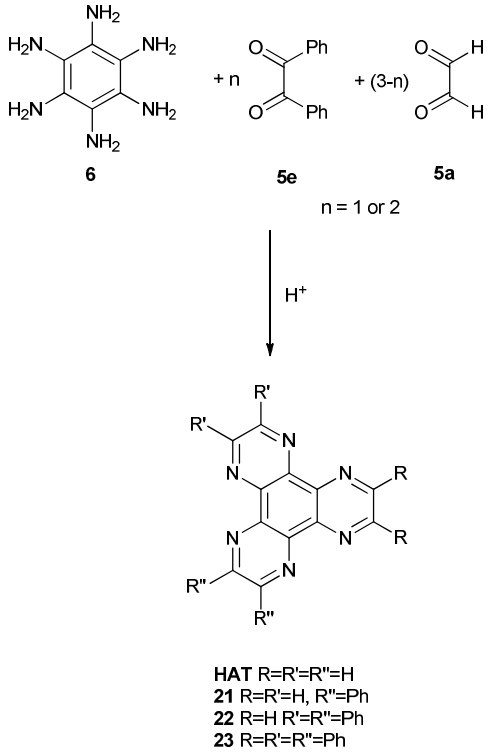

Scheme 7 Aleatory method for the synthesis of non-trigonal HATs.

2.2 Synthesis of not trigonal HATs

Most of the **HAT** derivatives synthesized so far have a trigonal symmetry, probably because of the lack of selective methods for the synthesis of non-trigonal analogues. Until recently, the only way to obtain non-trigonal derivatives was a aleatory method based on the condensation of hexaaminobenzene (**6**) with more than one α–diketone at a time thus providing inevitably a complex mixture of products. For example, the reaction of one equivalent of **6** with one or two equivalents of benzil (**5e**) followed by two or one equivalents respectively of glyoxal (**5a**)[37] yields a complex mixture of products (**HAT**, **21-23**, scheme 7) that is difficult to purify.

Thus, in recent years the need to develop synthetic strategies that allow the synthesis and investigation of non-trigonal **HATs** has become clear.

In 1997, Moucheron reported an easy access to pyrazino[2, 3-f] quinoxaline-5,6- diamine (**3**) in a single step by condensation between hexaaminobenzene (**6**) and glyoxal (**5a**) under stoichiometric control in a mixture of ethanol and water (Scheme 8).[38] This easy access to the diaminoderivative **3** paved the way for the synthesis of nontrigonal **HAT** derivatives by reaction with other α-diketones. Thus, condensation between **3** and 1,10-phenanthroline-5,6-dione **24** yields the nontrigonal **HAT** derivative **25** selectively (Scheme 8).[38]

We have employed this synthetic strategy in order to obtain donor-acceptor materials for nonlinear optical (NLO) applications in which the electron deficient **HAT** core is connected to electron rich groups through double or triple bonds (**26-30**, Figure 7). [39]

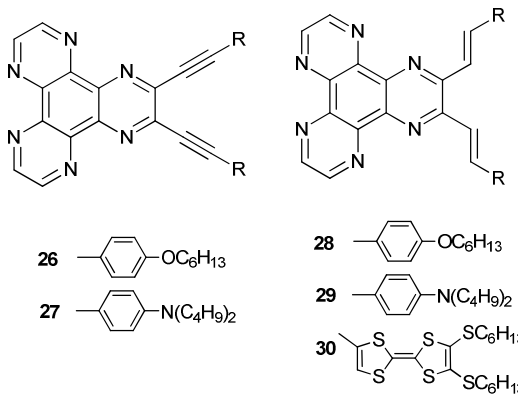

Fig. 7 Nontrigonal donor-acceptor-donor **HAT** derivatives.

Other synthetic approaches involving the use of oxocarbons (monocyclic polycarbonyl compounds) such as 2,3,5,6-tetrahydroxy-*p*-benzoquinone (**31**), hexaketocyclohexane (**9**) or rhodizonic acid (**4**) as starting materials (scheme 9) have also been explored. Thus, condensation between 2,3,5,6-tetrahydroxy-*p*-benzoquinone (**31**) and *o*-phenylenediamine **32**, followed by oxidation with nitric acid, affords a tetraketo derivative **33** which can be condensed in acidic media with other substituted *o*-phenylenediamine derivatives (**34a,b**) to yield the final non-trigonal **HAT** derivatives **35a,b** (Scheme 9).[40]

In the previous section we have shown how hexaketocyclohexane (**9**) can be condensed with unsaturated 1,2-diamines to reach trigonal **HATs** easily. Alternatively, **9** can be condensed with an *o*-phenylenediamino derivative (**30b**) in a carefully chosen reaction medium (formic acid at room

temperature) to afford a α-diketone **36** in very good yield (83%). This α-diketone can be further condensed with other different *o*-pheneylenediamine derivatives (**37a-c**) to form the corresponding nontrigonal **HAT** derivatives **38a-c** (Scheme 9).[40] On the other hand, the intermediate α-diketone derivative **36** can also be obtained from rhodyzonic acid (**4**) by condensation with an *o*-phenylenediamine derivative (**34b**), followed by oxidation (Scheme 9). Furthermore, Wang and coworkers reacted the α-diketone derivative **36** thus obtained with 2,3-diaminomaleonitrile (**10**) to afford the nontrigonal **HAT** derivative **39** with a high electron accepting capability due to the presence of the nitrile groups and with smectic liquid crystalline properties, these due to the long alkyl chains and the flat **HAT** core.[41]

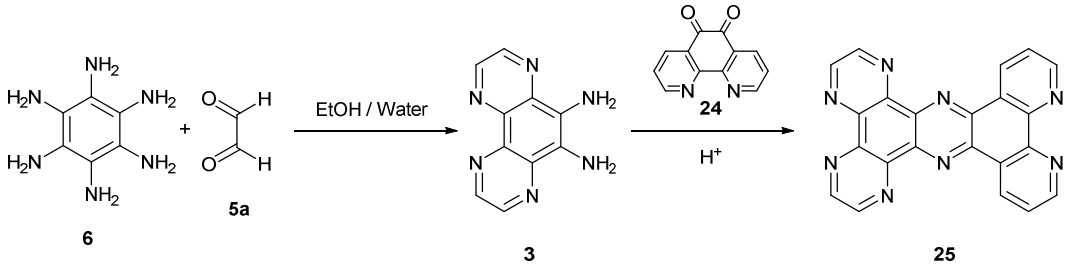

Scheme 8 First controlled synthesis of non-trigonal HATs.

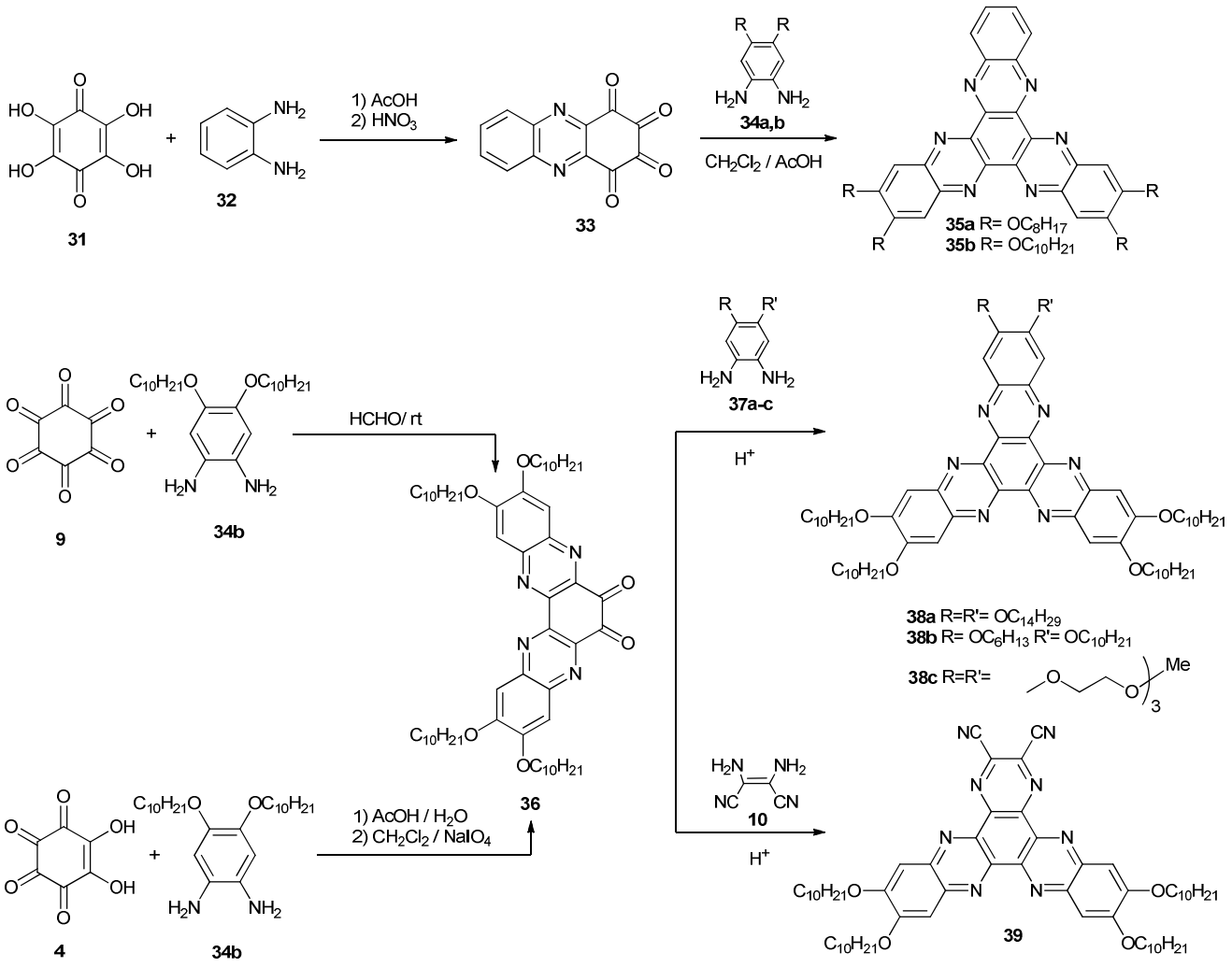

Scheme 9 Synthesis of nontrigonal **HAT** derivatives from different oxocarbons as starting materials

Cite this: DOI: 10.1039/c0xx00000x

www.rsc.org/xxxxxx

ARTICLE TYPE

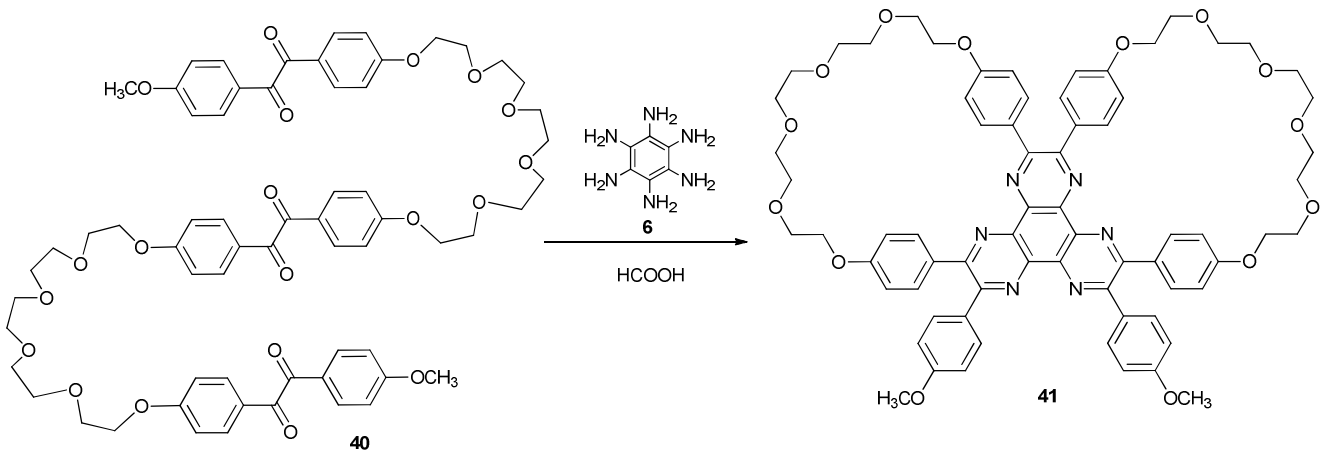

Scheme 10 Synthesis of an unsymmetrical bismacrocyclic **HAT** derivative

A completely different approach has been developed by Scondo and Fages for the synthesis of nontrigonal **HAT** derivatives laterally bridged with two macrocyclic units (**41**, Scheme 10). The procedure involves the condensation of a linear trisbenzil precursor (**40**) with hexaaminobenzene (**6**) acting as both a reagent and template (Scheme 10). Here, the stepwise creation of the six imine bonds, leading to the formation of the **HAT** core and the concomitant construction of the two lateral macrocycles, was reasoned to imply the wrapping of one molecule of the linear trisbenzil precursor (**40**) around the hexaaminobenzene (**6**) nucleus in a sequence of one bimolecular and two intramolecular condensations.[42]

The novel routes toward non trigonal **HATs** open up a field of novel materials and applications of **HAT** derivatives, as will be outlined in the following sections.

2.3 Post-synthesis functionalization of HAT derivatives

In almost all of the previous synthetic sequences the last step consists on the formation of the **HAT** nucleus. In this section, we will present functionalized **HAT** derivatives that can be further modified.

The first example of post-synthesis functionalization of a **HAT** derivative was based on the conversion of the functional groups attached to the **HAT** core and it has already been presented in scheme 3.[29] Thus, the cyano groups of hexacyano **HAT** (**11**) can be reduced to the hexaamido derivative (**12**) which can be converted to the corresponding hexa(methylcarbonyl) analogue (**13**) which can be further hydrolysed to the hexacarboxylic acid **HAT** derivative (**14**). In addition, the hexa(methylcarbonyl) derivative (**13**) has been reported to react with different amines to yield the corresponding amides.[43]

Czarnik et al. reported the synthesis of **HAT**-trisimides **44a-d** by reaction of **HAT**-trianhydride (**42**) with different amines (**43a-d**, Scheme 11). In addition, they explored the influence of different amounts of **HAT**-trianhydride (**42**) in polymerization reactions between pyrromellitic dianhydride and 4,4'-oxydianiline (**43d**). In these reactions, **42** is used as a crosslinking agent in the synthesis of polyimides due to its trifunctional character.[44]

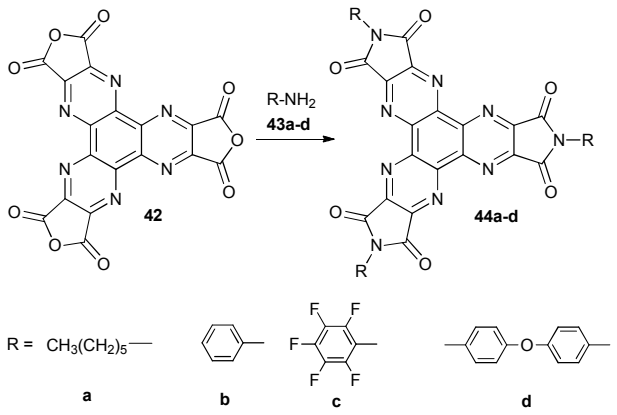

Scheme 11 HAT-trisimide derivatives obtained by post-synthesis functionalization

Another functionalization based on a functional group transformation has been reported by Aumiller *et al*. which have been able to synthesize hexakis-(dihalomethyl) HATs (**46** and **47**) and hexaformyl **HAT** (**48**) by halogenation and oxidation reactions of hexamethylhexaazatriphenylene (**45**, scheme 12) respectively.[45]

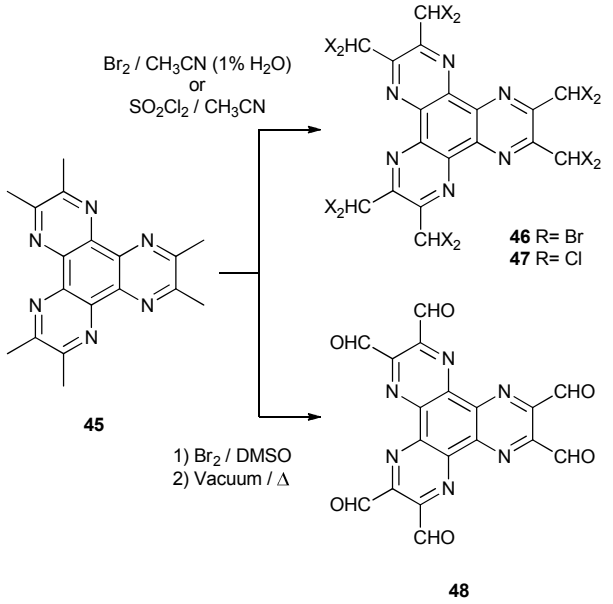

Scheme 12 HAT derivatives obtained by post-synthesis functionalization

Our group have reported the synthesis of a dibromomethyl substituted **HAT** derivative (**49**) and its further conversion to the corresponding diphosphonate derivative (**50**) which can undergo Horner-Wadsworth-Emmons olefination reactions with different aromatic aldehydes to yield donor-acceptor-donor HAT derivatives (**28-30**, Scheme 13) with nonlinear optical properties. Hexacyano-**HAT** (**11**) has also been used as the substrate for nucleophilic aromatic substitutions where the CN groups act as leaving groups. Thus, the reaction of **11** with alkyl thiols yielded the corresponding hexahexylthio derivatives **52**.[46] In contrast, analogous reaction of **11** with alkyl alcohols afforded **HAT** derivatives in which only three CN groups are substituted (**51a,b** scheme 14).[47] This different behaviour can be rationalized in terms of the higher electron donor ability of the alkyloxy groups that deactivate the neighbour CN groups for further substitution reactions. The previous proposed mechanism could explain this fact, due to the weaker electron donating ability of alkylthio groups in comparison with alkyloxy groups, the deactivation of the CN groups being in this case smaller, thus allowing them to react until all of the groups have been substituted. A similar behaviour has been observed for the reaction of hexachloro**HATNA 18a** with alkylthiols and alkylalcohols (Scheme 14). Total replacement of the chlorine atoms, upon reaction of **18a** with alkyl thiols, was observed yielding derivatives **53-56**[48] as electron transporting discotic materials.[49] On the other hand, similar reaction between **18a** and different alkyl alcohols did not provide characterizable products.[50]

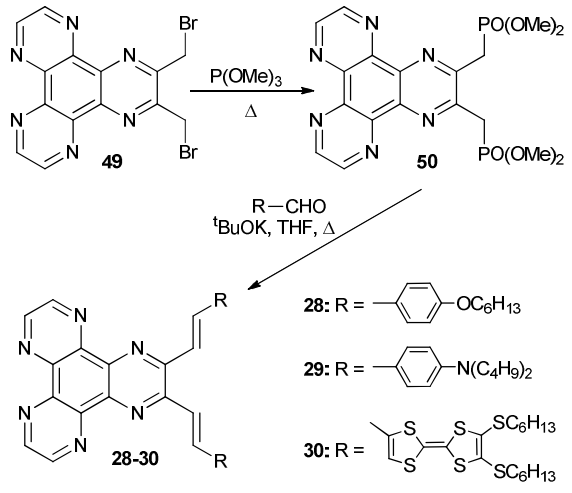

Scheme 13 Donor-acceptor-donor HAT derivatives obtained by post-synthesis functionalization

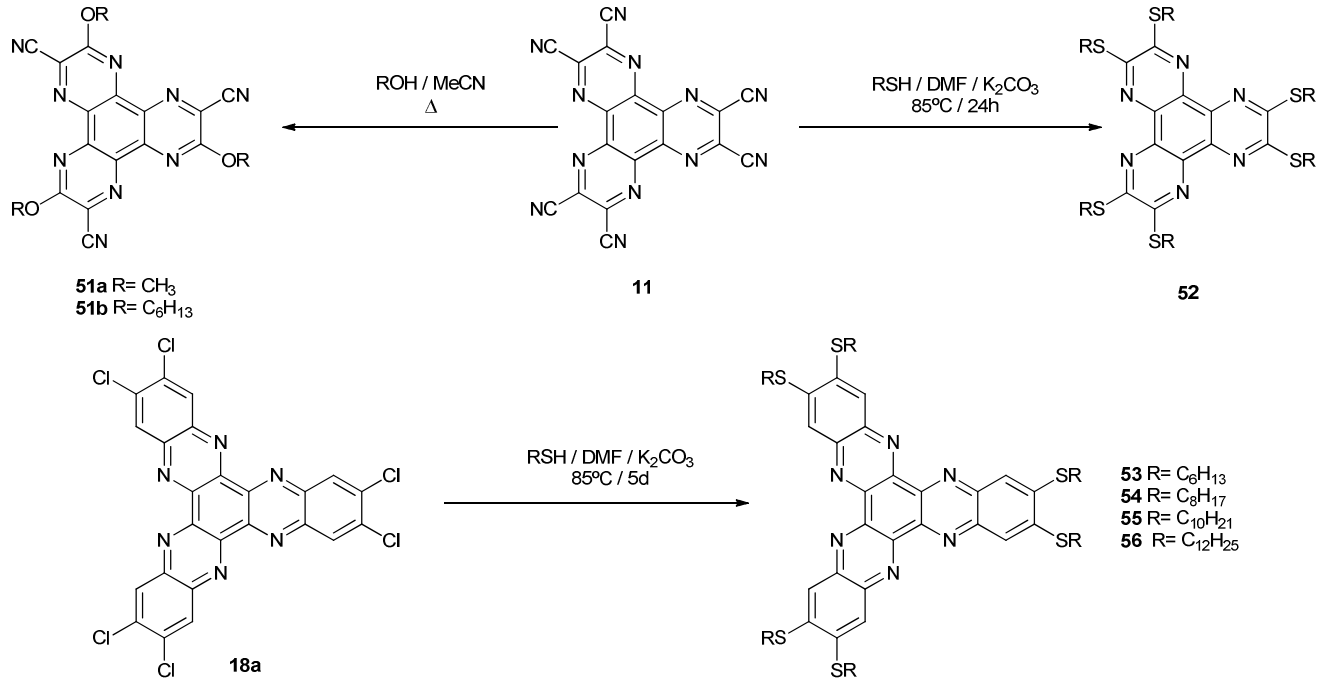

Scheme 14 Post synthesis functionalization of HATs based on aromatic nucleophilic substitution

Cite this: DOI: 10.1039/c0xx00000x

www.rsc.org/xxxxxx

ARTICLE TYPE

It can thus be seen that the possibility of obtaining **HAT** derivatives endowed with functional groups greatly enhance the possibility of incorporating the **HAT** moiety in novel molecular and macromolecular materials as well as in supramolecular assemblies.

2.4 Expanding the HAT core conjugation

The first example of a **HAT** derivative with two-dimensional expansion of the π-conjugated system (**57**, Figure 8) was reported by Lehn and coworkers in 1996 in the search of rigid ligands for polymetallic molecular architectures. The novel **HAT** derivative was obtained by reaction of hexaaminobenzene (**6**) with a suitable diketone to yield only the symmetrical product.[51] Other **HAT** derivative with two-dimensional expansion of the π-conjugated system is the planar conjugated macrocycle **61** (Figure 10) which has also been used as a ligand. After coordination of **61** with three Co ions, the $[CoN_4]_3$ complex shows an excellent behavior as nonprecious metal catalysts (NPMCs) for fuel cell applications.[52, 53] In this case, the compound was obtained through a multistep reaction sequence after the **HAT** ring was formed as depicted in Scheme 15.

However, the main driving force for the development of **HAT** derivatives with extended π-conjugation has been the search for novel organic semiconductors. Large-sized semiconductors with an expanded π-electron system tend to have a positive influence on the charge carriers mobility due to the increase of the self-assembling aggregative nature between the stacked molecules as well as the increase of the orbital overlap between the π-orbitals of the molecules. For example, the *p*-type self-assembling semiconductor hexabenzocoronenes[1] with an expanded π-electron system are well-known as good carrier-transporting materials.[54] On the other hand, the *n*-type self-assembling semiconductors are very often limited to small- and medium-sized aromatics.[55]

Thus, the creation of new large-sized self assembling *n*-type semiconductors including **HAT**, the tuning of their HOMO and LUMO values together with the study of their self-assembling properties both in solution and in the solid state has been a hot subject of research in last recent years.

In this regard, Wang and coworkers synthesized a series of *n*-type **HAT** derivatives (**63-66**, Figure 9).[56] It is observed that the absorption and emission spectra are red-shifted with the increase of the pyrazine unit number. In particular, the LUMO energy levels are drastically decreased from -3.54 eV (**63**) to -4.02 eV (**66**), even lower than a well-known *n*-type material PCBM(-3.8 eV) used in organic photovoltaics.[57]

We and others have synthesized **HAT** derivatives with two-dimensional expansion of the π-conjugated system such as **58**[58], **59**,[59] **60**[15] and **62**[60] (Figure 8) with the aim to investigate their self-assembling properties both in solution and in the solid state as it will be summarized in the following section.

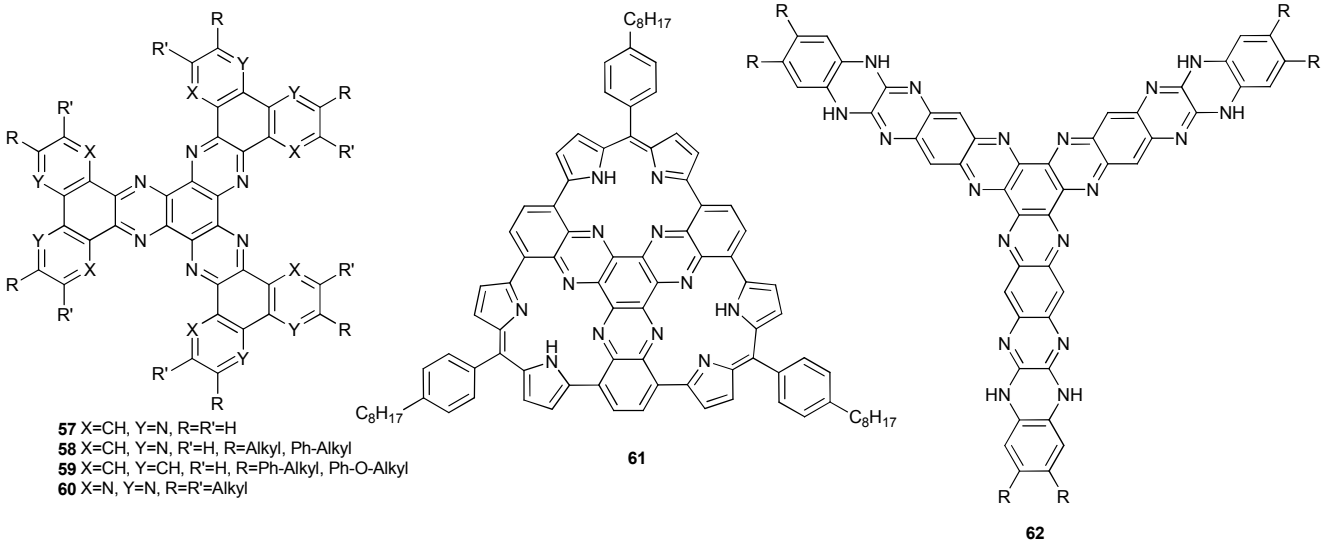

Fig. 8 HAT derivatives with two-dimensional expansion of the π-conjugated system

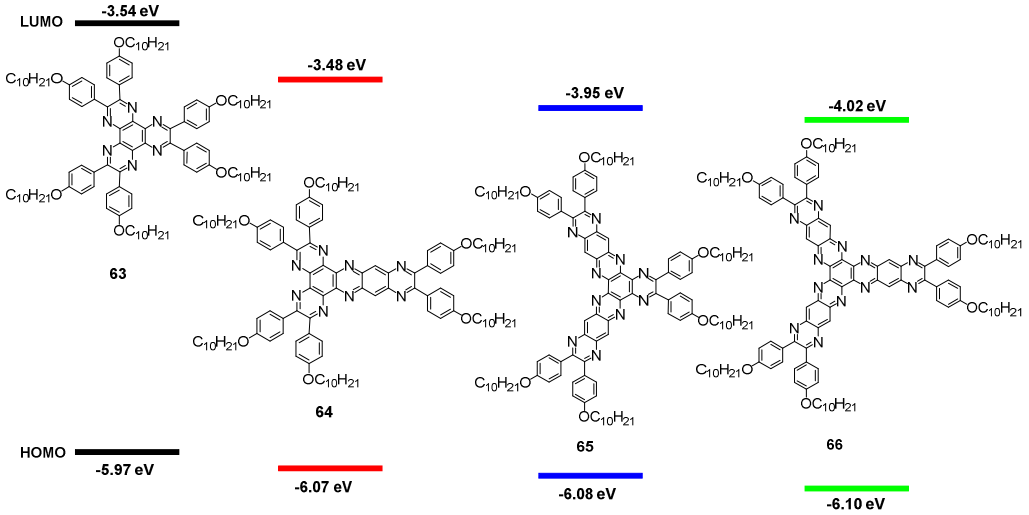

Fig. 9 Frontier orbitals tuning of a series of **HAT** derivatives (**63-66**) with different number of pyrazine units. Adapted with permission from Org. *Lett*, 2011, 13, 4378-4381. Copyright 2011 American Chemical Society

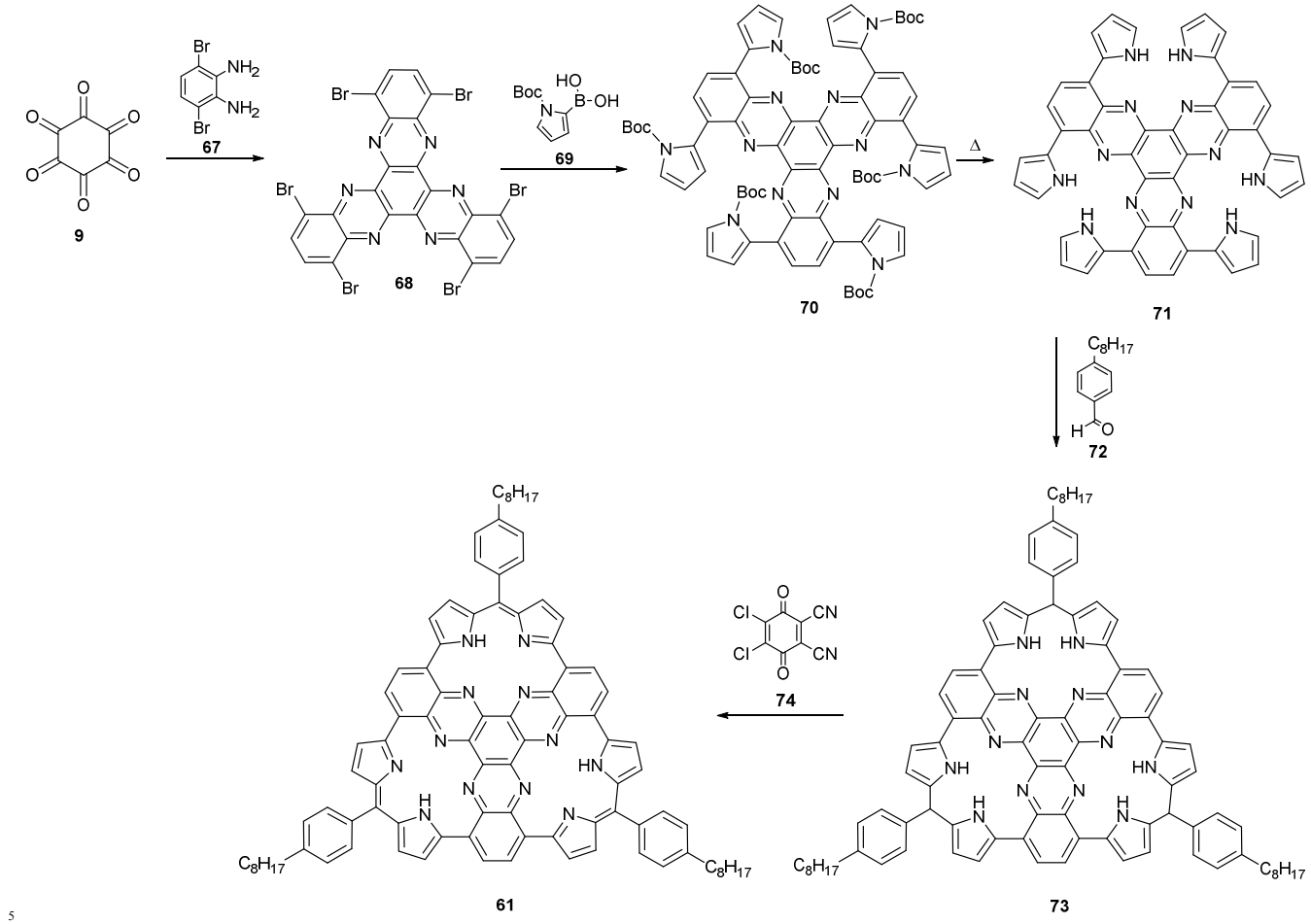

Scheme 15 Multistep synthesis of planar conjugated macrocyclic HAT derivative **61**

HAT derivatives directly conjugated with strong electroactive moieties (**75**, **76**, **77**, Figure 10) have been also synthesized. Liu and coworkers reported the synthesis of a redox-active tri-star molecule **75** combining the strong electron donor tetrathiafulvalene (TTF) and **HAT**. The target compound was obtained via the direct condensation reaction of hexaketocyclohexane (**9**) with a TTF derivative endowed with a diamino functionality.[61]

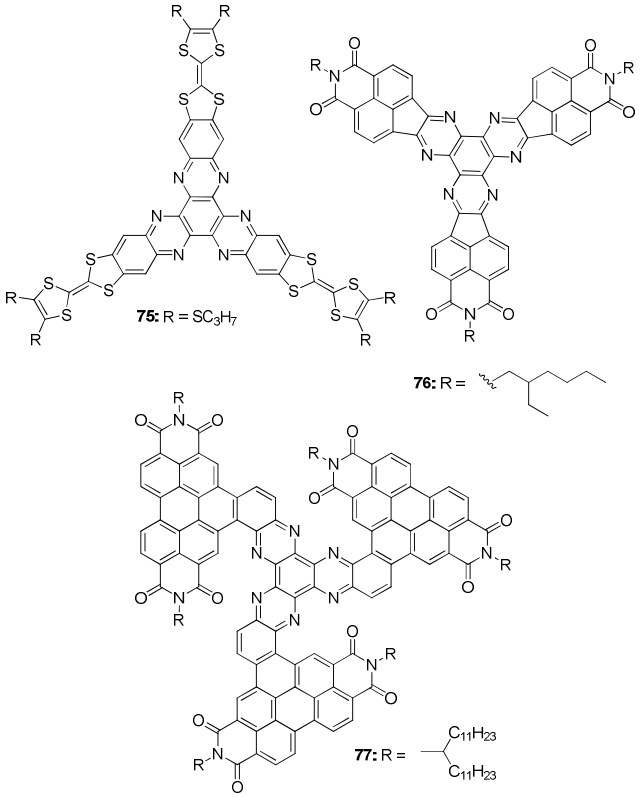

Figure 10 HAT derivatives directly conjugated with the strong electron donor tetrathiafulvalene (**75**) and the strong electron acceptors naphthalimide (**76**) and perylene bisimide (**77**)

On the other hand, in the frame of a systematic study of a family of *n*-type semiconducting naphthalimide-based pyrazinacenes, we have recently reported the synthesis of a **HAT** derivative directly conjugated with the strong electron acceptor naphthalimide (**76**).[62] The synthesis was carried out *via* the direct condensation of hexaaminobenzene (**6**) with a naphthalimide derivative endowed with a diketone functionality. It was shown that, in comparison with linear analogues, the discotic shape of **HAT** derivative **76** improves the film forming properties which is of interest for its use in devices.

Xiao and coworkers have reported the synthesis of an *n*-type star shaped molecule **77** that contains a **HAT** core fused with three perylene-3,4,9,10-tetracarboxylic acid bisimide (PBI) "arms" at the bay sites, which is composed of 25 fused six-membered aromatic rings. Interestingly, an *n*-type charge carrier mobility of 3.34 x 10^{-3} cm^2 V^{-1} s^{-1} was obtained for **77** by steady-state space charge-limited currents (SCLC) measurements, which is considerably higher than 8.71 x 10^{-5} cm^2 V^{-1} s^{-1} as determined for the PBI monomer.[63]

In the next section we will review how some of these **HAT** derivatives with extended π-cores have a strong tendency for aggregation, both in solution and in the solid state.

3 Self-assembling properties of HAT derivatives

Molecular self-assembly via noncovalent interactions has been employed as a tool for obtaining supramolecular architectures. Among these noncovalent interactions, the controlled self-assembly of π-conjugated molecules into ordered supramolecular architectures via π- π stacking is a subject of increasing research interest for the tailoring of their functionalities, and for their application in organic electronic devices.[64] Such ordered supramolecular aggregates are more attractive candidates for electron transporting materials than glassy-type amorphous aromatics with unfavorable positional and energy disorder.[65]

The outcome of the self-assembly at the molecular scale can be visualized at different levels such as (i) three dimensional (3D) ordered liquid crystals (LC) in the solid state,[66] (ii) one dimensional (1D) micro/nanostructures[67] and (iii) assemblies on solid surfaces.[68] We will review how **HAT** derivatives are used to generate supramolecular architectures at the three above mentioned levels and we will also summarize the available research on the self-assembling properties of **HAT** derivatives in solution.

3.1 Self-assembly in solution

As it has been already mentioned, **HAT** derivatives can be self-assembled both in solution and in the solid state. Although most of the applications of the supramolecular assemblies are based on solid-state materials, the first evidences for the aggregation are provided by means of spectroscopic techniques very often performed in solution. For example, Ishi-I and co-workers, in the search of new large-sized self-assembling *n*-type semiconductors, investigated the aggregation properties of a family of **HAT** derivatives with two-dimensional expansion of the π-conjugated system (**57-58**, Figure 8) by means of UV-vis, fluorescence, ^{1}H-NMR spectroscopies and MALDI-TOF mass spectrometry.[58,59] They observed concentration- and temperature dependent spectral changes in 1,1,2,2-tetrachloroethane solutions which were attributed to dynamic exchange between monomer and aggregate species. The trends observed are very similar to those of the π-stacked aggregates with an H-type parallel stacking mode which is rationalized by the molecular exciton model.[69] The aggregation of these HAT derivatives is also reflected in the fluorescence spectra. In 1,1,2,2-tetrachloroethane, a significant concentration dependence was observed due to the dynamic exchange between the monomer and aggregates species, as found in the UV-vis spectra. They also observed in ^{1}H-NMR line-broadening effects arising from the aggregation. By addition of trifluoroacetic acid-D_1, the broad peaks became sharp according to aggregate dissociation. Sharpening of the ^{1}H-NMR signals can be also appreciated at temperatures higher than 100 ºC indicating also aggregate dissociation at higher temperatures. Interestingly, a direct evidence for aggregation could be also obtained by MALDI-TOF mass spectrometry in which assemblies of three, four and even five molecules could be detected.

A similar study has been also reported by Wang et al. for **HAT** derivatives with tunable LUMO levels (**63-66**, Figure 9) where a growing tendency towards molecular aggregation with increased number of fused aromatic rings is observed.[56]

In the frame of a joint theoretical and experimental study, we investigated the aggregation behaviour in solution of the so-called **tri-HAT** derivative **60** (Figure 8) which has the same amount of fused aromatic ring as those systems described by Ishi-I (**57-58**, Figure 8) but containing six more nitrogen atoms in the conjugated backbone.[15] We investigated the electronic and molecular structure of these novel molecules bearing three fused **HAT** moieties and fully characterized them by means of optical and vibrational Raman spectroscopy, electrochemistry, solid state UV, inverse photoemission spectroscopy (UPS and IPES), and by comparison with quantum-chemical calculations. Concerning the aggregation in solution, concentration and temperature-dependent UV-vis and fluorescence measurements provide a similar behaviour to that reported by Ishi-I for HAT derivatives **57-58**

(Figure 8) with redshifted emission upon increased concentration. The molecular aggregation was investigated by QM/MM calculations on dimer models considering two different types of conformations, π-stacked and T-shaped arrangements, either with parallel or antiparallel dispositions. The energy profiles obtained predict that the antiparallel π-stacking interaction is the most stable conformation for **60** as well as for pristine **HAT**. This conclusion was also supported by photophysical data. Indeed, upon dimerization, the lowest excited energy level is expected to redshift in both parallel (perfectly co-facial) and anti-parallel configurations. However, the emission from this state in the parallel configuration is prohibited due to symmetry. Analyses of the different energy contributions indicate that electrostatic interactions are responsible for the stabilization of the antiparallel cofacial arrangement in relation to the parallel one in both **HAT** and **tri-HAT 60** dimers.

In 2014, Zhao and coworkers have used the ability of **HAT** derivatives for self-assembly to produce an unusual chiral amplification phenomenon in a very simple four component supramolecular system constructed by the coassembly of achiral hexa-2-pyridyl-HAT (**78**) with aminoacid derivatives **79-81** (Figure 11).[70]

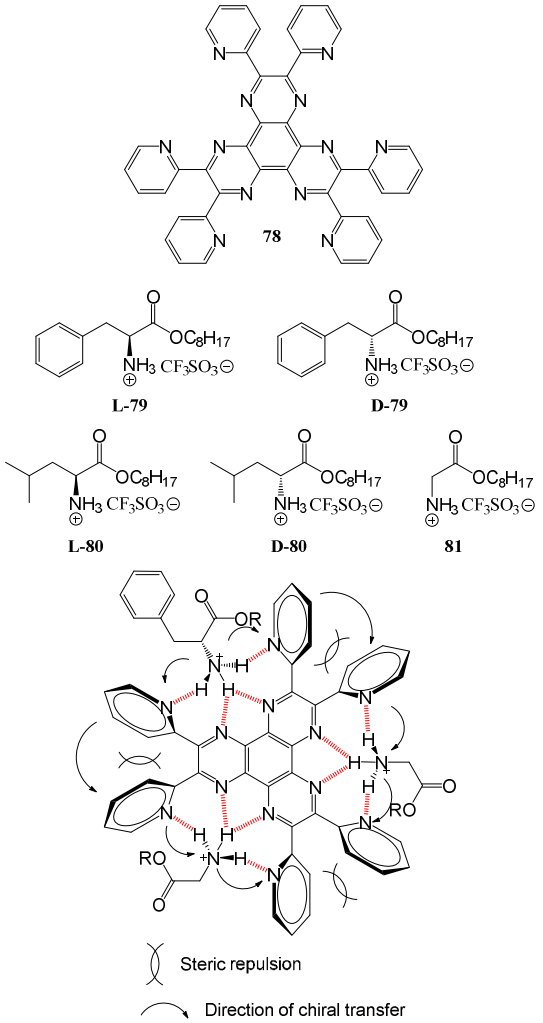

Fig. 11 top: chemical structures of achiral hexa-2-pyridyl-HAT (**78**) and aminoacid derivatives **79-81**. Bottom: Schematic illustration of the origin of the "sergeant-and-soldiers" principle on the basis of the transfer of chirality from the D-phenylalanine derivative to the other part of the complex.

The coassembly of achiral **HAT** derivative **78** and chiral aminoacids allow to construct propeller-like supermolecules driven by intermolecular hydrogen bonding. Both the "sergeants-and soldiers" principle and "majority-rules" effect are applicable in these discrete four-component supermolecules, which are the simplest supramolecular system ever reported that exhibit chiral amplification.

It can be concluded from these studies that the extension of the π-cores is a useful approach not only to tune the electronic properties of these materials but also to enhance their tendency for aggregation and even to participate in chiral amplification.

3.2 Self-assembly in the bulk. Liquid crystal behaviour and charge transport properties

Discotic liquid crystals (DLCs)[71, 72] have attracted the attention of many research groups since their discovery by Chandrasekhar in 1977[73] and many efforts have been made to exploit DLCs in organic electronic devices.[74]

Simple discotic mesogens such as triphenylene (**82**, Figure 12) derivatives have a more or less rigid planar core with typically six or eight flexible chain substituents laterally attached to the core.[66] Thus, in 1988 it was reported that 2,3,6,7,10,11-hexakis(hexylthio)triphenylene (**83**, figure 12) can order in a columnar liquid crystalline structure.[75]

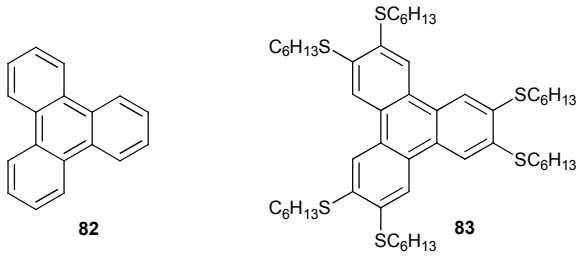

Fig. 12 Structure of triphenylene **82** and a mesogen triphenylene derivative **83**

This discovery was followed by the observation of a charge carrier mobility (μ) of μ = 0.1 cm^2 V^{-1} s^{-1} for **83** in the ordered columnar liquid crystal (LC) state which was the best value in that time for a non-crystalline organic compound.[76] By that time, the charge carrier mobilities of other mesogens based on hexabenzocoronene or phthalocyanine aromatic cores were also investigated [77] and values of μ as high as 0.1 cm^2 V^{-1} s^{-1} were reported for the columnar mesophase of hexabenzocoronene derivatives.[78] However, most of the discotic mesogens reported at that time were better hole carriers than electron carriers creating, therefore, the need for new electron acceptor discotic mesogens.

HAT, incorporating six nitrogen heteroatoms within a triphenylene core, is a good electron acceptor and therefore it was expected that it should facilitate electron injection and collection. Because of its structural similarity with triphenylene (**82**), **HAT** derivatives were then proposed as good candidates to be investigated as electron-deficient mesogens.

In 1985, Kohne and Praefcke synthesized a family of HAT derivatives endowed with alkyl and aryl functionalities (6c,6d,6g,6h, Scheme 2) with the aim to explore their liquid crystalline properties by analogy with the parent triphenylene analogues. However, liquid crystalline properties were not

observed by any of these compounds.[26] Although Bushby and coworkers reported the ability of HAT derivatives to enhance the mesophase ranges by mixing with triphenylene derivatives[79], seminal work in the development of liquid crystalline HAT derivatives was performed by Lehmann, Geerts and coworkers that, in a series of papers, investigated the mesophase characterization of discotic mesogens based on **HAT** derivatives (**52**, **53**, **84**, Figure 13).[46, 48, 80]

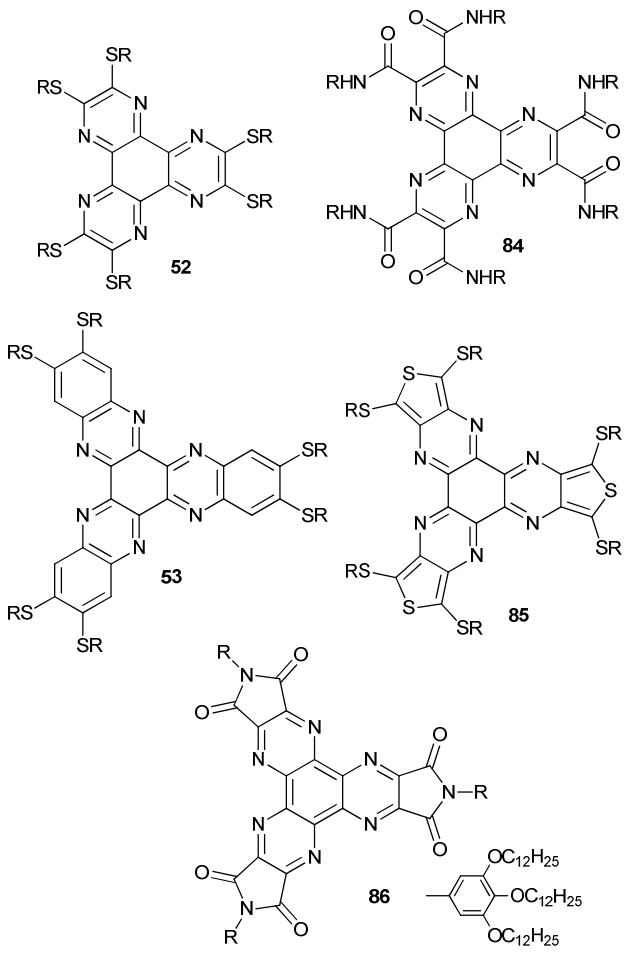

Fig. 13 HAT derivatives used to investigate their thermotropic liquid crystalline behavior

Surprisingly, it was found that hexathialkylhexaazatriphenylenes (**52**, Figure 13) do not form columnar LC phases like their corresponding triphenylene analogues, probably because of the large negative charges on the nitrogen atoms, which lead to the repulsion of the adjacent cores.[46] In **HAT** derivative **84** (Figure 13), hydrogen bonds were used to counterbalance and overcome this Coulombic repulsion, leading to the formation of a discotic mesophase with charge-carrier mobility ca. 0.1 $cm^2\ V^{-1}\ s^{-1}$, as determined by microwave conductivity measurements).[43] The amide hydrogen bonds serve as non-covalent "clamps" in the crystal phase of hexacarboxamidohexaazatriphenylene (**84**, R = H, Figure 13). The resulting interplanar distance is as short as 3.32 Å which is significantly smaller (3.50-4.00 Å) than the one that was found for other semiconducting columnar mesogens.

Meijer and coworkers synthesized hexaazatriphenylene-hexacarboxy triimide (**86**, Figure 13) which combines **HAT** as the acceptor core and 3,4,5-tridodecyloxyphenyl groups to introduce mesogenic character.[81] The electron deficient LC material shows photoinduced electron transfer with poly-3-hexylthiophene as a donor which would make it interesting to be tested in organic solar cells. However, to the best of our knowledge, there are so far no reports on organic solar cells fabricated with this **HAT** derivative.

HAT derivatives with alternating donor alkoxy side chains and nitrile acceptor substituents (**51b**, Scheme 14) have been also investigated as potential mesogens. Only the derivative with the longer hexyl chain exhibit liquid crystalline behavior. For this particular derivative the intracolumnar disk-to-disk distance is of 3.39 Å. The presence of the alkoxy groups in the electron deficient **HAT** nucleus over-rides the non existing π-complexation.[47]

In contrast with **HAT** derivatives **52**, the larger hexaazatrinaphtylene analogues (**53**, Figure 13) exhibit at least one LC mesophase before decomposition around 250 ºC[46, 48] which is in agreement with the enhancement in the tendency for aggregation with the extension of the π-cores as it was observed in solution. The electron mobility was found to be higher in the crystalline than in the liquid crystalline phases (helical phase), with maximum values of 0.9 and 0.3 $cm^2V^{-1}s^{-1}$ respectively.[82, 83] The difference in mobility between the LC and the crystal phases has been rationalized in terms of the order lost in the columnar mesophase due to the movements of the disks that can deform the columns preventing a correct electron jumping between them.

Similar **HATNA** derivatives with six decyloxy side chains have been also reported to show LC behavior and they have been used to investigate the orientational packing of this discotic mesogens when they are in a confined space, i.e., between two flat glass substrates. It is observed that the thermal state of the mesogen during molecular stacking is crucial for an conveniently oriented columnar aggregation.[84]

We have investigated the LC properties of **triHAT** derivatives **60** (Figure 8) with a two-dimensional expansion of the π-conjugated system.[85] The higher number of heterocyclic N atoms makes **triHAT** derivatives better electron acceptors than unsubstituted **HAT**. Derivatives with *n*-hexyl and *n*-decyl alkyl chains reveal mesomorphic properties, thus confirming the benefitial effect of conjugation extension in order to achieve liquid crystalline properties. However, the study of the mesomorphic properties of the **HAT** derivative with shorter alkyl chains was impeded by its decomposition before reaching its clearing point.

The mesogenic properties of a **HAT** analogue of **56**, in which the peripheral benzene rings were replaced by thiophene moieties (**85**, Figure 13), were also investigated[80] but it was found that the hexaalkylsulfanylhexaazatriisothianaphthene derivatives (**85**) do not show mesogenic properties. The authors rationalize this behavior in terms of Coulomb repulsion effects linked to the charge distribution found in the aromatic cores which could prevail over the stabilizing forces induced by van der Waals interactions.[80]

Ishi-I and coworkers demonstrated that the use of alkyl chains to obtain **HAT** derivatives is not necessary with LC properties. They report that HATs with six aromatic side chains (**87**, Figure 14) aggregate both in liquid crystalline and in organogel phases.[86]

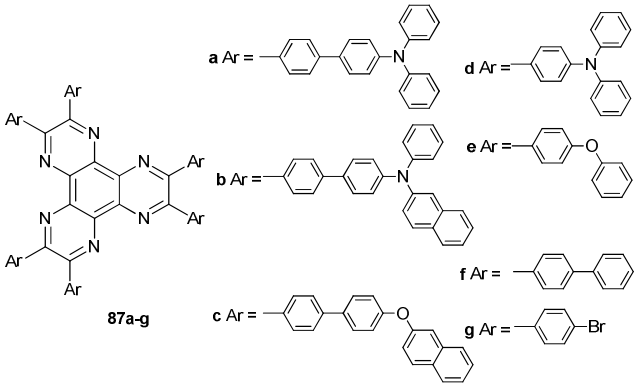

Fig. 14 HAT derivatives with aromatic side chains investigated as potential liquid crystal materials

In derivatives **87a-c**, the aromatic side chains with terminal flexible groups make up soft regions that cooperatively stabilize the liquid crystalline and organogel supramolecular structures together with the hard regions of the **HAT** core and therefore have crystalline behaviour with two-dimensional hexagonal packings. In contrast, the analogues with shorter aromatic chains did not show LC behaviour.

Chemical doping of discotic liquid crystals is well known and, in some cases, it produces enhanced mesophase ranges.[87] Hence, Bushby, Lozman and coworkers reported that substantially enhanced mesophase ranges can be obtained by mixing 2,3,6,7,10,11-hexakis(hexyloxy)triphenylene (**88a**, n = 6, Figure 15) with a **HAT** derivative with a larger polyaromatic core (**89**, Figure 15).[79] The special stability of these π-stacked systems is not the result of either charge-transfer or (net) quadrupolar interactions but instead arises from a complementary polytopic interaction (CPI). This strategy provides a tool in order to develop π-stacking tectons in supramolecular chemistry as an alternative to, for example, hydrogen bonds.[88] In this regard, formation of CPI compounds with triphenylene derivatives and **89** (Figure 15) can be used not only to enhance the mesophase range of triphenylene-based discotic liquid crystals but also to induce mesophase behaviour in non-mesogenic triphenylene derivatives,[89,90,91] to improve their conductivity and alignment properties,[89,92,93] to induce microphase separation in block copolymer systems,[91] and to order fullerene C_{60} molecules in helical columnar structures.[94]

Big efforts have been made in order to shed light, with the help of quantum-chemical calculations, on the nature of charge transport at the molecular scale in discotic materials based on **HAT** derivatives and to establish structure-transport properties relationships.[95,80,96,82,15] Charge transport in discotic liquid crystals is usually expected to correspond to a phonon-assisted hopping regime, as is the case in amorphous organic thin films[97] or molecular crystals at high temperature.[98] In such a regime, the charges are localized over a single molecule and jump from site to site to yield a current. A major parameter governing the charge mobility, be it in a (localized) hopping or (delocalized) band regime, is the transfer integral *t* which describes the strength of the interactions between adjacent molecules. Quantum chemical calculations demonstrate that the amplitude of the transfer integrals is strongly dependent on geometric fluctuations, in particular ring rotations and translations between consecutive molecules in the columns of the mesophase while an increase in the size of the conjugated core does not necessarily ensure better transport properties. Thus, charge mobilities result from a subtle interplay between the size, nature of the conjugated core and side chains, and relative positions of the molecules in the columns.[95,80]

Based on quantum-chemical calculations Brédas, Cornil and coworkers predicted a significant increase in the charge mobility when going from triphenylene to hexaazatrinaphthylene which was further confirmed by measurements carried out with the pulse radiolysis time-resolved microwave conductivity technique.[99] Kippelen, Marder and coworkers reported effective mobilities of 0.07 $cm^2V^{-1}s^{-1}$ for **HATNA** derivatives endowed with alkyl ester and pentafluorobenzyl ester side chains (**90**, **91**, Figure 16).[100] The effective charge carrier mobility was studied by the steady-state space-charge limited current technique. It is worth mentioning that this measurements were obtained from noncrystalline films. By using also the steady-state space-charge limited current technique, Chi and coworkers reported mobilities of 3.4 x 10^{-5} $cm^2V^{-1}s^{-1}$ for HAT derivatives end functionalized with dicarboximide groups (**92**, Figure 16).[101]

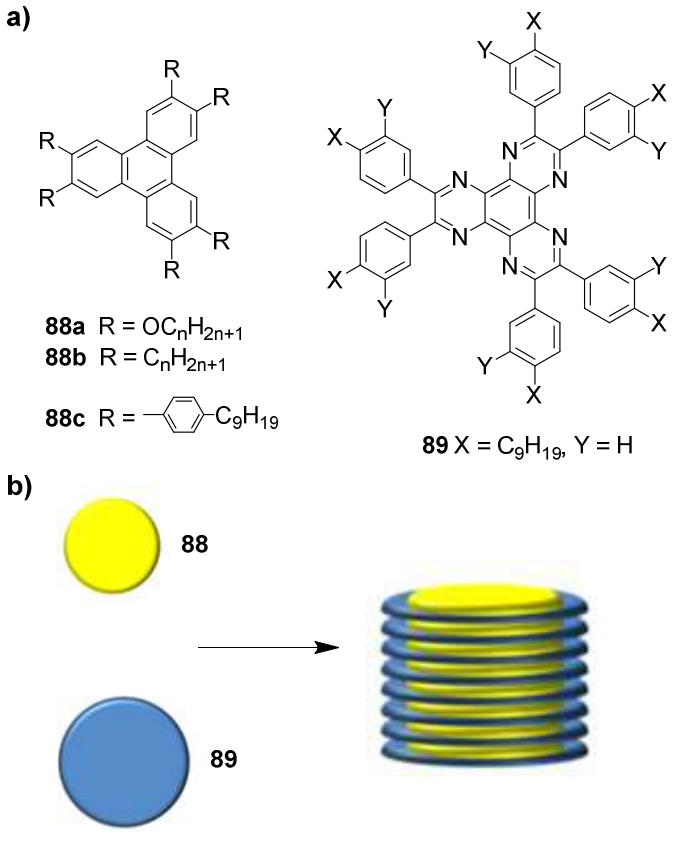

Fig. 15. a) Triphenylene (**88**) and **HAT** derivatives (**89**) that exhibit complementary polytopic interaction (CPI). **b)** Representation of the stacking of **88** and **89** in an alternating manner.

To the best of our knowledge, the highest mobility measured for a **HAT** derivative is 0.9 $cm^2V^{-1}s^{-1}$ measured using the pulse-radiolysis time-resolved microwave conductivity technique for hexa(alkylsulfanyl) **HATNA** derivatives (**56**, R = $C_{10}H_{21}$ and $C_{12}H_{25}$ Figure 13).[82] This mobility was observed for the columnar solid phase while a mobility of 0.3 $cm^2V^{-1}s^{-1}$ was measured in the liquid crystalline state. Due to the different techniques employed, the mobilities of **56** cannot be directly compared to the above mentioned mobilities for other **HAT** derivatives. It is observed that along the columns, mesogens do not pack in an eclipsed conformation and therefore adjacent molecules are rotationally or translationally displaced. Interestingly, it is observed that the side-chains have a strong

influence on the intracolumnar ordering of these molecules which contrasts with the results of studies on larger discotic molecules, such as hexabenzocoronenes,[78] for which the mobilities in the LC phase are found to be primarily independent of the side chains. Futhermore, transition temperatures above 200 ºC were too high for practical use.

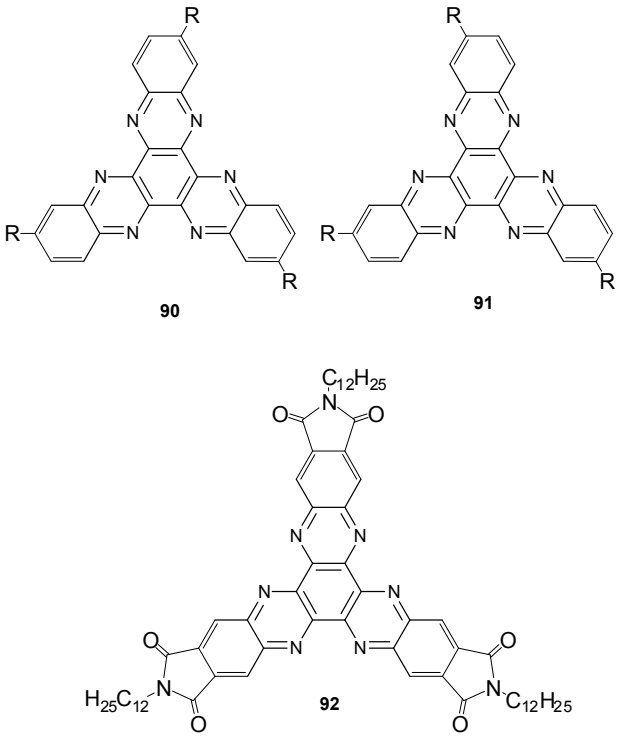

Fig. 16 HATNA derivatives used to measure charge carrier mobilities

In 2014, Hanna and coworkers have synthesized a series of self-organizing *n*-type hexaazatrinaphthylenes with various bay-located side chains (**93-95**, Figure 17) which are able to form long-range molecular columns with self-directed growth directions. [102]

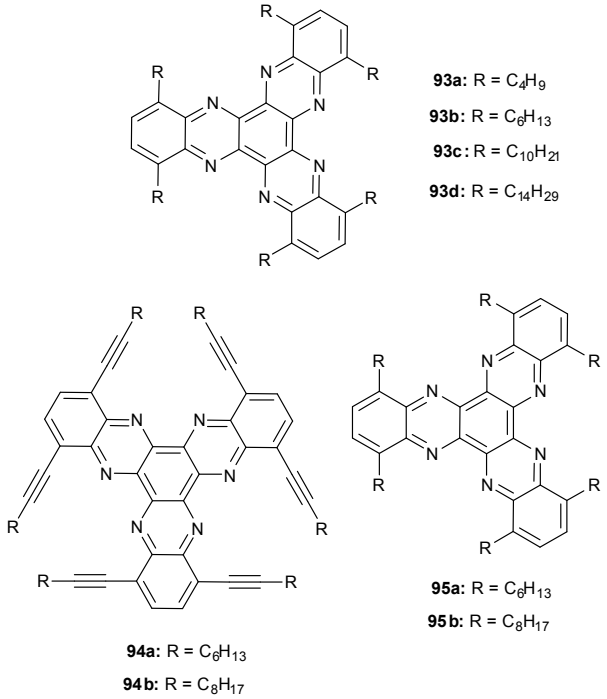

Fig. 17 Bay-substituted **HATNA** derivatives used to measure charge carrier mobilities

In particular, alkyl substituted **HATNA**s organize themselves as "in plane" molecular columns with axes parallel to substrates, whereas the columnar orientation of the **HATNA**s with alkylethynyl or alkylthio groups strongly depends on the side chains (Figure 18). Interestingly, the derivative with octylthiochains exhibits "out-of-plane" molecular columns, in which electron mobility of up to 10^{-3} $cm^2V^{-1}s^{-1}$ was determined by the time-of-flight technique, highlighting the fact that such molecular columns based on bay-substituted **HATNA**s are promising *n*-type semiconductors for electronic device applications.[102]

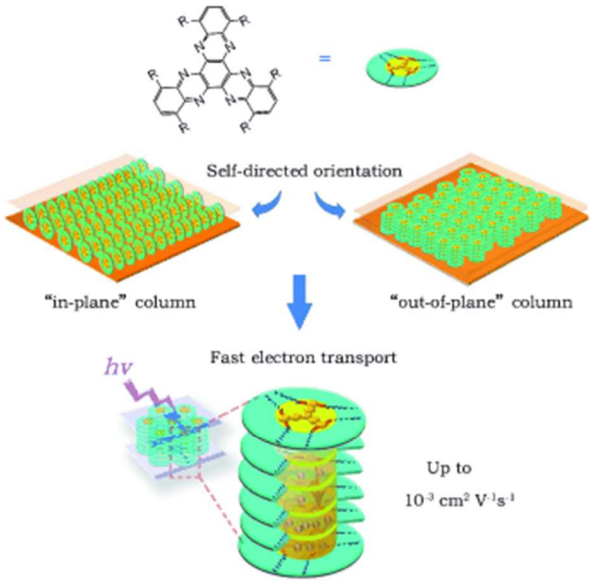

Fig. 18 Schematic diagram representing "in plane" and "out of plane" molecular columns with the fastest electron transport observed for the "out-of-plane" molecular columns. Reproduced from Ref. 102. Copyright 2014 Wiley-VCH Verlag GmbH & Co. KGaA, Weinheim

Thus, it has been already demonstrated that the electron deficient core of **HAT** facilitates the electron carrier transport and, by selecting appropriate substituents at specific locations, it is possible to achieve long-range molecular columns for fast charge transport.

3.3 Self assembling on surfaces

Assembly of individual molecules and formation of molecular nanostructures on surfaces have attracted increasing attention as molecular and nanoscale engineering becomes an integral part of miniaturization in electronic and photonic devices.[68] With this aim, in the last recent years some efforts have been devoted to investigate the molecular self-assembly of **HAT** derivatives on solid surfaces.[103,104,105,106,106] Molecular self-assembly on solid surfaces is an intricate process involving a balance between adsorbate–adsorbate and adsorbate–substrate interactions and therefore different morphologies have been observed depending on the investigated **HAT** derivatives and substrates.

Samori and coworkers reported on the structural and electronic properties of *N*-(2-ethylhexyl)-substituted hexacarboxamido-hexaazatriphenylene (**84**, R = 2-ethylhexhyl, Figure 13) physisorbed on surfaces.[107] On electrically conductive substrates such as highly oriented pyrolitic graphite (HOPG), scanning tunneling microscopy (STM) investigations at the solid/liquid interface highlighted the formation of ordered monolayers with molecules assembled face-on with respect to the basal plane of the surface forming rows of dimers of the molecule in an oblique (near to rectangular) 2D lattice (Figure 19a). Furthermore, Kelvin probe force microscopy experiments (KPFM) showed that the surface potential in multilayered samples was 4.53 eV. This estimation is of fundamental importance in molecular electronics because it enables the elucidation and correct tuning of differences in energy levels between molecular nanostructures and electrodes, thereby allowing optimization of charge injection.

Ha and coworkers reported their STM investigations on the morphological behavior of 1-2 monolayers (ML) of unsubstituted **HATNA** (Scheme 1) deposited on Au(111).[104] The first ML consisted of molecules flat on the surface (Figure 19b), arranged in one of three different ordered phases depending on annealing parameters. Regardless of phase, the substrate influences the spatial charge distribution in the organic layer, as evidenced by the visibility of the Au(111) reconstruction features. The substrate-molecule interaction is weak because the desorption temperature is relatively low and ordered multilayers are not formed.

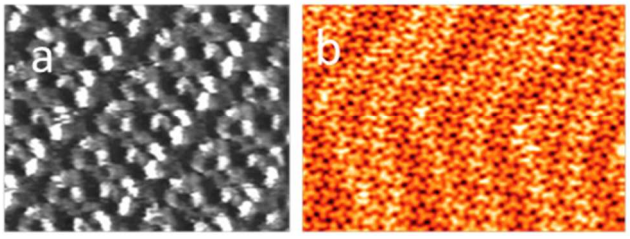

Fig. 19 STM image of a) *N*-(2-ethylhexyl)-substituted hexacarboxamido-hexaazatriphenylene (**84**, R = 2-ethylhexhyl, Figure 13) at the tetradecane/HOPG interface. Reproduced from Ref. 107 Copyright 2006 Wiley-VCH Verlag GmbH & Co. KGaA, Weinheim. b) **HATNA** on Au(111). Reprinted with permission from *J. Phys. Chem. C*, 2007, 111, 10493-10497. Copyright 2007 American Chemical Society

Shortly after these studies, Xu et al. reported on the investigation and control of the orientation of **HATNA** derivatives on surfaces by tailoring the molecular structures and through the adjustment of external stimuli.[108] They demonstrated that it is possible to adjust the strength of the adsorbate–substrate interaction by changing the surface charge density and to subsequently form tunable assembled structures on the substrate surface (Figure 20). For this purpose, they use electrochemical scanning tunneling microscopy (ECSTM) which is a tool that effectively combines STM with electrochemical techniques.[109] They were able to induce that **HAT** molecules organize in flat or vertical orientations on the Au(111) surface by applying electrode potentials. The possibility of tuning the molecular orientation on surfaces has been proposed as an approach to build nanostructures or thin films with controllable molecular orientations for electronic applications.

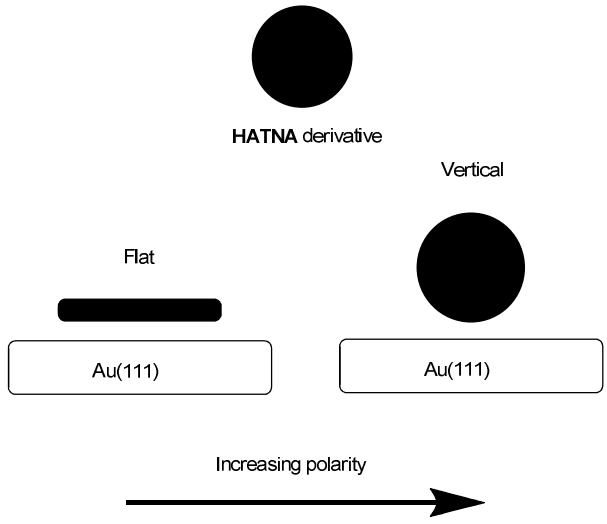

Fig. 20 Schematic diagram of the orientational transition of **HATNA** derivatives on Au(111) with varied electrode potentials.

Ha and coworkers have probed by STM the Layer-by-layer growth of tris{2,5-bis(3,5-bis-trifluoromethyl-phenyl)-thieno}[3,4-*b*,*h*,*n*]-1,4,5,8,9,12-hexaaza-triphenylene (THAP, **96**, Figure 19) on Au(111)[106] because of its interest as electron transport material.[110-112] They show that at least 4 parallel ordered monolayers can be grown where the molecules align parallel to the surface and, at least the first three monolayers, have a bidimensional hexagonal close packing (hcp, figure 21, left). Thus, in the growth from the first to fourth monolayers, each layer induces the order and lattice vector directions of the successive layer.

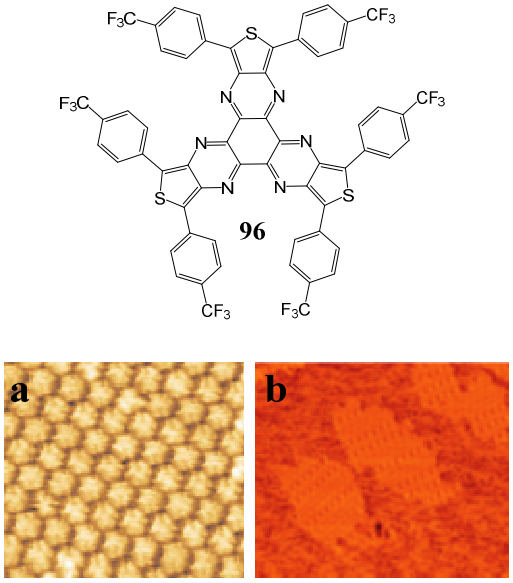

Fig. 21 Chemical structure of THAP (**104**) and STM images of a) one monolayer of **96** on Au(111) (Reprinted with permission from S. D. Ha, Q. Zhang, S. Barlow, S. R. Marder, and A. Kahn. *Phys. Rev. B*, 2008, 77, 085433. Copyright 2008 by the American Physical Society) and b) submonolayer coverage of **96** on Ag(110). Reprinted with permission from *J. Phys. Chem. C*, 2008, 112, 9803–9807. Copyright 2008 American Chemical Society.

The above shown assemblies of individual molecules on surfaces have been investigated on "nonreactive" substrates such as Au or HOPG with which molecules interact relatively weakly. However, Salomon and coworkers have also studied the balance between molecule–substrate and molecule–molecule interactions for THAP **96** (Figure 21) and different metals. First, the electronic properties of **96** films deposited layer by-layer on medium and high work function metallic substrates (Ag and Au) was investigated by means of ultraviolet and X-rays photoemission spectroscopies. With Ag(110) a charge transfer occurs from the metal to the LUMO of the **96** molecule, leading to the occupation of a new interface gap state. No evidence of charge transfer or chemical reaction is observed for **96** adsorbed on Au(111) which indicates a weaker interaction.[111]

Following this study, the structural aspects of the adsorption of THAP **96** (Figure 21) on a clean Ag(110) surface was also investigated via STM showing that the molecule–substrate interaction plays also an important role as well in defining the structure of the full monolayer.[106] In contrast with the 4 parallel ordered monolayers of **96** grown on Au(111), small adjacent islands were observed when **96** was evaporated on Ag(110) (Figure 21). While intermolecular van der Waals forces dominate in the Au(111) case, a stronger molecule–substrate chemical interaction occurs in the Ag(110) case.

The ability for self-assembling together with the versatility of functionalization and electrochemical characteristics of HAT derivatives make these materials good candidates for further development of self-organized nanostructures on surfaces.

3.3 Nano and microstructures built by Self assembly

Nanoscience has experienced a spectacular rise in the last two decades stimulated by advances in the synthesis and interdisciplinary investigation of the properties of lowdimensional nanostructures and nanomaterials in which at least one of the dimensions falls in the 1-100 nm.[113] In this context, the supramolecular self-assembly of small organic molecules into well-defined micro/nanowires or micro/nanobelts represents a simple, efficient approach to the construction of micro/nanostructures with high aspect ratios.[114] With this aim, **HAT** derivatives have been chosen as the basic scaffold because of its excellent π-π stacking ability, as well as attractive electro-optical properties.

Jen and coworkers reported the first example of nanostructures based on **HAT** derivatives by patterning robust self-assembled alkylamide-tethered **HATNA** derivatives (**97, 98**, Figure 22) into nanorods and nanowires by microcontact printing.[115] Compound **97** has good solubility in $CHCl_3$; however, it gels easily in mixed solvents such as $CHCl_3$/hexane (v/v) 1:1) owing to enhanced amide-amide hydrogen bonding in a less polar environment. A morphological study reveals that **97** forms self-organized nanowires with a diameter of ~20 nm and a length over 10 μm in the gel.

The self-assembling properties of **98** are very different from those of **97** in $CHCl_3$. The introduction of π-conjugated diacetylene groups further enhances the π-π stacking between the molecules. The shortened flexible alkyl groups also reduce the solvation of the molecules in $CHCl_3$. As a result, the binding force between the molecules increases, and they start to aggregate at a lower concentration. Furthermore, the diacetylene units in **98** can be used for the fixation of the supramolecular nanowires by photo-cross-linking produced by exposing the self-assembled nanowires to a 18 W UV lamp. In addition, the microcontact printing[116] has been used to form patterns of nanowires and nanorods of **98**. The self-assembled nanostructures were first spin-coated onto a patterned polydimethylsiloxane (PDMS) stamp, which was then allowed to generate conformal contact with a SiO_2/Si substrate for 30 s to transfer the nanostructures to the surface. These nanostructures could be directly transferred to SiO_2/Si substrate without the need of any surface modification, and they formed robust patterns after postpolymerization by UV treatment (Figure 22).[115]

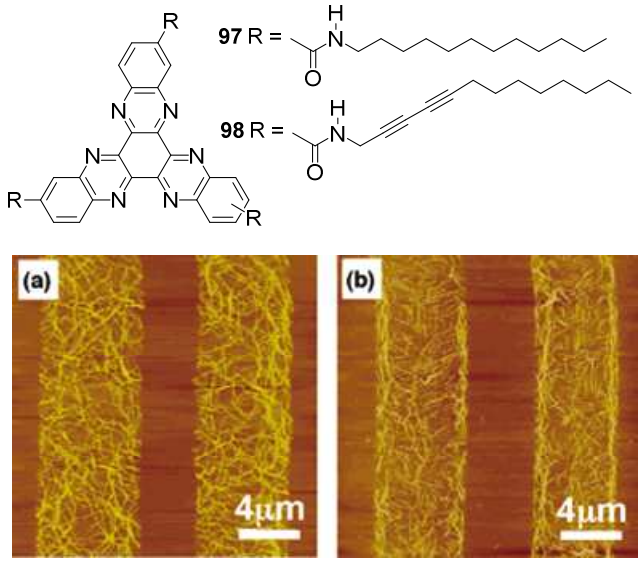

Fig. 22 Chemical structure of alkylamide-tethered **HATNA** derivatives (**97, 98**) and AFM images of (a) nanowires and (b) nanorods pattern of **98** on SiO_2/Si fabricated by microcontact printing. Reprinted with permission from *J. Am. Chem. Soc.,* 2006, 128, 13042-13043. Copyright 2006 American Chemical Society.

Li and coworkers have reported the fabrication of microbelts through the coassembly of hexa-2-pyridyl-hexaazatriphenylene (**78**, Figure 23) with primary alkyl ammonium triflate. The strategy was first to construct hydrogen-bonded complexes between **78** and primary alkyl ammoniums to mimic covalently bonded π-core alkyl chain structures, and then the complexes self-assembled into microbelts driven by π-π stacking in the π core and van derWaals interactions between the peripheral alkyl chains.[117]

No well-defined aggregates could be observed from the sample obtained from a chloroform solution of **78** indicating that the π core itself was not a good building block for self-assembly. This suggests that a side chain might be necessary to promote ordered aggregation. However, when n-dodecyl ammonium triflate (DAT) was introduced into a solution of **78** in chloroform, flocculent material precipitated out after standing for several minutes. A SEM image revealed that it consisted of well defined microbelts of 1 to 2 μm in width and tens of micrometers in length. The formation of a stable hydrogen-bonded **78**-alkyl ammonium complex is believed to be the condition for this sequential self-assembly process, through which the complex could further self-assemble into microbelts (Figure 23). This approach might offer a promising way to construct novel supramolecular architectures via the coassembly of simple components without the need to synthesize supramolecular building blocks with complicated chemical structures.

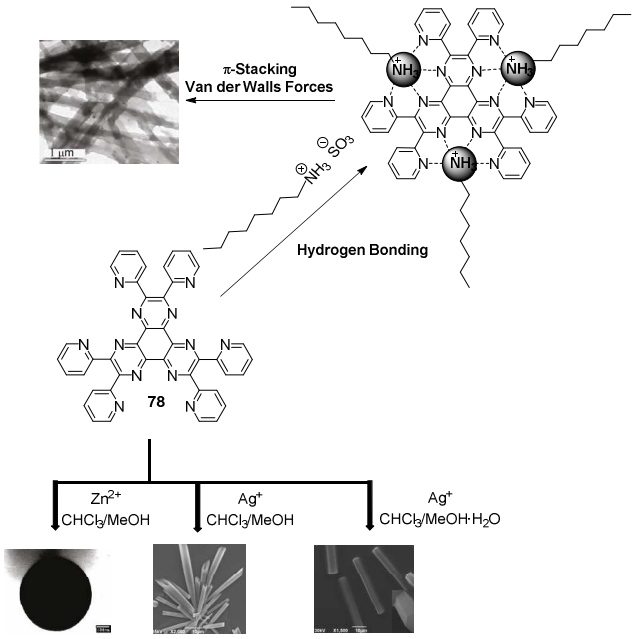

Fig. 23. Chemical structure of hexa-2-pyridyl-hexaazatriphenylene (**78**), its hydrogen bonding complex with n-dodecyl ammonium triflate (DAT) and TEM images of microbelts fabricated from the **78**/DAT mixture (Upper part). On the lower part are represented (left) the TEM image of the microspheres constructed from the **78**/Zn^{2+} mixture, (middle) and the SEM image of **78**/Ag^{+} microtubes and (right) SEM image of **78**/Ag^{+} microrods. Adapted with permission from *Langmuir*, 2010, 26, 13048-13051 and *Chem. Mater.*, 2011, 23, 1505-1511. Copyright 2010 and 2011 American Chemical Society.

Li and coworkers have also described the construction of three well-defined discrete microstructures—microspheres, microtubes, and microrods— that have been fabricated through metalorganic coordination between hexa-2-pyridyl-hexaazatriphenylene (**78**, Figure 23) and different transition metal ions.[118] It is interesting to point out that deriving from the same organic unit, the resulting microspheres and microtubes (microrods) exhibit dramatic difference in dimension (0D vs 1D) as a result of different coordination manners of zinc and silver with **78** because of different coordination numbers and size and also by processing the coordination in different solvents.

The approaches described above represent promising methods to construct self-organized molecular assemblies in a tunable way and prove the suitability of HAT derivatives as a π core to build nano and microsutructures.

4. HAT-CN, a special case of study

1,4,5,8,9,11-Hexaazatriphenylene hexacarbonitrile, or **HAT-CN** (IUPAC name: Dipyrazino[2,3-f:2',3'-h]quinoxaline-2,3,6,7,10,11-hexacarbonitrile, **11**, Scheme 3), is a cyanoazacarbon, $C_{18}N_{12}$, first reported by Czarnik and co-workers.[30, 119] It is a strong electron-deficient discotic heterocyclic molecule with a deep-lying lowest unoccupied molecular orbital (DL-LUMO) level (~5.1 eV) and therefore a large electron affinity that acts as an electron-accepting unit. One consequence of this is that it avoids self π-complexation in its neutral form. In fact, in **HAT-CN** crystals, obtained from a methanol/acetonitrile mixture, the planar **HAT-CN** molecules do not align in a parallel manner via π–π stacking, but rather form a staircase-like chain motif with a perpendicular arrangement. The intermolecular spacing is 3.75 Å, which is larger than the expected van der Waals radii sum of 3.54 Å. The overall crystal packing is mainly dominated by CN-π interactions which leads to a complicated, but highly symmetric, 3D hexagonal arrangement.[120, 121] Through this weak intermolecular interaction the self-π-complexation can be avoided, which helps to preserve the large molecular electron affinity in the solid state.[120]

Concerning with its electrochemical behavior, three reductions steps are typically seen in cyclic voltammetry measurements.[122] Although these three reductions are more or less reversible, depending on the conditions, the voltage separation is sufficient for three distinct species to be identified that at appropriate fixed potentials by spectroelectrochemistry. Upon treatment with tetra-*n*-butylammonium oxalate, **HAT-CN** is reduced, leaving **[tetra-n-butylammonium][HAT-CN]** salt and CO_2 gas. Magnetic susceptibility measurements on this salt show its ferromagnetic behavior with an estimate Curie temperature of Tc ~ 3K. In contrast with the staircase-like chain motif with a perpendicular arrangement observed for neutral **HAT-CN**, the molecular structure of **[tetra-*n*-butylammonium][HAT-CN]** is dominated by the stacking of the **HAT-CN** radical anions which form π-stacked pairs at the remarkably short distance of 3.110Å. The pair of anions is rotated by 60° with respect to each other, which allows the staggering of the nitrile groups even though the rest of the atoms are almost fully eclipsed with a slip distance of only 1.457Å. Each close pair is in turn slip-stacked with respect to its neighboring pairs, with an approximately half-molecule slip, or step, of 5.837Å between adjacent pairs, and a somewhat longer interplanar spacing of 3.302 Å between the slipped pairs (Figure 24). These closely associated pairs of ions are likely responsible for the low temperature ferromagnetism.[123] Dunbar and coworkers investigated also the ability of reduced forms of **HAT-CN** to be used as ligands. Most binary compounds of the first row transition metals with discrete or extended polymeric structure exhibit paramagnetic behavior with the exception of a polymeric [**Cu-HAT-CN**] phase which behaves as a canted antiferromagnet

below 6 K.[120] No structural information was provided for this system. In spite of these observations, the magnetic properties of **HAT-CN** derivatives remain still relatively unexplored. Kitagawa and coworkers demonstrated the effect of the coordination mode of the oxidation states of HAT-CN that can be achieved through a self-assembly process with copper(I) ions and ferrocene derivative coligands. Interestingly, it is observed that the coordination mode of HAT-CN exerts a drastic effect on its reduction potentials through the "normal" effect of σ polarization.[124]

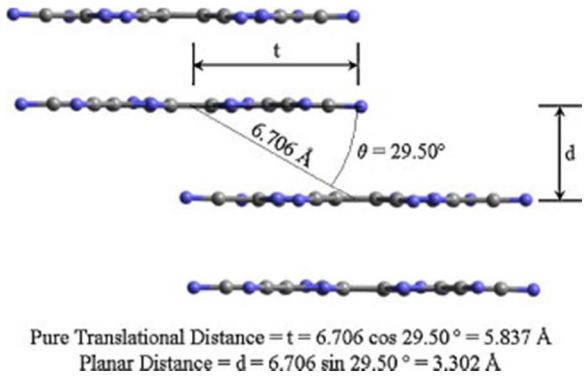

Fig. 24. Vectors between adjacent pairs of $HAT(CN)_6$ anions. Reproduced from *Synthetic Met.*, 2009, 159, 1667-1671. Copyright 2009, with permission from Elsevier.

Concerning with its optical properties, **HAT-CN** has a wide band gap of 3.3 eV and it is therefore highly transparent in the visible spectral range.[125] Thus, the UV/vis absorption spectrum shows an onset at ~370 nm (3.35 eV) and a peak at 320 nm (3.88 eV). Furthermore, **HAT-CN** is characterized by an infrared band at 2243 cm^{-1} (C≡N).[126]Another interesting features of **HAT-CN** are its good hole injection characteristics,[126,126,127,128] and its low refractive index of about 1.7 in the visible wavelength.[129] It has very high stability even under ambient air conditions and it can be thermally evaporated at a low temperature below 300 ºC in vacuum.[129]

Furthermore, it has been found that **HAT-CN** is selectively soluble in 2-propanone and is insoluble in other solvents commonly utilized for solution processing (such as toluene, chlorobenzene, 1,2-dichlorobenzene, 1,2,4-trichlorobenzene, chloroform, and 1,2-dichloromethane). This unique characteristic facilitate its use as a universal hole-injection layer in multilayer solution-processed devices.[130]

Electron mobility in thin films of **HAT-CN** has been found to be $\mu_e \sim 10^{-4}$ cm^2/Vs as determined by time of flight measurements.[123]

Because of all this features, **HAT-CN** has found interest for a variety of studies and applications that will be summarized below.

4.1 HAT-CN for (opto)electronic applications

Organic semiconductors have been developed vastly in the past decades as materials for organic (opto)electronic applications due to their numerous advantages such as low cost, mechanical flexibility or versatility of chemical design and synthesis. Organic semiconductors are intensively used as active thin films and electron and hole transporting materials in (opto)electronic devices such as light-emitting-diodes (OLEDs),[131] solar cells (OSCs),[132] organic field-effect transistors (OFETs) and sensors.[133]

Recently, transition metal oxides (TMOs) or organic dopants possessing a deep lying-LUMO level have received significant attention for their powerful roles in organic semiconductors. TMOs or organic dopants increase the conductivity and carrier density of organic films when they are doped in an organic semiconductor.[134] In addition, thin layers of the materials can enhance the injection efficiency of charge carriers from the electrode to the organic layer by adjusting the work function of the electrodes[135,136] including carbon nanotube electrodes.[137] Furthermore, **HAT-CN** has some additional advantages as the low refractive index (1.7) which is lower than that of other TMOs, and it effectively protects organic layers below the **HAT-CN** layer from sputtering damage during the formation of a transparent electrode.[129] In contrast to TMOs, **HAT-CN** is highly conductive and transparent, even in layers that are several tens of nanometers thick, thereby minimizing the optical and electrical power loss and improving the performance of organic electronic devices. Thus, also naked **HAT-CN** layers have been widely used in place of doped layers because of the good electrical properties of pristine **HAT-CN** layers.[138,139] The molecular alignment and nanostructure of **HAT-CN** thin films on organic surfaces has been investigated. **HAT-CN** molecules have been found to stack with a $(001)_{hex}$ preferred orientation on different organic surfaces and the orientation is maintained with increasing thickness.[138] Even more interestingly, because the electronic properties of organic electronic devices depend strongly on the specific electrode-semiconductor interface, some efforts have been also devoted to investigate the layer growth, thermal stability and desorption behavior of **HAT-CN** on different electrodes. It has been found that, in contrast to growth on organic surfaces as indicated above, the thermal stability and preferred orientation of the **HAT-CN** molecules is related to the thickness of the film and the nature of the electrode substrate.[140,141]

Thus, the role of **HAT-CN** either as dopant or as naked layers has been tested in the following devices:

*4.1.1. **HAT-CN** in organic light emitting diodes (OLEDs)*

Conventional OLEDs are formed by selected organic materials (sometimes consisting of several layers) deposited between two electrodes. Usually the organic layers consist in an emitting layer (EML) between an electron injection layer (EIL) and a hole injection layer (HIL).(Figure 25).

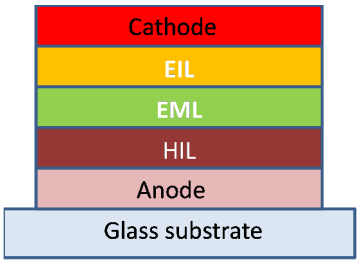

Fig. 25 Schematic structure of a conventional OLED

Optimized carrier injection from the electrodes to the emitting layer is usually desired, with the goal of manufacturing efficient and reliable organic light-emitting diodes (OLEDs). In general, large energy barriers between the organic emitting materials and the electrodes will cause high operation voltage, low electroluminescence (EL) efficiency, and fast degradation in OLEDs. One efficient strategy in order to enhance hole injection and lower operation voltage in OLEDs involves the use of a doped hole-injection layer HIL (Fig. 25) which is typically made

by doping a strong electron acceptor material (*i.e.*, p-type dopant), in a hole transport material to generate free charges in the injection transport layer.[127, 142-144] The enhanced electroluminescence performance is attributed to the formation of charge transfer complexes in doped organic host materials through electron transfer from organic molecules to the dopants.[145] In this respect, **HAT** has been successfully used as a highly efficient *p*-type dopant with common hole transport materials in OLEDs and compared favorably with inorganic dopants in terms of power efficiency, half lifetime and lower temperatures for thermal evaporation.[145-148]

An alternative strategy to optimize hole injection barriers comprises the use of basic **HAT-CN** layers in place of doped layers.[149] It has been found that such **HAT-CN** acceptor interlayers significantly reduce the hole injection barriers for organic semiconductors. With this aim, HAT-CN has been successfully employed as interlayer in different OLED architectures[150,151,151,152,146] including multi-stacked,[153,154] inverted,[128,129,155] tandem, [126,126,156,157] p-i-n[158] and phosphorescent OLEDs.[159-166] Thus, this approach proved to be very useful to improve the driving voltage of OLEDs, avoiding the more complex processing of doping layers.

*4.1.2. **HAT-CN** in organic solar cells (OSCs)*

Intensive work is currently done in search of high efficiency solar cells with low-cost fabrication. In this respect, in recent years, there has been a growing interest in organic-based photovoltaic technology. Organic semiconductors show great promise owing to their synthetic variability, low-temperature processing, and the possibility of producing lightweight, flexible, easily manufactured, and inexpensive solar cells.[167, 168, 169]

HAT-CN has been used in both small-molecule-based and semiconducting polymers-based organic photovoltaics. Thus, the efficiency of a copper phthalocyanine (CuPc):C_{60} based Organic Solar Cells (OSCs) can be improved by using a hole- transporting **HAT-CN** templating layer at the ITO anode that results in an ordered, vertical standing CuPc morphology. **HAT-CN** induces an ordered vertical phase in contrast to the more conventional flat lying orientation using strongly binding templates such as perylene-3,4,9,10-tetracarboxylic dianhydride (**PTCDA**).[170] This reduces the layer resistance to charge transport between the CuPc donor and the ITO anode, thereby significantly increasing both short circuit current (J_{sc}) and field factor (FF) and hence the cell power conversion efficiency (PCE).

HAT-CN has been also used as electron conducting window layer for separating the photoactive region from the cathode in organic small-molecule-based p-i-n type solar cells. The use of **HAT-CN** in this type of devices was prevented by its exceptionally high electron affinity, estimated 4.8 eV, which introduces an electron injection barrier to the photoactive acceptor material C_{60}. Nevertheless, the introduction of doped and undoped C_{60} intermediate layers efficiently removes the injection barrier and allows for using **HAT-CN** as window layer in small-molecule-based p-i-n type solar cells.[171]

The use of **HAT-CN** as the organic interlayer for hole collection at the anode in semiconducting polymer-based organic photovoltaics has been also demonstrated. Thus, the open circuit voltage (V_{OC}), FF and power conversion efficiency of inverted OSCs based on poly(3-hexylthiophene)(P3HT): [6,6]-phenyl C61-butyric acid methyl ester (PCBM) can be greatly improved by inserting a **HAT-CN** interlayer between the active layer and the cathode.[172]

The above examples show the relatively unexplored possibilities of **HAT-CN** to improve the performances of OSCs.

*4.1.3. **HAT-CN** in organic field effect transistors (OFETs)*

Due to the potential applications in integrated circuits for large area, flexible, and ultralow-cost electronics, organic field-effect transistors (OFETs) have received much attention all over the world.[173] Although the performance of *n*-type OFETs has improved in last recent years, compared to *p*-type semiconductors, fewer *n*-type semiconductors have been investigated.[55] Thus, because of the *n*-type character of **HAT-CN**, irts performance in OFETs has been investigated. A mobility of 2.5 x 10^{-4} cm^2/Vs with an ON/OFF ratio of up to 2 x 10^4 has been measured at room temperature in a bottom-contact n-channel OFET with SiO_2 dielectric and gold drain/source electrodes.[174]

HAT-CN has been also investigated in magnetoresistive field effect transistors. The phenomenon of organic magnetoresistance, usually abbreviated to OMAR, refers to the change in electrical resistivity in sandwich structures of nonmagnetic metals and organic materials under a magnetic field.[175] The OMAR phenomenon has been studied in various organic materials with the aim to address fundamental questions about spin transport and spin manipulation in organic materials, but also because of its promising potential for the construction of lightweight, flexible, and multifunctional electronic devices without the use of ferromagnetic compounds.[176]. Until recently, OMAR was nearly always analyzed in two terminal devices. For a deeper understanding of OMAR, it is of high importance to explore this phenomenon in organic field-effect transistors (OFETs), because this (three-terminal) device geometry allows the verification of the charge carrier sign in the conducting channel as well as the determination of the corresponding mobility. In 2012, Saragi and coworkers reported for the first time on magnetoresistive field effect transistors sensitive to ultrasmall magnetic fields (< 5 mT) by using a charge transport layer achieved by mixing **HAT-CN** as a strong electron acceptor and 2,2',7,7'-tetrakis-(*N*,*N*-di-*p*-methylphenylamino)-9,9'-spirobifluorene (spiro-TTB) as electron donor (Figure 26).[177]

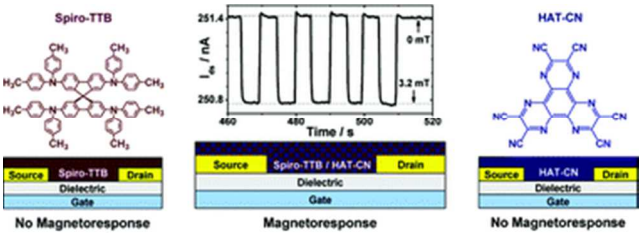

Fig. 26 Schematic representation of the experimental schemes reported in Ref. 177. On the left and right side, non-magnetoresistive field-effect transistors based on *p*-type Spiro-TTB and *n*-type **HAT-CN**, as well as the corresponding chemical structures, are shown. Devices with a mixture of Spiro-TTB and HAT-CN show a significant response to an external magnetic field of 3.2 mT (depicted in the middle). Reproduced from Ref. 177 with permission from The Royal Society of Chemistry

This blends leads to a high density of coulomb-correlated Intermolecular Radical Pair (IRP) states with magnetic-field-dependent formation, dissociation and interaction rates. The amount of IRP states can be tuned by changing the blending composition and, as a result, the magnetoresponse of the devices can be adjusted as well. Thus, the use of **HAT-CN** in donor-acceptor blends in organic semiconductor devices is a powerful tool to fabricate magnetoresistive devices.

*4.1.4. Noncovalent functionalization of graphene with **HAT-CN** for the design of conductive graphene electrodes with tailored work function*

It has been demonstrated that the electronic properties of graphene can be tuned by metal doping or chemical modification. However, it has been shown that the induced structural defects produced by these modifications can easily destroy the excellent properties of graphene, especially its high carrier mobility.[178] On the contrary, noncovalent functionalization, through physisorption of electron withdrawing/donating molecules on the graphene surface, has been reported to be a simple and effective scheme to nondestructively dope graphene.[179] Chen and coworkers have recently performed density functional theory (DFT) calculations to assess the electronic structure of graphene overlaid with a monolayer of electro-active conjugated molecules including **HAT-CN**. Calculations show that **HAT-CN** adopts AB-stacking and keeps its planar geometry when adsorbed on graphene; there is no significant distortion of graphene with a rumpling of less than 0.1 Å; the mean distance between graphene and **HAT-CN** is around 3.2 Å (Figure 27). Interestingly, the noncovalenet functionalization results in a work function modification that scales with the electron transfer from graphene, in line with the formation of an interfacial dipole. The use of the Boltzmann transport equation combined with the deformation potential theory shows that large charge carrier mobilities are maintained upon noncovalent functionalization of graphene, thereby suggesting that molecular doping is an attractive approach to design conductive graphene electrodes with tailored work functions.

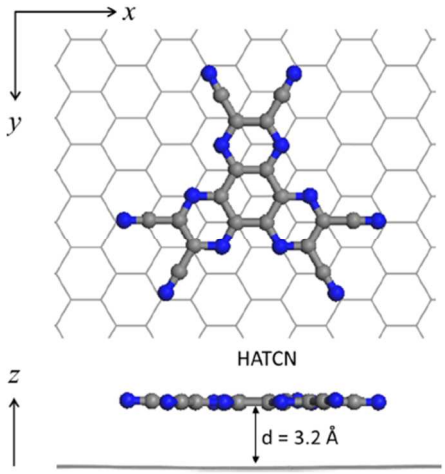

Fig. 27 Top and side view of the most stable configuration of **HAT-CN** adsorbed on graphene. *x*–*y* plane is the graphene plane, and *z* is normal to the graphene plane. Adapted with permission from *J. Phys. Chem. Lett.,* 2013, 4, 2158-2165. Copyright 2013 American Chemical Society.

4.2 HAT-CN in immobilized one-dimensional columnar charge transfer assemblies

Charge-transfer complexes are combinations of charge donating (D) and charge-accepting (A) materials. While the constituting compounds tend to be unipolar semiconductors, the CT complex can have entirely different properties; it can be an ambipolar semiconductor, a metal, or even a superconductor.[180] Apart from their electronic properties, many CTCs have also been reported to show interesting long-wavelength optical absorption bands that are not observed in their constituting materials.[181]

For a variety of applications using charge transfer (CT) complexes, long range structural ordering of donor/acceptor assemblies are important. In this respect, **HAT-CN** among other acceptors has been found to form CT complexes with amphiphilic triphenylene derivatives **99a,b** shown in Figure 28. Aida and coworkers have used mesoporous silicates to provide highly ordered, unidimensional channels that are optimal for the long-range structural ordering of this charge transfer assemblies.[182]

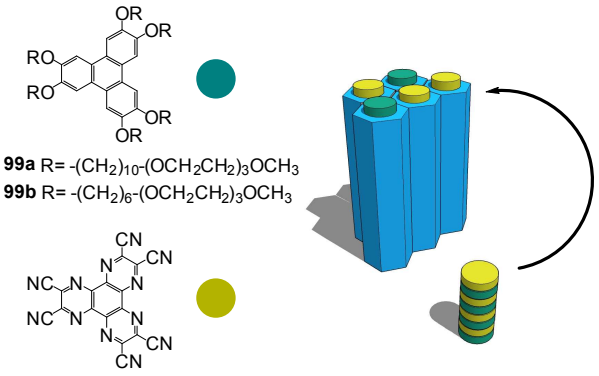

Fig. 28 Formulas of triphenylene donors **99a,b** and acceptor **HAT-CN** and a schematic representation of a mesoporous silica film containing one-dimensional charge transfer (CT) assemblies immobilized in a hexagonal array of nanoscopic channels.

The mesostructured silica films were fabricated by using the triphenylene-based CT complexes as templates for sol-gel synthesis. The silica wall segregates the individual CT columns, which display neither solvatochromism nor guest-exchange activity, and exhibits red-shifted absorption bands, possibly as a consequence of a long-range structural ordering. Furthermore, the donor/acceptor molar ratio, which is related to photoconductive properties, can be varied over a wide range from 1:1 to 9:1.

This seminal contribution paved the way for the use of mesoporous silicates with unidirectional nanoscopic channels as good scaffolds for ensuring long-range ordering of columnar assemblies of functional groups in order to develop anisotropic optoelectronic properties.[183]

4.3 Interactions between anions and HAT-CN

In last recent years, the presence of noncovalent interactions of anions has garnered much interest with the goal of designing anion-specific molecular sensors and receptors,[184] for applications in biological and medicinal chemistry, e.g. transmembrane anion π-slides.[185] In 2002, the term "anion-π interaction" was used by Deyà, Frontera et al. to describe the interaction of anions with electron-deficient arenes.[186] Several studies have shown that certain arenes possessing strong electron-accepting abilities and large quadrupole moments undergo significant changes in their absorption and emission spectra upon interaction with anions.[187] In these systems, the π-acceptor/anion interaction involves charge transfer (CT),[188] which in several cases is accompanied by the appearance of highly colored solutions or crystals, rendering them promising candidates for designing selective anion-sensing receptors.[189]

Considering the high π-acidity of **HAT-CN**, due to the conjugated cyano groups, its high molecular polarizability, and positive quadrupole moment, it was sugested that **HAT-CN** could be a particularly attractive heterocyclic system to establish anion- or lone pair–π contacts.[190] Thus, Dunbar and coworkers showed the existence of CT bands in the complexation process of **HAT-**

CN with several halide anions (i.e., X = Cl^-, Br^-, and I^-) using THF as solvent. The dominant multisite CT interactions afforded extremely high values ($K_{CT,X}$ = (1−4) × 10^3 M^{-1}) as compared to those typically determined (1−10 M^{-1}) for related complexes also displaying CT-bands.[187]

Shortly afterwards, Ballester and coworkers reported experimental evidence indicating that the nature of the interaction established between **HAT-CN** with mono- or polyatomic anions switches from the almost exclusive formation of reversible anion−π complexes, featuring a markedly charge transfer (CT) or formal electron-transfer (ET) character, to the quantitative and irreversible net production of the anion radical [**HAT-CN**]$^{\bullet-}$ and the dianion [**HAT-CN**]$^{2-}$ species.[191]

The high stability of the distinctly colored complexes assembled with different anions as directing elements and the simultaneous multisite CT interactions in which **HAT-CN** engages are unique in the literature of this area. These are highly desirable features for the design of anion-sensing receptors. These seminal studies pave the way for further studies of interactions of **HAT-CN** with other anions.

4.4 HAT-CN as source for patterned graphene growth

Since the successful isolation of graphene via mechanical exfoliation of graphite,[192,193] various methods of graphene synthesis have been developed, including chemical vapor deposition (CVD),[194,194,195]chemical reduction of graphene oxides,[196,197,198] and organic synthesis from micromolecules.[199,200] However, one limitation is that for these procedures it is necessary to physically transfer the grown graphene onto desired substrates for subsequent device processing. Thus, intense efforts are currently focusing on developing alternative synthetic methods that can avoid transfer and the introduction of defects into the graphene sheet associated with the transfer process. In this respect, in 2015 Sun and coworkers have reported a simple, transfer-free method capable of synthesizing N-doped graphene directly on dielectric substrates at temperatures as low as 600 ºC using **HAT-CN** as polycyclic aromatic hydrocarbon as the carbon source.[201] The carrier mobility of N-doped graphene from **HAT-CN** was measured at 1835 cm^2 V^{-1} s^{-1} without optimization and a square resistance of 850 Ω/cm^2 at the lowest growth temperature (~ 600 ºC) which is compatible with direct growth on glass substrates.

Thus, this method should provide a possible route to directly grow graphene on a variety of substrates, for example, quartz or glass, without the need for any transfer process.

5. Miscellaneous studies and applications for HAT derivatives

In addition to the self-assembling properties of **HAT** derivatives and the applications outlined above for **HAT-CN**, there are additional interesting studies and applications found for other **HAT** derivatives that will be reviewed below.

5.1 HAT derivatives and energy transfer processes

Energy transfer in donor-acceptor systems is an important process in a natural photosynthetic system[202] as well as for the development of light harvesting antennas which are important and practically useful for the design of artificial photovoltaics.[203] In this respect, taking advantage of the strong tendency for self-assembly of **HAT**, Ishi-I and coworkers designed and prepared an energy transfer system based on the incorporation of **HAT** possessing perylenebisimide (**PBI**) acceptor moiety into **HAT**-based columnar-type aggregates (Figure 29).[204]

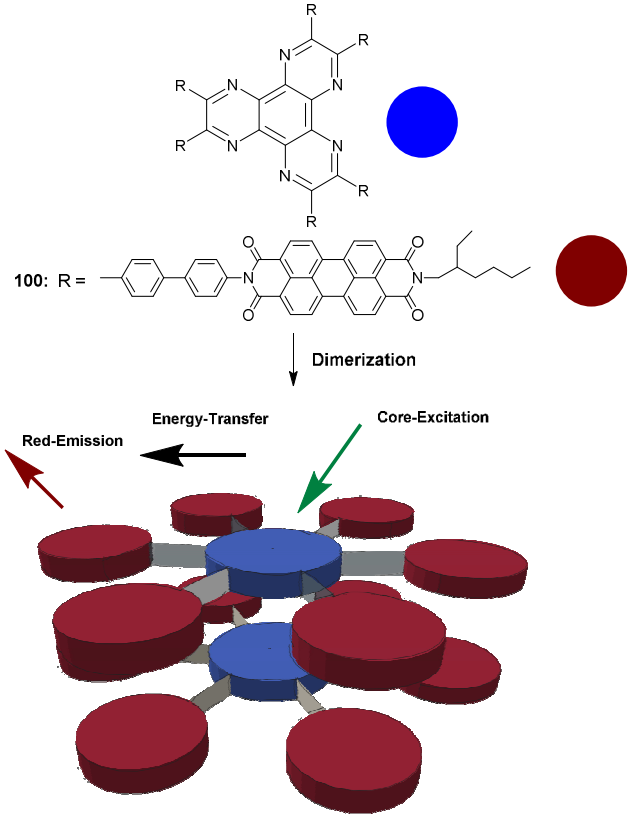

Fig. 29 Formulas of **HAT-PBI** assembly (**100**) and a schematic representation of the dimer aggregates that exhibit energy transfer process from the HAT core to the peripheral PBI moieties

PBI was selected as the acceptor moiety because of its strong accepting nature, suitable overlap of its absorption spectrum with the fluorescence spectrum of the **HAT** chromophore used as energy donor moiety, and good separation between the fluorescence spectra of the **HAT** and **PBI** chromophores.

In order to investigate the energy transfer process, a film of a **HAT** derivative with six octyloxy-containing biphenyl groups (**HAT-OC8**) doped with 5 mol % **HAT-PBI 100** was prepared by spin coating. It was observed that in the presence of **HAT-PBI 100** the emission from **HAT-OC8** was quenched even upon excitation of the HAT chromophore. In addition, the **PBI** emission upon indirect excitation of the **HAT** chromophore was enhaced by a factor of 4 times compared to that observed upon direct excitation of the **PBI** chromophore which indicates the efficient light harvesting properties of the **HAT-OC8** based medium. The energy transfer phenomenon can be easily visualized by change in the emission color from green **HAT** emission to red PBI emission.

Another efficient energy transfer system based on **HAT** derivatives and triphenylene (**TP**) derivatives endowed with (diphenylaminobiphenyl)biphenyl (DAB), phenoxybiphenyl (POB) and biphenyl (BP) groups was reported. In this case the **HAT** derivatives act as energy-acceptor. Thus, in 1:1 mixtures of **TP** /**HAT**, the blue emission from **TP** was completely quenched and only the green emission from **HAT** was detected and, even in the presence of 10 equivalent of **HAT**, the quenching of **TP-DAB** emission occurred significantly. Thus, an energy transfer system can be created by combination of triphenylene and **HAT** moieties with structural similarity and electronic complementarity.[205]

It can be concluded from these results that **HAT** derivatives can be efficiently used to provide self-assembled light harvesting and energy transfer systems.

5.2 Nonlinear optical (NLO) properties of HAT derivatives

Nonlinear optics is the branch of optics that describes the behavior of light in media where the dielectric polarization responds nonlinearly to (the electric field component of) light. The doubling of the frequency of the incident beam, through the second harmonic generation (SHG) process, constitutes one example of nonlinear optical (NLO) phenomena that is currently exploited in laser components as well as in optical information processing and data storage devices.[206]

The most important class of molecules that has received significant attention in this field are donor-acceptor dipolar molecules in which the ease of polarization in one direction within the molecule is easier than that in the opposite direction.[207] However, Zyss and coworkers[208] showed that octupolar molecules with C3 symmetry exhibit first hiperpolarizability comparable to those of the donor-acceptor dipoles and a great deal of interest have been devoted to the use of this type of systems for NLO applications.[209] Indeed, the lack of permanent dipole moment of octupolar structures, usually associated with an improved hyperpolarizability and with a good transparency, constitutes a strong advantage over more classic dipolar structures for many applications.[210] In this respect, the **HAT** moiety has been identified as a good scaffold to build octupolar systems and the NLO properties of some **HAT** derivatives (**101-103**, Figure 30) have already been investigated.[211,212] Thus, we have recently explored the electron-withdrawing property of HAT by ramifying and fully substituting its six peripheral positions with electron donor arms giving rise to new octupolar extended HAT dyes **101a,b**, **102a,b** (Figure 30) in a donor-to acceptor pattern with modulation of the charge transfer character. In addition, we have compared the nonlinear optical behavior of these charge transfer compounds with that of **103**[15] which consists of the fusion of three **HAT** molecules and that, without relying on donor−acceptor derived noncentrosymmetry (as necessitated in linear conjugated structures), epitomizes the purely octupolar implementation of noncentrosymmetry.[211,212]

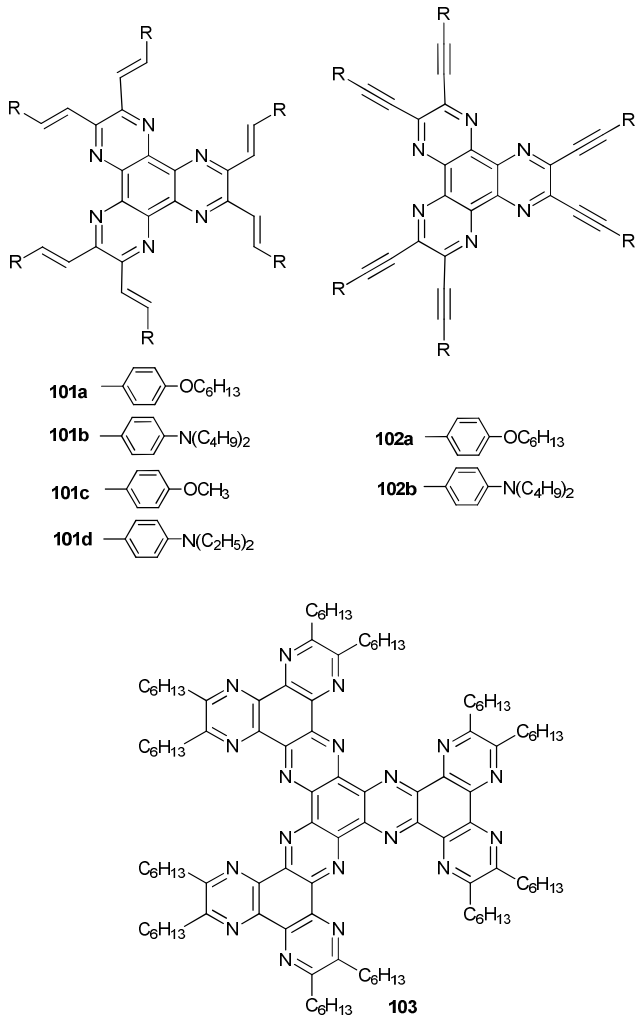

Fig. 30 Formulas of octupolar HAT derivatives for NLO

First hyperpolarizability (β) values between 250 and 510 x 10^{-30} esu were found for the charge transfer compounds **101a,b**, **102a,b**. Among them it was observed that the amine derivatives turned out to enhance the NLO activity due to their large electron donor capacity. On the other hand, a β value of 690 x 10^{-30} esu was found for **103**. The conclusion of this study was that the modulation of the second order optical response is a balance of charge transfer and octupolar contributions.

Cho and coworkers found that the NLO properties of **HAT** derivatives **101c-d** can be increased by complexation of the **HAT** derivatives with Cu(I) at the center of the octupolar molecules. This behavior is in agreement with the increase in the acceptor strength of the HAT moiety upon complexation.[211]

Apart from the NLO optical properties of **HAT** derivatives with C3 symmetry, we have also explored in a joint theoretical-experimental study the nonlinear optical properties of V-shaped **HAT** derivatives with C2 symmetry (**26-30**, Figure 7).[39] β values between 30 and 66 x 10^{-30} esu were determined and it was found that by varying the type of linkage and the nature of the donor moiety, the electrochemical properties as well as the absorption spectra of the well-defined asymmetric donor- acceptor

conjugated systems can easily be tuned and, again, the highest values were obtained for **HAT** derivatives containing the more electron-rich dibutylamino moiety.

The study of multiphoton-absorbing materials is another research field that has grown rapidly in the area of organic nonlinear optical materials because of its broad technological impact. The technologically useful multiphoton excitation-based applications, especially by two-photon absorption TPA, have drawn considerable attention including (but not limited to) three-dimensional (3D) fluorescence imaging, photodynamic therapy, nonlinear optical transmission, optical power limiting, up-converted lasing, three-dimensional data-storage, 3D microfabrication, and uncaging of bioactive species.[213] Two-photon absorption (TPA) is a process whereby molecules simultaneously absorb two photons and is inherently weak at normal light intensities. From the design point of view it has been identified that donor-acceptor substitution can enhance the two-photon absorption activity of molecules through an increase in the transition dipole moment or the dipole moment difference between the ground and excited states. Furthermore, TPA crosssections (δ) can also be enhanced by intermolecular interactions, such as intercalation and self-assembling to form dimers and aggregates.[214] With this in mind, Ishi-I and coworkers synthesized a family of donor-acceptor **HAT** derivatives bearing six electron-donating moieties **104-d** (Figure 31).[215]

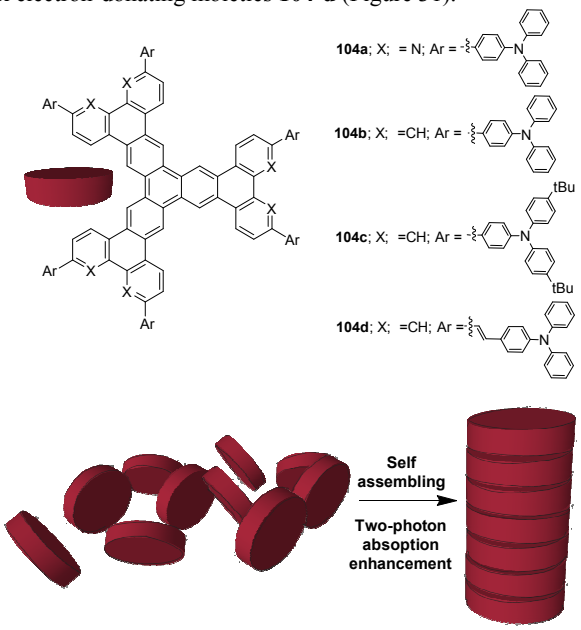

Fig. 31 Formulas of TPA dyes **104a-d** based on **HAT** and schematic representation of the enhancement of the TPA nature by self-assembly. Adapted from *Tetrahedron*, 2013, 69, 29-37. Copyright 2013, with permission from Elsevier

An enhancement of the two-photon absorption cross-section was observed for the self-assembled **104b** system to give a δ value of 1460 GM (at 870 nm), which is 1.4 times larger than the value for the non-aggregative **104c** (1080 GM at 850 nm) system bearing bulky *tert*-butyl groups. The δ value increased with expansion of the π-electron system from **104b** to **104d** (2560 GM at 850 nm). Compared to the phenanthrene-fused **104b** system, the phenanthroline-**104a** demonstrated a larger δ value (2420 GM at 870 nm). Thus, the order of the two-photon absorption nature was determined to be in agreement with the aggregative nature of the molecules.

We have also investigated the TPA properties of **HAT** derivatives **101a-b** and **102a-b** (Figure 30).[212] We found that in this family of compounds that the increase of the TPA crosssection (δ) values is consistent the rise of the first hyperpolarizability (β) and with the decrease of the experimental and theoretical HOMO-LUMO gaps. The linear relationship between β and δ values can be a useful guide for developing new strategies to synthesize compounds with great NLO and TPA properties.

The above contributions show how the chemical design of suitable molecular structures is an efficient method to tune nonlinear optical properties.

5.3 HAT derivatives as photoinitiators for polymerization reactions

The photoinitiating systems play an important role in free radical polymerization (FRP), thiol-ene polymerization (TEP), cationic polymerization (CP) or free radical promoted cationic polymerization (FRPCP) and interpenetrated polymer networks (IPN) synthesis. Great efforts are being devoted to the design of UV, visible and near IR sensitive photoinitiating systems working upon exposure to monochromatic or polychromatic lights, under high or low intensity sources, in laminate, inert atmosphere or under air.[216]

In this respect, phenazine derivatives have been used in photopolymerization reactions and benzo [2,3-b]phenazines have been found to be quite efficient photosensitisers in radical as well as cationic polymerization processes, but only upon high intensity Xenon lamp exposure.[217] **HAT** derivatives exhibit enhanced light absorption properties compared to the previously used phenazine analogues which exhibit only UV light absorption. This is due to the fact that the lowest energy transition exhibits a π/π* character and involves strongly delocalized molecular orbitals. Thus, basic **HATNA** as well as other **HATNA** derivatives (**105**, **106**, Figure 32) have been proposed as suitable photoinitiators and it has been recently shown that **HAT-** based three component photoinitiating systems allow efficient radical polymerization of acrylates and cationic of epoxides upon exposure to easily accessible, energy saving and cheap LEDs at 385, 395 and 405 nm as well as a laser diode at 405 nm or a halogen lamp.[218]

The excellent absorption properties in the 380 to 425 nm range resulting from the presence of strongly delocalized molecular orbitals are promising for the development of other derivatives exhibiting a red-shifted absorption.

5.4 HAT derivatives for molecular recognition and sensors

Different **HAT** derivatives have been designed and synthesized with the aim to use them for molecular recognition and sensors.

Badjic and coworkers synthesized internally functionalized and dynamic cavitands of type **107a-c** (Figure 33) which can be used as "claws" for selectively "grabbing" small chemical analytes such as CBr_4.[219]

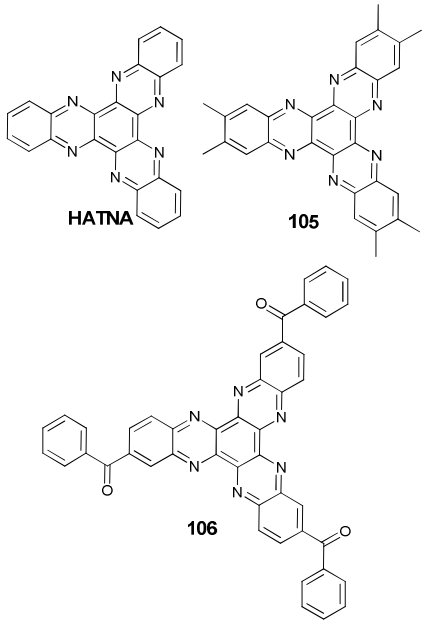

Fig. 32 Formulas of **HATNA** derivatives us as photoinitiators in photopolymerization reactions.

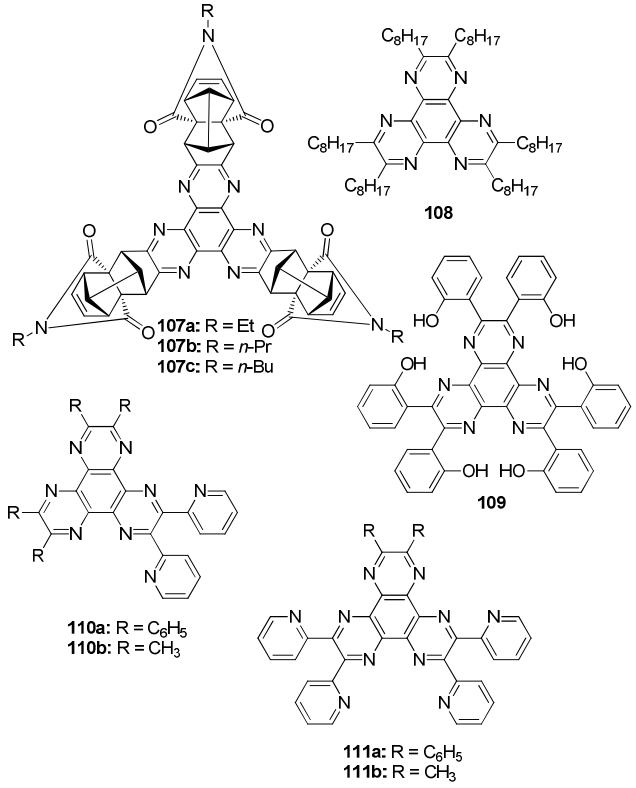

Fig. 33 Formulas of **HAT** derivatives used for molecular recognition and sensors

Organogels based on **HAT** derivative **108** (Figure 33) have been used for silver(I) recognition.[220] The strong stacking between the large planar **HAT** core and the van der Waals forces of the six aliphatic chains of this C_3-symmetric molecules greatly facilitate the formation of organogels in several solvents. It is observed that introduction of silver(I) salts result in the formation of silver-**108** complexes which led to the destruction of the organogels due to the collapse of the well- ordered molecular arrangement. Fifteen nitrates were tested, with the metals ranging from alkali, alkaline-earth to transition metals and, remarkably, only Ag^+ was found capable of breaking the organogel which was ascribed to the strong complexation between **108** and Ag^+ in aqueous medium. This is a nice example that suggests a new way for the fabrication of gel-based sensing systems or smart soft materials.

HAT derivatives have been also used as chemosensors capable of selectively and efficiently detect fluoride anions. Thus, **HAT** derivative **109** (Figure 33) displays a high degree of F^- discrimination both in organic solvent and aqueous mixture by direct deprotonation of phenolic OHs.[221] Compound **109** is fluorescence silent, which might be attributed to the charge transfer between electron-deficient **HAT** core and electron-rich phenol units. Therefore, the fluorescence emission of **109** could not be turned on upon addition of anions ant its recognition behavior had to be investigated using UV-vis spectroscopy. Thanks to the high acidity of the phenolic OH units and the strong intramolecular hydrogen bonds formed between them and the **HAT** core, the formation of intermolecular hydrogen-bonding between the OHs and anions was blocked and thus only direct deprotonation of OHs by F^- could occur, which led to a high selectivity to fluoride over other anions.

The same **HAT** derivative **109** has been also recently used for selective recognition of Cu^{2+} through the formation of coordination polymer which further aggregates into metal-organic nanospheres. The polymer is formed through the coordination interactions between the phenolic hydroxyl groups of **109** and Cu^{2+}. It exhibits distinct color changes and absorption variation toward Cu^{2+} without being interfered by other competing metal ions and a satisfactory visual detection limit of 6.25×10^{-6} M can be reached.[222] This is a good example of how coordination polymers can also exhibit high selectivity and sensitivity as chemosensors for the recognition of metal cations.

While the introduction of phenolic substituens in the **HAT** core produce fluorescence silent derivatives, introduction of other less electron-donating aromatic rings makes the compounds emissive.[223] This is interesting considering that, due to operability and sensitivity, fluorescent sensors are powerful tools for the detection of metal ions and widely used not only in environmental monitoring but also in biological studies. Thus, **HAT** derivative **78**[117,118] (Figure 33) with electron-defficient pyridine substituents has been found to have excellent fluorescent selectivity for Cd^{2+} over many other metals (K^+, Na^+, Ca^{2+}, Mg^{2+}, Mn^{2+}, Fe^{2+}, Ni^{2+}, Co^{2+}, Cu^{2+}, Ag^+, Hg^{2+}, Zn^{2+}, and Cr^{3+}).[118] This fact is of interest, as developing a Cd^{2+} selective fluorescence sensor that can discriminate Cd^{2+} from Zn^{2+} as a consequence of the similar chemical properties of Cd^{2+} and Zn^{2+} has been a great challenge. Thus, compared with the weak fluorescence in solution of the free HAT derivative **78**, the emission color of the solution changes from dark to bright blue after addition of Cd^{2+} ions. The monitoring event can be even observed in a naked-eye experiment under UV-vis light irradiation because the emission color changes perceptively from dark to bright blue. The recognition process of Cd^{2+} by **78** is reversible. This was demonstrated by addition of an equal amount of an ethylenediaminetetraacetic acid (EDTA) aqueous solution into the glowing **78**-Cd^{2+} solution, which recovers the original emission of **78** (Figure 34).

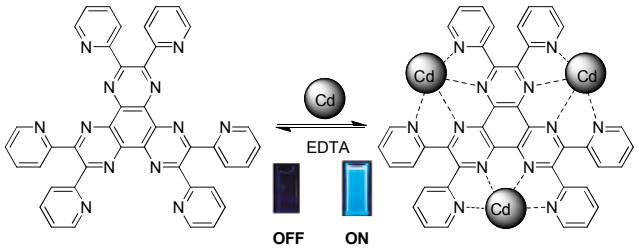

Fig. 34 Reversible recognition process of Cd^{2+} by **HAT** derivative **78** showing the fluorescent complex (right) and the non-fluorescent free HAT derivative **78** (left)

Inspired by the pioneering work described above, a series of **HAT** derivatives with different coordination structures, such as non-centrosymmetric HATs, have been designed and synthesized in order to obtain different fluorescence sensors for different metal ions.[224,225] Thus, two C_2-symmetrical **HAT** derivatives (**110a**, **111a**, Figure 33) bearing different number of pyridine and phenyl groups were synthesized.[224] The two C_2-symmetrical **HAT** derivatives **110a** and **111a** are architecturally different in their coordination geometry compared with the symmetrical analogue **78**. Both **110a** and **111a** exhibit ratiometric and colorimetric fluorescence recognition of Zn^{2+} nearly without interference by many other background metal ions, including alkali ions, alkaline earth ions and a wide range of transition metal ions, including Cd^{2+}. Compound **110a**, with a detection limit of 0.095 μM, is more sensitive toward Zn^{2+} than **111a**.

Considering that Cd^{2+} has similar electronic structure but larger size relative to Zn^{2+}, it has been shown that replacing the phenyl groups with smaller substituents, such as methyl groups, thus reducing the steric hindrance to metal ions and enhancing the binding ability to Cd^{2+}, is an efficient strategy for the design of Cd^{2+} response fluorescent sensors. With this aim, two C_2-symmetrical **HAT** derivatives bearing methyl groups instead of phenyl rings (**110b**, **111b**, Figure 33) have been synthesized and investigated as chemosensors.[225] They both exhibit selective turn-on fluorescent recognition of Cd^{2+} ion that is nearly unaffected by many other background metal ions including Na^+, K^+, Ca^{2+}, Mg^{2+}, Mn^{2+}, Fe^{2+}, Co^{2+}, Ni^{2+}, Cu^{2+}, Zn^{2+}, Ag^+ and Pb^{2+}.

One common strategy to improve the sensitivity of chemical sensors consists on enhancing the fluorescence emission of the complex formed between sensor and analyte. Thus, a novel **HAT** derivative (**112**, Figure 34) that retain the receptor structure of **78** but with an extended chromophoric group has been prepared with the aim of getting a more sensitive response to the Cd^{2+} ion.[226] The detection limit of 0.02 μM is remarkably lower than that of the parent **HAT** derivative **78** due to the extension of the chromophoric group with pyrene in **112** that exaggerates the fluorescence response. Interestingly, **112** exhibit water tolerance, low cytotoxicity and cell membrane permeability which allow for its use as in vivo sensor of intracellular Cd^{2+} levels.

The strategy of extending the conjugated systems of the chromophore has been also used for other **HAT** derivatives (**113**, **114**, Figure 35) used as Hg^{2+} fluorescent chemosensors. The novel derivative **113** is analogous to **112** but the peripheral pyridine moieties substituted by phenyl rings. Thus, through this alteration of the binding site, the two **HAT**-based sensors can selectively respond to different metal ions. The detection limits of **113** and **114** are 2.8 and 3.1 nM which is lower than the toxic level of Hg^{2+}. Thus, this **HAT** derivatives suitable for the detection of sub-micromolar level of Hg^{2+} in many biological and environmental systems.[227] Furthermore, these sensors maintain their fluorescence sensing properties on test paper, which makes their practical application more convenient.

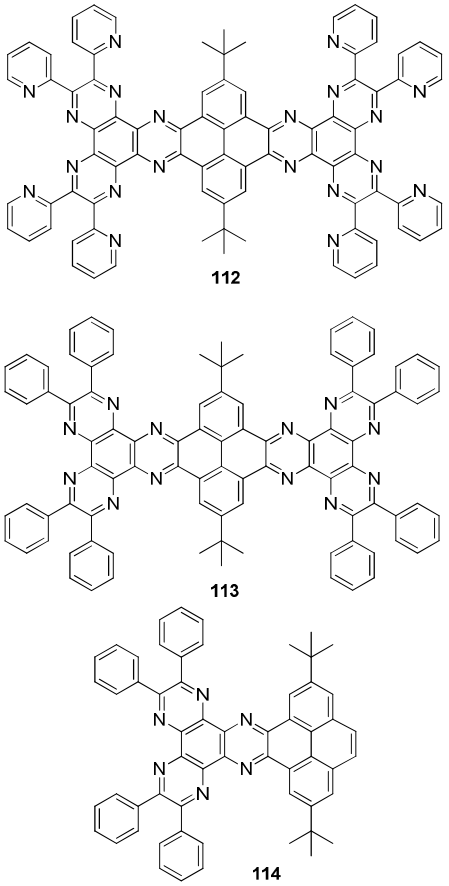

Fig. 35 Formulas of **HAT** with extended pyrene chromophores used for molecular recognition and sensors

These studies show that by appropriate design **HAT** derivatives can be used as efficient and selective fluorescent chemosensors for small chemical analytes and a variety of ions.

5.5 HAT derivatives as scaffolds for microporous frameworks

Until recently, organic polymers have not been considered as materials for gas storage because polymers generally have enough conformational and rotational freedom to pack space efficiently and thus do not offer high surface areas. However, the polymers of intrinsic microporosity (PIMs) have been developed that are composed wholly of fused ring subunits designed to provide highly rigid and contorted macromolecular structures that pack space inefficiently.[228] In the search of polymers for hydrogen storage, McKeown, Budd and coworkers developed a polymer of intrinsic microporosity (PIM) based on **HAT** (**115**, Figure 36).[229]

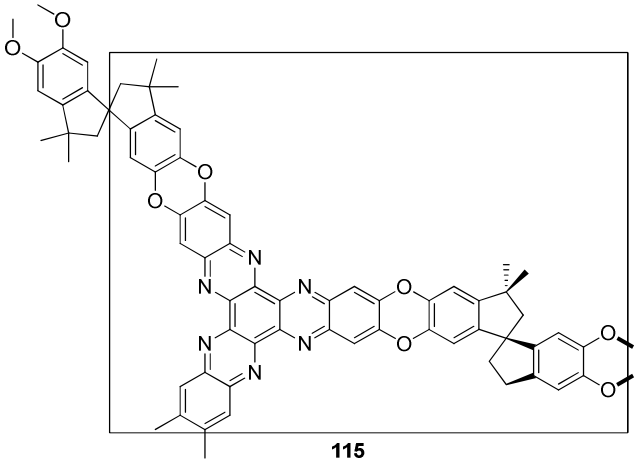

Fig. 36 Formula of the **HAT** network polymer with intrinsic porosity **115**.

The polymer can be obtained by reaction between hexachlorohexaaza-trinaphthylene (**18a**, Figure 5) and a spirocyclic bis(cathecol) monomer. A Brunauer–Emmett–Teller (BET) surface area of 820 m^2g^{-1} was measured for **115** by nitrogen adsorption at 77 K. The measurements for H_2 adsorption reveals that **115** adsorbs significant quantities of H_2 (1.4 % by mass) at relatively low pressures with saturation being reached at less than 10 bar pressure and with most of the adsorption taking place below 1 bar. Calculations show that the maximum number of hydrogen molecules adsorbed per fused-ring of the polymeric repeat unit is approximately 0.43 H_2 per ring. One interesting characteristic of this system is that unlike other types of microporous materials (zeolites, MOFs), the structures of this system is not necessarily constrained by a fixed network structure and may be dissolved in suitable solvents and swollen by suitable nonsolvents. Thus, polymer structural manipulation can be used to optimize H_2 adsorption; for example, the rapid removal of solvent from the swollen network could generate additional free volume and thus provide greater accessible surface area.

An important class of porous frameworks are those named π-conjugated microporous polymers (CMPs) which consist on an extended π-conjugated system and inherent nanopores.[230,231] The combination of the porous structure and the characteristics of π-conjugated systems open the field for new applications. Thus, Jiang and coworkers reported the synthesis of porous framework based on an aza-fused CMPs with the general structure (**116**, Figure 37a) and highlighted their functions in supercapacitive energy storage and electric power supply.[232]

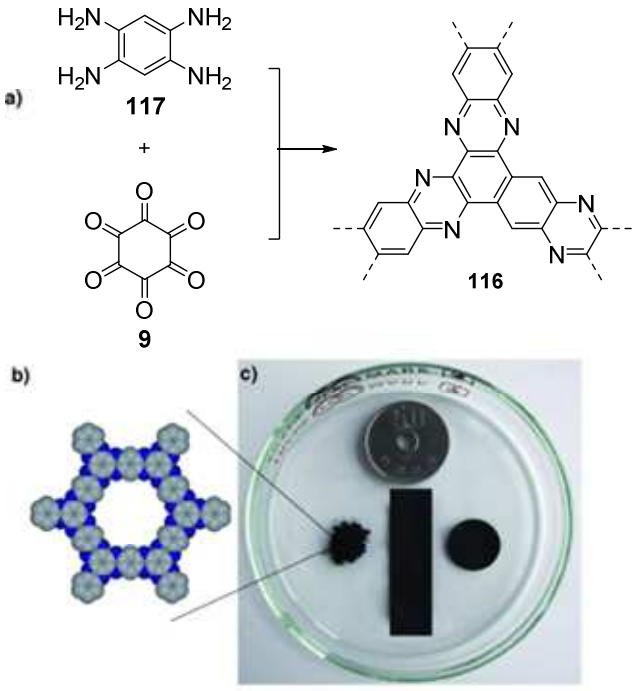

Fig. 37 a) Synthesis of the aza-fused π-conjugated microporous polymer **116**. b) The elementary pore structure of Aza-CMPs calculated using the Gaussian03 program at B3LYP/3-21G(d) level (the carbon network is gray and nitrogen is blue). c) Photographic image of the powder and flexible thin films with different shapes of **116**. Reproduced from Ref. 232 Copyright 2011 Wiley-VCH Verlag GmbH & Co. KGaA, Weinheim.

Different Aza-CMPs with the general structure **116** were ionothermally synthesized by a condensation reaction of 1,2,4,5-benzenetetramine (**117**) with hexaketocyclohexane (**9**) at 300, 350, 400, 450, and 500 °C. BET areas of up to 1200 m^2g^{-1} were obtained for the polymer obtained at higher temperatures. Aza-MPs are amorphous and they can be used to prepare free standing flexible thin film electrodes films with different shapes (Figure 37c). Galvanostatic charge-discharge cycling experiments with disk-shaped films were done in order to test the supercapacitive performance. The highest capacitance measured was of 946 Fg^{-1} which is superior to the specific capacitance of nitrogen-enriched porous carbon materials and state-of-the art carbon nanostructures such as graphenes and carbon nanotubes and exceeds that of the best values of supercapacitors with a redox ruthenium oxide electrode.[233] The energy density is higher than those of nanostructured porous carbon materials and reaches the regime of batteries such as Pb-acid, NiCd and even lithium ion battery. Furthermore, it has an excellent cycle life as well.

More recently, Jiang and coworkers have synthesized another **HAT**-based CMP (**118**, Figure 38) as a new platform for lithium-battery energy storage with a built-in redox active skeleton and permanent nanopores.[234] The **HAT**-based CMP (**118**) was synthesized via Sonogashira cross-coupling polycondensation of 1,4-diethynylbenzene and hexaiodoHATNA in the presence of tetrakis-(triphenylphosphine) palladium and copper iodide catalyst and diisopropylamine base.

The CMP strategy provides a useful platform for crosslinking redox-active modules into highly stable porous electrodes (the porosity of **118** was revealed by a BET surface area of 616 m^2g^{-1}); such organic cathode materials have been long pursued in the exploration of next-generation green batteries.[235,236] It is worth pointing out that the structural features of the CMP work

together in energy storage with lithium-ion batteries because the **HAT**-based built from redox-active units that serve as energy-storing and power supplying modules, it bears inherent open nanopores that are accessible to lithium ions and it possesses a high surface area that facilitates the charge dynamics. Thus, it has been found that batteries fabricated with **118** exhibit a near-unity coulombic efficiency, high capacity and energy density, and enable repetitive energy storage and supply with good cycle stability.

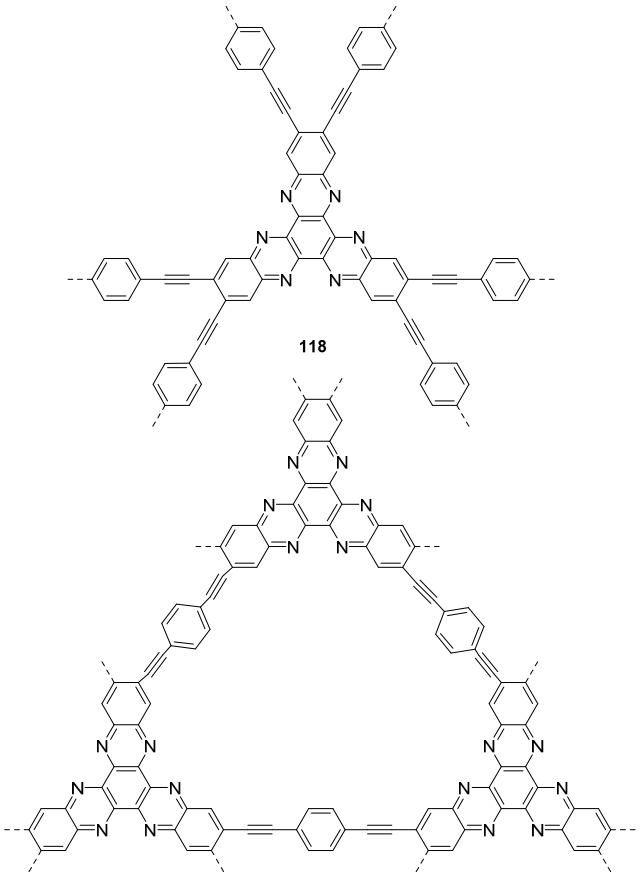

Fig. 38 Schematic representation of the **HAT**-based CMP **118** (upper part) and its elementary pore structure (lower part).

The above examples demonstrate the enormous potential of **HAT**-derived CMPs as green electrode materials for designing high-energy storage and power supply devices.

Summary and Conclusions

The first three decades after the synthesis of **HAT** have witnessed a great interest on this system from the synthetic, theoretical and applications point of view. As for the applications, it has revealed itself as a basic scaffold in the areas of organic materials and nanoscience.

The structural behaviour of **HAT** has been investigated showing that, because of its discotic D_{3h} symmetry and planarity, the **HAT** core has a strong tendency towards π-π stacking. Furthermore, the presence of six nitrogen atoms with sp^2 hybridization provides **HAT** a good electron acceptor ability as demonstrated by electrochemical and UPS/IES experiments.

Thus, the understanding of the particular structural and, moreover, electron acceptor ability of **HAT** as well as the establishment of accessible method for the synthesis and functionalization of this unique molecule has allowed the smart design of materials with tailored properties.

In the review we have summarized the main general synthetic methods for the synthesis of **HAT** derivatives with D_{3h} symmetry. We have also highlighted the few examples of synthetic strategies toward **HAT** derivatives with non-trigonal symmetry which open up the way for the development of V-shaped NLO materials or the tuning of the liquid crystalline properties, among others. We have also outlined the main synthetic strategies for the post-synthesis functionalization of **HAT** derivatives which has allowed the incorporation of a variety of functionalities to **HAT** including electroactive moieties. We have summarized the main synthetic strategies followed to expand the **HAT** core conjugation with the aim to create n-type self-assembling semiconductors.

The outcome of the self-assembly of **HAT** derivatives at the molecular level has been investigated at different levels. (i) **HAT**-based three dimensional ordered liquid crystals have been prepared and *n*-type charge carrier mobilities have been measured for some **HAT** derivatives. (ii) **HAT** derivatives have revealed as excellent scaffolds for the development of self-organized nanostructures on different surfaces. It has been found that by using electrochemical scanning tunnelling microscopy it is possible to induce **HAT** molecules to organize in flat or vertical orientations on metallic surfaces which is a suitable way to build nanostructures or thin films with controllable molecular orientations for electronic applications. (iii) Different **HAT** derivatives have been used for the production of nano and microstructures including microbelts, microtubes or microspheres by using additional hydrogen bonding or metalorganic coordination interactions.

We have also reviewed the main applications found for **HAT** derivatives. In this respect we have remarked the special character of a **HAT-CN**, a **HAT** derivative endowed with six electron accepting nitrile groups. **HAT-CN** is a strong electron-deficient discotic heterocyclic molecule with a deep-lying lowest unoccupied molecular orbital (DL-LUMO) level (~5.1 eV) which has found extensive application as charge transport layer or as dopant in different (opto)electronic devices such as organic light emitting diodes, organic solar cells, organic filed effect transistors including magnetoresistive field effect transistors. It has also been used (i) for the work function tuning of graphene through noncovalent interactions, (ii) for the development of unidirectional nanoscopic channels m (iii) for applications related with its ability of anion-π interactions and (iv) as source for the production of N-doped graphene.

Other important applications of **HAT** derivatives have been also summarized. By attaching suitable light harvesting antennas such as perylene bisimide derivatives to the **HAT** core it has been possible to show that **HAT** derivatives can be efficiently used to provide self-assembles light harvesting and energy transfer systems.

Because of it octupolar character with trigonal symmetry appropriately functionalized **HAT** derivatives have proven as

suitable materials for NLO applications and as chromophores of multiphoton absorption.

By attaching appropriate functionalities **HAT** derivatives can be efficiently used as efficient and fluorescent selective sensors of small chemical analytes such as CBr_4, fluoride anions or metal ions including Zn^{2+}, Cd^{2+}or Hg^{2+}.

HAT derivatives can be also used as high performance photoinitiators for the ring opening polymerization of epoxy monomers as well as for the free radical polymerization of (meth)acrylates.

Very recently, **HAT** derivatives have also proved to be excellent scaffolds for the development of microporous frameworks, including conjugated microporous polymers (CMP). Thus, batteries fabricated with HAT-based CMPs have been found to exhibit a near unity coulombic efficiency, high capacity and energy density that enable energy storage and supply with good cycle stability.

In summary, **HAT** is a molecule whose interesting electronic properties have challenged the creativity and inventiveness of chemists in areas such as organic, polymer, supramolecular and materials chemistry as well as in nanoscience. The knowledge accumulated during this years of research based on this system will certainly lead to novel applications for this unique molecule.

Acknowledgements

Financial support from Spanish Government (Project MAT2014-52305-P) and a UCM-BSCH joint project (GR3/14) is acknowledged. The authors wish to give credit to the scientists who have participated in the development of this research field whose names are cited in the references.

Notes and references

[a] *Departamento de Química Orgánica, Facultad de Química, Universidad Complutense de Madrid, E-28040 Madrid, Spain. Fax: +34-91-394103; Tel: +34-01-3945142; E-mail: segura@ucm.es*

[b] *Department of Environmental and Technological Chemistry, Universidad Rey Juan Carlos, Madrid 28933*

1. J. Wu, W. Pisula and K. Müllen, *Chem. Rev.*, 2007, 107, 718-747.
2. M. Bendikov, F. Wudl and D. F. Perepichka, *Chem. Rev.*, 2004, 104, 4891-4946.
3. J. E. Anthony, *Chem. Rev.*, 2006, 106, 5028-5048.
4. J. E. Anthony, *Angew. Chem. Int. Ed.*, 2008, 47, 452-483.
5. W. Jiang, Y. Li and Z. Wang, *Chem. Soc. Rev.*, 2013, 42, 6113-6127.
6. K. Takimiya, I. Osaka, T. Mori and M. Nakano, *Acc. Chem. Res.*, 2014, 47, 1493-1502.
7. S. S. Zade and M. Bendikov, *Angew. Chem. Int. Ed.*, 2010, 49, 4012-4015.
8. D. Biermann and W. Schmidt, *J. Am. Chem. Soc.*, 1980, 102, 3163-3173.
9. I. Kaur, M. Jazdzyk, N. N. Stein, P. Prusevich and G. P. Miller, *J. Am. Chem. Soc.*, 2010, 132, 1261-1263.
10. L. Zhang, Y. Cao, N. S. Colella, Y. Liang, J. L. Bredas, K. N. Houk and A. L. Briseno, *Acc. Chem. Res.*, 2015, 48, 500-509.
11. U. H. F. Bunz, J. U. Engelhart, B. D. Lindner and M. Schaffroth, *Angew. Chem. Int. Ed.*, 2013, 52, 3810-3821.
12. L. Chen, Y. Hernandez, X. Feng and K. Müllen, *Angew. Chem. Int. Ed.*, 2012, 51, 7640-7654.
13. S. Kitagawa and S. Masaoka, *Coord. Chem. Rev.*, 2003, 246, 73-88.
14. S. Barlow, Q. Zhang, B. R. Kaafarani, C. Risko, F. Amy, C. K. Chan, B. Domercq, Z. A. Starikova, M. Y. Antipin, T. V. Timofeeva, B. Kippelen, J. L. Bredas, A. Kahn and S. R. Marder, *Chem. Eur. J.*, 2007, 13, 3537-3547.
15. R. Juárez, M. M. Oliva, M. Ramos, J. L. Segura, C. Alemán, F. Rodríguez-Ropero, D. Curcó, F. Montilla, V. Coropceanu, J. L. Brédas, Y. Qi, A. Kahn, M. C. Ruiz Delgado, J. Casado and J. T. López Navarrete, *Chem. Eur. J*, 2011, 17, 10312-10322.
16. H. Grove and J. Sletten, *J. Chem. Crystallogr.*, 2000, 30, 123-130.
17. A. Bondi, *J. Phys. Chem.*, 1964, 68, 441-451.
18. R. Foster, 1969, 233-234.
19. N. Defay, D. Maetens and R. Nasielski-Hinkens, *Org. Magn. Rsonance*, 1984, 22, 340-344.
20. R. Wang, T. Okajima, F. Kitamura, N. Matsumoto, T. Thiemann, S. Mataka and T. Ohsaka, *J. Phys. Chem. B*, 2003, 107, 9452-9458.
21. R. Nasielski-Hinkens, M. Benedek-Vamos, D. Maetens and J. Nasielski, *J. Organomet. Chem.*, 1981, 217, 179-182.
22. R. Nietzki and A. W. Schmidt, *Ber. Dtsch. Chem. Ges.*, 1888, 21, 1227-1230.
23. B. Eistert, H. Fink and H.-K. Werner, *Liebigs Ann.*, 1962, 657, 131-141.
24. S. Skujins and G. A. Webb, *Tetrahedron*, 1969, 25, 3935-3945.
25. A. R. Farminer, S. Skujins and G. A. Webb, *J. Mol. Struct.*, 1971, 10, 121-134.
26. B. Kohne and K. Praefcke, *Liebigs Ann. Chem.*, 1985, 522-528.
27. D. Z. Rogers, *J. Org. Chem.*, 1986, 51, 3904-3905.
28. V. M. Boddu, D. S. Viswanath, T. K. Ghosh and R. Damavarapu, *J. Hazard. Mater.*, 2010, 181, 1-8.
29. M. S. P. Sarma and A. W. Czarnik, *Synthesis*, 1988, 72-73.
30. K. Kanakarajan and A. W. Czarnik, *J. Org. Chem.*, 1986, 51, 5241-5243.
31. B. Gao, Y. Liu, Y. Geng, Y. Cheng, L. Wang, X. Jing and F. Wang, *Tetrahedron Lett.*, 2009, 50, 1649-1652.
32. S. Choudhary, C. Gozalvez, A. Higelin, I. Krossing, M. Melle-Franco and A. Mateo-Alonso, *Chem. Eur. J*, 2014, 20, 1525-1528.
33. C. W. Ong, S.-C. Liao, T. H. Chang and H.-F. Hsu, *J. Org. Chem.*, 2004, 69, 3181-3185.
34. S. Barlow, Q. Zhang, B. R. Kaafarani, C. Risko, F. Amy, C. K. Chan, B. Domercq, Z. A. Starikova, M. Y. Antipin, T. V. Timofeeva, B. Kippelen, J.-L. Brédas, A. Kahn and S. R. Marder, *Chem. Eur. J*, 2007, 13, 3537-3547.
35. M. Luo, H. Shadnia, G. Qian, X. Du, D. Yu, D. Ma, J. S. Wright and Z. Y. Wang, *Chem. Eur. J*, 2009, 15, 8902-8908.
36. I. M. Piglosiewicz, R. Beckhaus, W. Saak and D. Haase, *J. Am. Chem. Soc.*, 2005, 127, 14190-14191.
37. J. Nasielski, C. Moucheron, C. Verhoeven and R. Nasielski-Hinkens, *Tetrahedron Lett.*, 1990, 31, 2573-2576.
38. C. Moucheron, M. A. Kirsch-De and S. Choua, *Inorg. Chem.*, 1997, 36, 584-592.
39. R. Juarez, M. Ramos, J. L. Segura, J. Orduna, B. Villacampa and R. Alicante, *J. Org. Chem.*, 2010, 75, 7542-7549.
40. M.-C. Yeh, S.-C. Liao, S.-H. Chao and C. W. Ong, *Tetrahedron*, 2010, 66, 8888-8892.
41. B. Gao, L. Zhang, Q. Bai, Y. Li, J. Yang and L. Wang, *New J. Chem.*, 2010, 34, 2735-2738.
42. P. Secondo and F. Fages, *Org. Lett.*, 2006, 8, 1311-1314.
43. R. I. Gearba, M. Lehmann, J. Levin, D. A. Ivanov, M. H. J. Koch, J. Barbera, M. G. Debije, J. Piris and Y. H. Geerts, *Adv. Mater.*, 2003, 15, 1614-1618.
44. K. Kanakarajan and A. W. Czarnik, in *Polym. Commun.*, 1989, vol. 30, ch. 171, p. 3.
45. W. D. Aumiller, C. R. Dalton and A. W. Czarnik, *J. Org. Chem.*, 1995, 60, 728-729.
46. O. Roussel, G. Kestemont, J. Tant, H. V. de, R. G. Aspe, J. Levin, A. Remacle, I. R. Gearba, D. Ivanov, M. Lehmann and Y. Geerts, *Mol. Cryst. Liq. Cryst.*, 2003, 396, 35-39.
47. T.-H. Chang, B.-R. Wu, M. Y. Chiang, S.-C. Liao, C. W. Ong, H.-F. Hsu and S.-Y. Lin, *Org. Lett.*, 2005, 7, 4075-4078.
48. G. Kestemont, V. d. Halleux, M. Lehmann, D. A. Ivanov, M. Watson and Y. H. Geerts, *Chem. Commun.*, 2001, 2074 - 2075.
49. J. Clark, R. Archer, T. Redding, C. Foden, J. Tant, Y. Geerts, R. H. Friend and C. Silva, *J. Appl. Phys.*, 2008, 103, 124510.

50. C. W. Ong, S.-C. Liao, T. H. Chang and H.-F. Hsu, *Tetrahedron Lett.*, 2003, 44, 1477-1480.
51. K. Warnmark, O. Heyke, J. A. Thomas and J.-M. Lehn, *Chem. Commun.*, 1996, 2603-2604.
52. L. Arnold, S. R. Puniredd, M. C. von, W. Pisula, N. Koshino, H. Higashimura, M. Baumgarten, M. Wagner and K. Muellen, *J. Porphyrins Phthalocyanines*, 2012, 16, 564-575.
53. R. Liu, M. C. von, L. Arnold, N. Koshino, H. Higashimura, M. Baumgarten and K. Mullen, *J. Am. Chem. Soc.*, 2011, 133, 10372-10375.
54. A. C. Grimsdale and K. Müllen, *Angew. Chem. Int. Ed.*, 2005, 44, 5592-5629.
55. Y. Zhao, Y. Guo and Y. Liu, *Adv. Mater.*, 2013, 25, 5372-5391.
56. M. Wang, Y. Li, H. Tong, Y.-X. Cheng, L.-X. Wang, X.-B. Jing and F.-S. Wang, *Org. Lett.*, 2011, 13, 4378-4381.
57. H. Zhao, X. Guo, H. Tian, C. Li, Z. Xie, Y. Geng and F. Wang, *J. Mater. Chem.*, 2010, 20, 3092-3097.
58. T. Ishi-I, K. Yaguma, R. Kuwahara, Y. Taguri and S. Mataka, *Org. Lett.*, 2006, 8, 585-588.
59. T. Ishi-i, R. Hirashima, N. Tsutsumi, S. Amemori, S. Matsuki, Y. Teshima, R. Kuwahara and S. Mataka, *J. Org. Chem.*, 2010, 75, 6858-6868.
60. C. Tong, W. Zhao, J. Luo, H. Mao, W. Chen, H. S. O. Chan and C. Chi, *Org. Lett.*, 2012, 14, 494-497.
61. C. Jia, S. X. Liu, C. Tanner, C. Leiggener, L. Sanguinet, E. Levillain, S. Leutwyler, A. Hauser and S. Decurtins, *Chem. Commun.*, 2006, 1878-1880.
62. H. Herrera, P. de Echegaray, M. Urdanpilleta, M. J. Mancheno, E. Mena-Osteritz, P. Bauerle and J. L. Segura, *Chem. Commun.*, 2013, 49, 713-715.
63. Z. Zhao, Y. Xiao, Y. Zhang and H. Wang, *RSC Adv.*, 2013, 3, 21373-21376.
64. S. I. Stupp and L. C. Palmer, *Chem. Mater.*, 2013, 26, 507-518.
65. P. Strohriegl and J. V. Grazulevicius, *Adv. Mater.*, 2002, 14, 1439-1452.
66. B. R. Kaafarani, *Chem. Mater.*, 2010, 23, 378-396.
67. F. S. Kim, G. Ren and S. A. Jenekhe, *Chem. Mater.*, 2010, 23, 682-732.
68. L. Xu, L. Yang and S. Lei, *Nanoscale*, 2012, 4, 4399-4415.
69. M. Kasha, H. R. Rawls and M. A. El-Bayoumi, *Pure Appl. Chem.*, 1965, 11, 21.
70. B. Nie, T.-G. Zhan, T.-Y. Zhou, Z.-Y. Xiao, G.-F. Jiang and X. Zhao, *Chem. Asian J.*, 2014, 9, 754-758.
71. H. K. Bisoyi and S. Kumar, *Chem. Soc. Rev.*, 2010, 39, 264-285.
72. S. Kumar, *Chem. Soc. Rev.*, 2006, 35, 83-109.
73. S. Chandrasekhar, B. K. Sadashiva and K. A. Suresh, *Pramana - J Phys*, 1977, 9, 471-480.
74. S. Laschat, A. Baro, N. Steinke, F. Giesselmann, C. Hägele, G. Scalia, R. Judele, E. Kapatsina, S. Sauer, A. Schreivogel and M. Tosoni, *Angew. Chem. Int. Ed.*, 2007, 46, 4832-4887.
75. E. Fontes, P. A. Heiney and W. H. de Jeu, *Phys. Rev. Lett.*, 1988, 61, 1202-1205.
76. D. Adam, P. Schuhmacher, J. Simmerer, L. Haussling, K. Siemensmeyer, K. H. Etzbachi, H. Ringsdorf and D. Haarer, *Nature*, 1994, 371, 141-143.
77. A. M. van de Craats and J. M. Warman, *Adv. Mater.*, 2001, 13, 130-133.
78. A. M. v. d. Craats, J. M. Warman, A. Fechtenkötter, J. D. Brand, M. A. Harbison and K. Müllen, *Adv. Mater.*, 1999, 11, 1469-1472.
79. E. O. Arikainen, N. Boden, R. J. Bushby, O. R. Lozman, J. G. Vinter and A. Wood, *Angew. Chem., Int. Ed.*, 2000, 39, 2333-2336.
80. M. Lehmann, V. Lemaur, J. Cornil, J.-L. Brédas, S. Goddard, I. Grizzi and Y. Geerts, *Tetrahedron*, 2004, 60, 3283-3291.
81. K. Pieterse, P. A. van Hal, R. Kleppinger, J. A. J. M. Vekemans, R. A. J. Janssen and E. W. Meijer, *Chem. Mater.*, 2001, 13, 2675-2679.
82. M. Lehmann, G. Kestemont, R. G. Aspe, C. Buess-Herman, M. H. J. Koch, M. G. Debije, J. Piris, H. M. P. de, J. M. Warman, M. D. Watson, V. Lemaur, J. Cornil, Y. H. Geerts, R. Gearba and D. A. Ivanov, *Chem. Eur. J.*, 2005, 11, 3349-3362.
83. G. Kestemont, H. V. de, M. Lehmann, D. A. Ivanov, M. Watson and Y. H. Geerts, *Chem. Commun.*, 2001, 2074-2075.
84. W. Zheng, Y.-T. Hu, C.-Y. Chiang and C. W. Ong, *Int. J. Mol. Sci.*, 2010, 11, 943-955.
85. R. Juárez, M. Ramos, M. Lehmann and J. L. Segura, *Synth. Met.*, 2014, 195, 222-227.
86. T. Ishi-i, T. Hirayama, K.-i. Murakami, H. Tashiro, T. Thiemann, K. Kubo, A. Mori, S. Yamasaki, T. Akao, A. Tsuboyama, T. Mukaide, K. Ueno and S. Mataka, *Langmuir*, 2005, 21, 1261-1268.
87. K. Praefcke and J. Holbrey, *J. Inclusion Phenom. Mol. Recognit. Chem.*, 1996, 24, 19-41.
88. O. R. Lozman, R. J. Bushby and J. G. Vinter, *J. Chem. Soc., Perkin Trans. 2*, 2001, 1446-1452.
89. N. Boden, R. J. Bushby, Z. Lu and O. R. Lozman, *Liq. Cryst.*, 2001, 28, 657-661.
90. N. Boden, R. J. Bushby, G. Cooke, O. R. Lozman and Z. Lu, *J. Am. Chem. Soc.*, 2001, 123, 7915-7916.
91. N. Boden, R. J. Bushby, Q. Liu and O. R. Lozman, *J. Mater. Chem.*, 2001, 11, 1612-1617.
92. T. Kreouzis, K. J. Donovan, N. Boden, R. J. Bushby, O. R. Lozman and Q. Liu, *J. Chem. Phys.*, 2001, 114, 1797-1802.
93. T. Kreouzis, K. Scott, K. J. Donovan, N. Boden, R. J. Bushby, O. R. Lozman and Q. Liu, *Chem. Phys.*, 2000, 262, 489-497.
94. R. J. Bushby, I. W. Hamley, Q. Liu, O. R. Lozman and J. E. Lydon, *J. Mater. Chem.*, 2005, 15, 4429-4434.
95. J. Cornil, V. Lemaur, J. P. Calbert and J. L. Brédas, *Adv. Mater.*, 2002, 14, 726-729.
96. X. Crispin, J. Cornil, R. Friedlein, K. K. Okudaira, V. Lemaur, A. Crispin, G. Kestemont, M. Lehmann, M. Fahlman, R. Lazzaroni, Y. Geerts, G. Wendin, N. Ueno, J.-L. Brédas and W. R. Salaneck, *J. Am. Chem. Soc.*, 2004, 126, 11889-11899.
97. H. Bässler, *Phys. Status Solidi B*, 1993, 175, 15-56.
98. C. Duke and L. Schein, *Phys. Today*, 1980, 33, 42-48.
99. V. Lemaur, D. A. da Silva Filho, V. Coropceanu, M. Lehmann, Y. Geerts, J. Piris, M. G. Debije, A. M. van de Craats, K. Senthilkumar, L. D. A. Siebbeles, J. M. Warman, J.-L. Brédas and J. Cornil, *J. Am. Chem. Soc.*, 2004, 126, 3271-3279.
100. B. R. Kaafarani, T. Kondo, J. Yu, Q. Zhang, D. Dattilo, C. Risko, S. C. Jones, S. Barlow, B. Domercq, F. Amy, A. Kahn, J.-L. Brédas, B. Kippelen and S. R. Marder, *J. Am. Chem. Soc.*, 2005, 127, 16358-16359.
101. J. Shao, J. Chang and C. Chi, *Org. Biomol. Chem.*, 2012, 10, 7045-7052.
102. X.-Y. Liu, T. Usui and J. Hanna, *Chem. Eur. J*, 2014, 20, 14207-14212.
103. M. Palma, J. Levin, V. Lemaur, A. Liscio, V. Palermo, J. Cornil, Y. Geerts, M. Lehmann and P. Samorì, *Adv. Mater.*, 2006, 18, 3313-3317.
104. S. D. Ha, B. R. Kaafarani, S. Barlow, S. R. Marder and A. Kahn, *J. Phys. Chem. C*, 2007, 111, 10493-10497.
105. X. Qing-Min, M. Hong, T. Neil, A. B. Julie and K. Y. J. Alex, *Nanotechnology*, 2007, 18, 335302.
106. E. Salomon, Q. Zhang, S. Barlow, S. R. Marder and A. Kahn, *J. Phys. Chem. C*, 2008, 112, 9803-9807.
107. M. Palma, J. Levin, V. Lemaur, A. Liscio, V. Palermo, J. Cornil, Y. Geerts, M. Lehmann and P. Samori, *Adv. Mater.*, 2006, 18, 3313-3317.
108. Q.-M. Xu, H. Ma, N. Tucker, J. A. Bardecker and A. K. Y. Jen, *Nanotechnology*, 2007, 18, 335302.
109. K. Gentz and K. Wandelt, *CHIMIA*, 2012, 66, 44-51.
110. C. K. Chan, F. Amy, Q. Zhang, S. Barlow, S. Marder and A. Kahn, *Chem. Phys. Lett.*, 2006, 431, 67-71.
111. E. Salomon, Q. Zhang, S. Barlow, S. R. Marder and A. Kahn, *Org. Electron.*, 2008, 9, 944-951.
112. W. Zhao, E. Salomon, Q. Zhang, S. Barlow, S. R. Marder and A. Kahn, *Phys. Rev. B: Condens. Matter Mater. Phys.*, 2008, 77, 165336.
113. *Handbook of Nanoscience, Engineering, and Technology, Third Edition*, CRC Press, 2012.
114. F. S. Kim, G. Ren and S. A. Jenekhe, *Chem. Mater.*, 2011, 23, 682-732.
115. H.-L. Yip, J. Zou, H. Ma, Y. Tian, N. M. Tucker and A. K. Y. Jen, *J. Am. Chem. Soc.*, 2006, 128, 13042-13043.

116. A. Perl, D. N. Reinhoudt and J. Huskens, *Adv. Mater.*, 2009, 21, 2257-2268.
117. Z.-Y. Xiao, X. Zhao, X.-K. Jiang and Z.-T. Li, *Langmuir*, 2010, 26, 13048-13051.
118. Z.-Y. Xiao, X. Zhao, X.-K. Jiang and Z.-T. Li, *Chem. Mater.*, 2011, 23, 1505-1511.
119. J. T. Rademacher, K. Kanakarajan and A. W. Czarnik, *Synthesis*, 1994, 1994, 378-380.
120. P. S. Szalay, J. R. Galán-Mascarós, R. Clérac and K. R. Dunbar, *Synth. Met.*, 2001, 122, 535-542.
121. P. S. Szalay, J. R. Galán-Mascarós, B. L. Schottel, J. Bacsa, L. M. Pérez, A. S. Ichimura, A. Chouai and K. R. Dunbar, *J. Cluster Sci.*, 2004, 15, 503-530.
122. J. C. Beeson, L. J. Fitzgerald, J. C. Gallucci, R. E. Gerkin, J. T. Rademacher and A. W. Czarnik, *J. Am. Chem. Soc.*, 1994, 116, 4621-4622.
123. J. R. Gallegos, A. H. Francis, N. W. Ockwig, P. G. Rasmussen, R. G. Raptis, P. R. Challen and I. Ouedraogo, *Synth. Met.*, 2009, 159, 1667-1671.
124. S. Furukawa, T. Okubo, S. Masaoka, D. Tanaka, H.-C. Chang and S. Kitagawa, *Angew. Chem. Int. Ed.*, 2005, 44, 2700-2704.
125. C. Falkenberg, S. Olthof, R. Rieger, M. Baumgarten, K. Muellen, K. Leo and M. Riede, *Sol. Energy Mater. Sol. Cells*, 2011, 95, 927-932.
126. L. S. Liao, W. K. Slusarek, T. K. Hatwar, M. L. Ricks and D. L. Comfort, *Adv. Mater.*, 2008, 20, 324-329.
127. S. Y. Kim, W. S. Jeon, T. J. Park, R. Pode, J. Jang and J. H. Kwon, *Appl. Phys. Lett.*, 2009, 94, 133303-133303.
128. S. M. Park, Y. H. Kim, Y. Yi, H.-Y. Oh and J. Won Kim, *Appl. Phys. Lett.*, 2010, 97, -.
129. J.-H. Lee, S. Lee, J.-B. Kim, J. Jang and J.-J. Kim, *J. Mater. Chem.*, 2012, 22, 15262-15266.
130. H.-W. Lin, W.-C. Lin, J.-H. Chang and C.-I. Wu, *Org. Electron.*, 2013, 14, 1204-1210.
131. K. Albrecht, K. Matsuoka, K. Fujita and K. Yamamoto, *Angew. Chem. Int. Ed. Engl.*, 2015, 54, 5677-5682.
132. Y. Sun, G. C. Welch, W. L. Leong, C. J. Takacs, G. C. Bazan and A. J. Heeger, *Nat. Mater.*, 2012, 11, 44-48.
133. L. Torsi, M. Magliulo, K. Manoli and G. Palazzo, *Chem. Soc. Rev.*, 2013, 42, 8612-8628.
134. K. Walzer, B. Maennig, M. Pfeiffer and K. Leo, *Chem. Rev.*, 2007, 107, 1233-1271.
135. M. T. Greiner, M. G. Helander, W.-M. Tang, Z.-B. Wang, J. Qiu and Z.-H. Lu, *Nat. Mater.*, 2012, 11, 76-81.
136. S. Winkler, J. Frisch, R. Schlesinger, M. Oehzelt, R. Rieger, J. Räder, J. P. Rabe, K. Müllen and N. Koch, *J. Phys. Chem. C*, 2013, 117, 22285-22289.
137. H. Lee, J. Lee, S. Park, Y. Yi, S. W. Cho, J. W. Kim and S. J. Kang, *Carbon*, 2014, 71, 268-275.
138. H. J. Kim, J.-H. Lee, J. W. Kim, S. Lee, J. Jang, H. H. Lee and J.-J. Kim, *J. Mater. Chem. C*, 2013, 1, 1260-1264.
139. H. Glowatzki, B. Bröker, R.-P. Blum, O. T. Hofmann, A. Vollmer, R. Rieger, K. Müllen, E. Zojer, J. P. Rabe and N. Koch, *Nano Lett.*, 2008, 8, 3825-3829.
140. P. Frank, T. Djuric, M. Koini, I. Salzmann, R. Rieger, K. Müllen, R. Resel, N. Koch and A. Winkler, *J. Phys. Chem. C*, 2010, 114, 6650-6657.
141. P. Frank, N. Koch, M. Koini, R. Rieger, K. Müllen, R. Resel and A. Winkler, *Chem. Phys. Lett.*, 2009, 473, 321-325.
142. Z. Liu, M. G. Helander, Z. Wang and Z. Lu, *J. Phys. Chem. C*, 2010, 114, 16746-16749.
143. J. Huang, Z. Xu and Y. Yang, *Adv. Funct. Mater.*, 2007, 17, 1966-1973.
144. J. Kido and T. Matsumoto, *Appl. Phys. Lett.*, 1998, 73, 2866-2868.
145. C.-H. Gao, X.-Z. Zhu, L. Zhang, D.-Y. Zhou, Z.-K. Wang and L.-S. Liao, *Appl. Phys. Lett.*, 2013, 102, 153301.
146. S. H. Cho, S. W. Pyo and M. C. Suh, *Synth. Met.*, 2012, 162, 402-405.
147. K. S. Yook, S. O. Jeon and J. Y. Lee, *Thin Solid Films*, 2009, 517, 6109-6111.
148. S. Lee, J.-H. Lee, K. H. Kim, S.-J. Yoo, T. G. Kim, J. W. Kim and J.-J. Kim, *Org. Electron.*, 2012, 13, 2346-2351.
149. B. Bröker, R. P. Blum, J. Frisch, A. Vollmer, O. T. Hofmann, R. Rieger, K. Müllen, J. P. Rabe, E. Zojer and N. Koch, *Appl. Phys. Lett.*, 2008, 93, 243303.
150. J. Niederhausen, P. Amsalem, J. Frisch, A. Wilke, A. Vollmer, R. Rieger, K. Müllen, J. P. Rabe and N. Koch, *Phys. Rev. B*, 2011, 84, 165302.
151. P. Amsalem, A. Wilke, J. Frisch, J. Niederhausen, A. Vollmer, R. Rieger, K. Müllen, J. P. Rabe and N. Koch, *J. Appl. Phys.*, 2011, 110, 113709.
152. S. E. Jang and J. Y. Lee, *Synth. Met.*, 2011, 161, 40-43.
153. T. Chiba, Y.-J. Pu, R.-I. Miyazaki, K.-I. Nakayama, H. Sasabe and J. Kido, *Org. Electron.*, 2011, 12, 710-715.
154. C. W. Joo, J. Moon, J.-H. Han, J. W. Huh, J. Lee, N. S. Cho, J. Hwang, H. Y. Chu and J.-I. Lee, *Org. Electron.*, 2014, 15, 189-195.
155. C. E. Small, S.-W. Tsang, J. Kido, S. K. So and F. So, *Adv. Funct. Mater.*, 2012, 22, 3261-3266.
156. S. Lee, J.-H. Lee, J.-H. Lee and J.-J. Kim, *Adv. Funct. Mater.*, 2012, 22, 855-860.
157. C.-H. Chang, Z.-J. Wu, Y.-H. Liang, Y.-S. Chang, C.-H. Chiu, C.-W. Tai and H.-H. Chang, *Thin Solid Films*, 2013, 548, 389-397.
158. K. S. Lee, I. Lim, S. H. Han and T. W. Kim, *Org. Electron.*, 2014, 15, 343-347.
159. L.-S. Cui, Y. Liu, X.-D. Yuan, Q. Li, Z.-Q. Jiang and L.-S. Liao, *J. Mater. Chem. C*, 2013, 1, 8177-8185.
160. J.-K. Bin, N.-S. Cho and J.-I. Hong, *Adv. Mater.*, 2012, 24, 2911-2915.
161. Y. H. Son, Y. J. Kim, M. J. Park, H.-Y. Oh, J. S. Park, J. H. Yang, M. C. Suh and J. H. Kwon, *J. Mater. Chem. C*, 2013, 1, 5008-5014.
162. S.-C. Dong, Y. Liu, Q. Li, L.-S. Cui, H. Chen, Z.-Q. Jiang and L.-S. Liao, *J. Mater. Chem. C*, 2013, 1, 6575-6584.
163. E. Najafabadi, K. A. Knauer, W. Haske and B. Kippelen, *Org. Electron.*, 2013, 14, 1271-1275.
164. D. Zhang, L. Duan, D. Zhang, J. Qiao, G. Dong, L. Wang and Y. Qiu, *Org. Electron.*, 2013, 14, 260-266.
165. Y. H. Son, M. J. Park, Y. J. Kim, J. H. Yang, J. S. Park and J. H. Kwon, *Org. Electron.*, 2013, 14, 1183-1188.
166. H. Sasabe, H. Nakanishi, Y. Watanabe, S. Yano, M. Hirasawa, Y.-J. Pu and J. Kido, *Adv. Funct. Mater.*, 2013, 23, 5550-5555.
167. L. Dou, J. You, Z. Hong, Z. Xu, G. Li, R. A. Street and Y. Yang, *Adv. Mater.*, 2013, 25, 6642-6671.
168. A. J. Heeger, *Adv. Mater.*, 2014, 26, 10-28.
169. K. Cnops, B. P. Rand, D. Cheyns, B. Verreet, M. A. Empl and P. Heremans, *Nat. Commun.*, 2014, 5, 3406.
170. B. E. Lassiter, R. R. Lunt, C. K. Renshaw and S. R. Forrest, *Opt. Express*, 2010, 18, A444-A450.
171. C. Falkenberg, S. Olthof, R. Rieger, M. Baumgarten, K. Muellen, K. Leo and M. Riede, *Sol. Energy Mater. Sol. Cells*, 2011, 95, 927-932.
172. S. O. Jeon and J. Y. Lee, *J. Ind. Eng. Chem.*, 2012, 18, 661-663.
173. H. Dong, X. Fu, J. Liu, Z. Wang and W. Hu, *Adv. Mater.*, 2013, 25, 6158-6183.
174. T. P. I. Saragi, T. Reichert, A. Scheffler, M. Kussler and J. Salbeck, *Synth. Met.*, 2012, 162, 1572-1576.
175. S.-T. Pham, Y. Kawasugi and H. Tada, *Appl. Phys. Lett.*, 2013, 103, 143301.
176. G. Veeraraghavan, T. D. Nguyen, S. Yugang, O. Mermer and M. Wohlgenannt, *Electron Devices, IEEE Transactions on*, 2007, 54, 1571-1577.
177. T. Reichert, T. P. I. Saragi and J. Salbeck, *RSC Adv.*, 2012, 2, 7388-7390.
178. S. Bruzzone and G. Fiori, *Appl. Phys. Lett.*, 2011, 99, 222108.
179. W. Chen, S. Chen, D. C. Qi, X. Y. Gao and A. T. S. Wee, *J. Am. Chem. Soc.*, 2007, 129, 10418-10422.
180. K. P. Goetz, D. Vermeulen, M. E. Payne, C. Kloc, L. E. McNeil and O. D. Jurchescu, *J. Mater. Chem. C*, 2014, 2, 3065-3076.
181. T. Matsushima, G.-H. Jin, Y. Kanai, T. Yokota, S. Kitada, T. Kishi and H. Murata, *Org. Electron.*, 2011, 12, 520-528.
182. A. Okabe, T. Fukushima, K. Ariga and T. Aida, *Angew. Chem. Int. Ed.*, 2002, 41, 3414-3417.
183. W. Otani, K. Kinbara and T. Aida, *Faraday Discuss.*, 2009, 143, 335-343.
184. C. Caltagirone and P. A. Gale, *Chem. Soc. Rev.*, 2009, 38, 520-563.

185. R. E. Dawson, A. Hennig, D. P. Weimann, D. Emery, V. Ravikumar, J. Montenegro, T. Takeuchi, S. Gabutti, M. Mayor, J. Mareda, C. A. Schalley and S. Matile, *Nat. Chem.*, 2010, 2, 533-538.
186. D. Quiñonero, C. Garau, C. Rotger, A. Frontera, P. Ballester, A. Costa and P. M. Deyà, *Angew. Chem. Int. Ed.*, 2002, 41, 3389-3392.
187. Y. S. Rosokha, S. V. Lindeman, S. V. Rosokha and J. K. Kochi, *Angew. Chem. Int. Ed.*, 2004, 43, 4650-4652.
188. B. P. Hay and V. S. Bryantsev, *Chem. Commun.*, 2008, 2417-2428.
189. B. Han, J. Lu and J. K. Kochi, *Cryst. Growth Des.*, 2008, 8, 1327-1334.
190. H. T. Chifotides, B. L. Schottel and K. R. Dunbar, *Angew. Chem. Int. Ed.*, 2010, 49, 7202-7207.
191. G. Aragay, A. Frontera, V. Lloveras, J. Vidal-Gancedo and P. Ballester, *J. Am. Chem. Soc.*, 2013, 135, 2620-2627.
192. K. S. Novoselov, A. K. Geim, S. V. Morozov, D. Jiang, Y. Zhang, S. V. Dubonos, I. V. Grigorieva and A. A. Firsov, *Science*, 2004, 306, 666-669.
193. K. S. Novoselov, D. Jiang, F. Schedin, T. J. Booth, V. V. Khotkevich, S. V. Morozov and A. K. Geim, *Proc. Natl. Acad. Sci.*, 2005, 102, 10451-10453.
194. C.-Y. Su, A.-Y. Lu, C.-Y. Wu, Y.-T. Li, K.-K. Liu, W. Zhang, S.-Y. Lin, Z.-Y. Juang, Y.-L. Zhong, F.-R. Chen and L.-J. Li, *Nano Lett.*, 2011, 11, 3612-3616.
195. B. Zhang, W. H. Lee, R. Piner, I. Kholmanov, Y. Wu, H. Li, H. Ji and R. S. Ruoff, *ACS Nano*, 2012, 6, 2471-2476.
196. Q. Zhuo, J. Gao, M. Peng, L. Bai, J. Deng, Y. Xia, Y. Ma, J. Zhong and X. Sun, *Carbon*, 2013, 52, 559-564.
197. W. Gao, L. B. Alemany, L. Ci and P. M. Ajayan, *Nat. Chem.*, 2009, 1, 403-408.
198. Q. Zhuo, Y. Ma, J. Gao, P. Zhang, Y. Xia, Y. Tian, X. Sun, J. Zhong and X. Sun, *Inorg. Chem.*, 2013, 52, 3141-3147.
199. F. Chen and N. J. Tao, *Acc. Chem. Res.*, 2009, 42, 429-438.
200. F. Ravani, K. Papagelis, V. Dracopoulos, J. Parthenios, K. G. Dassios, A. Siokou and C. Galiotis, *Thin Solid Films*, 2013, 527, 31-37.
201. Q. Q. Zhuo, Q. Wang, Y. P. Zhang, D. Zhang, Q. L. Li, C. H. Gao, Y. Q. Sun, L. Ding, Q. J. Sun, S. D. Wang, J. Zhong, X. H. Sun and S. T. Lee, *ACS Nano*, 2015, 9, 594-601.
202. W. S. Chow, *J. Biol. Phys.*, 2003, 29, 447-459.
203. W.-Y. Wong and C.-L. Ho, *Acc. Chem. Res.*, 2010, 43, 1246-1256.
204. T. Ishi-i, K.-i. Murakami, Y. Imai and S. Mataka, *Org. Lett.*, 2005, 7, 3175-3178.
205. T. Ishi-i, H. Tashiro, R. Kuwahara, S. Mataka, T. Yoshihara and S. Tobita, *Chem. Lett.*, 2006, 35, 158-159.
206. E. Garmire, *Opt. Express*, 2013, 21, 30532-30544.
207. S. R. Marder, *Chem. Commun.*, 2006, 131-134.
208. J. Zyss and I. Ledoux, *Chem. Rev.*, 1994, 94, 77-105.
209. O. Maury and H. Le Bozec, *Acc. Chem. Res.*, 2005, 38, 691-704.
210. G. Argouarch, R. Veillard, T. Roisnel, A. Amar, A. Boucekkine, A. Singh, I. Ledoux and F. Paul, *New J. Chem.*, 2011, 35, 2409-2411.
211. B. R. Cho, S. K. Lee, K. A. Kim, K. N. Son, T. I. Kang and S. J. Jeon, *Tetrahedron Lett.*, 1998, 39, 9205-9208.
212. M. M. Oliva, R. Juárez, M. Ramos, J. L. Segura, S. v. Cleuvenbergen, K. Clays, T. Goodson, J. T. L. Navarrete and J. Casado, *J. Phys. Chem. C*, 2012, 117, 626-632.
213. L. Guo and M. S. Wong, *Adv. Mater.*, 2014, 26, 5400-5428.
214. G. S. He, L.-S. Tan, Q. Zheng and P. N. Prasad, *Chem. Rev.*, 2008, 108, 1245-1330.
215. T. Ishi-i, S. Amemori, C. Okamura, K. Yanaga, R. Kuwahara, S. Mataka and K. Kamada, *Tetrahedron*, 2013, 69, 29-37.
216. J. V. Crivello and M. F. Aldersley, *J. Polym. Sci., Part A: Polym. Chem.*, 2013, 51, 801-814.
217. A. M. Szymczak, R. Podsiadły, K. Podemska and J. Sokołowska, *Coloration Technology*, 2012, 128, 378-386.
218. M.-A. Tehfe, F. Dumur, P. Xiao, J. Zhang, B. Graff, F. Morlet-Savary, D. Gigmes, J.-P. Fouassier and J. Lalevée, *Polymer*, 2014, 55, 2285-2293.
219. K. Hermann, M. Nakhla, J. Gallucci, E. Dalkilic, A. Dastan and J. D. Badjić, *Angew. Chem. Int. Ed.*, 2013, 52, 11313-11316.
220. Z.-G. Tao, X. Zhao, X.-K. Jiang and Z.-T. Li, *Tetrahedron Lett.*, 2012, 53, 1840-1842.
221. X. Zhang, J. Fu, T.-G. Zhan, L. Dai, Y. Chen and X. Zhao, *Tetrahedron Lett.*, 2013, 54, 5039-5042.
222. X. Zhang, J. Fu, T.-G. Zhan, X.-Z. Wang, L. Dai, Y. Chen and X. Zhao, *Tetrahedron Lett.*, 2014, 55, 6486-6489.
223. T. Hirayama, S. Yamasaki, H. Ameku, T. Ishi-i, T. Thiemann and S. Mataka, *Dyes Pigments*, 2005, 67, 105-110.
224. X.-H. Zhang, Q. Zhao, X.-M. Liu, T.-L. Hu, J. Han, W.-J. Ruan and X.-H. Bu, *Talanta*, 2013, 108, 150-156.
225. X.-H. Zhang, C.-F. Zhao, Y. Li, X.-M. Liu, A. Yu, W.-J. Ruan and X.-H. Bu, *Talanta*, 2014, 119, 632-638.
226. L.-L. Yang, X.-M. Liu, K. Liu, H. Liu, F.-Y. Zhao, W.-J. Ruan, Y. Li, Z. Chang and X.-H. Bu, *Talanta*, 2014, 128, 278-283.
227. S. Yoon, A. E. Albers, A. P. Wong and C. J. Chang, *J. Am. Chem. Soc.*, 2005, 127, 16030-16031.
228. P. M. Budd, E. S. Elabas, B. S. Ghanem, S. Makhseed, N. B. McKeown, K. J. Msayib, C. E. Tattershall and D. Wang, *Adv. Mater.*, 2004, 16, 456-459.
229. N. B. McKeown, B. Gahnem, K. J. Msayib, P. M. Budd, C. E. Tattershall, K. Mahmood, S. Tan, D. Book, H. W. Langmi and A. Walton, *Angew. Chem. Int. Ed.*, 2006, 45, 1804-1807.
230. A. I. Cooper, *Adv. Mater.*, 2009, 21, 1291-1295.
231. Z. Xie, C. Wang, K. E. deKrafft and W. Lin, *J. Am. Chem. Soc.*, 2011, 133, 2056-2059.
232. Y. Kou, Y. Xu, Z. Guo and D. Jiang, *Angew. Chem. Int. Ed.*, 2011, 50, 8753-8757.
233. J. P. Zheng, P. J. Cygan and T. R. Jow, *J. Electrochem. Soc.*, 1995, 142, 2699-2703.
234. F. Xu, X. Chen, Z. Tang, D. Wu, R. Fu and D. Jiang, *Chem. Commun.*, 2014, 50, 4788-4790.
235. M. Armand and J. M. Tarascon, *Nature*, 2008, 451, 652-657.
236. Z. Song and H. Zhou, *Energy Environ. Sci.*, 2013, 6, 2280-2301.